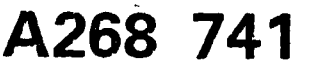

NAVAL POSTGRADUATE SCHOOL
Monterey, California

THESIS

An Application of Parameter Estimation
to the Stability and Control
of the
BQM-147 Unmanned Aerial Vehicle

by

Patrick John Quinn

June, 1993

Thesis Advisor: R.M. Howard

Approved for public release; distribution is unlimited.

REPORT DOCUMENTATION PAGE

1a Report Security Classification: Unclassified			1b Restrictive Markings	
2a Security Classification Authority			3 Distribution/Availability of Report	
2b Declassification/Downgrading Schedule			Approved for public release; distribution is unlimited.	
4 Performing Organization Report Number(s)			5 Monitoring Organization Report Number(s)	
6a Name of Performing Organization Naval Postgraduate School	6b Office Symbol (if applicable) AA		7a Name of Monitoring Organization Naval Postgraduate School	
6c Address (city, state, and ZIP code) Monterey CA 93943-5000			7b Address (city, state, and ZIP code) Monterey CA 93943-5000	
8a Name of Funding/Sponsoring Organization	6b Office Symbol (if applicable)		9 Procurement Instrument Identification Number	
Address (city, state, and ZIP code)			10 Source of Funding Numbers	
			Program Element No	Project No / Task No / Work Unit Accession No

11 Title (include security classification) An Application of Parameter Estimation to the Stability and Control of the BQM-147 Unmanned Aerial Vehicle

12 Personal Author(s) Quinn, Patrick J.

13a Type of Report	13b Time Covered From To	14 Date of Report (year, month, day)	15 Page Count *
Master's Thesis		1993 June these words	134

16 Supplementary Notation The views expressed in this thesis are those of the author and do not reflect the official policy or position of the Department of Defense or the U.S. Government.

17 Cosati Codes			18 Subject Terms (continue on reverse if necessary and identify by block number)
Field	Group	Subgroup	Aircraft Parameter Estimation

19 Abstract (continue on reverse if necessary and identify by block number)

Parameter estimation methods were used to obtain estimates of stability and control derivatives for the Marine Corps BQM-147 Unmanned Air Vehicle. The results from a simple PC-based linear model and those from a more robust non-linear model, pEst, were compared. A Cramer-Rao bound was used to assess the accuracy of the estimates for both methods. The bounds were high for both the longitudinal case and the lateral-directional case due to the limited maneuvers tested, high levels of noise in the same general frequency range as the control input, and the lack of body angle data. The linear model failed to provide estimates for the lateral-directional case. Though the results may be used as starting points for a dynamic model of the aircraft, it is recommended that the flight test procedures be modified to address the issues raised concerning noise, recorded signals and the need for repeated maneuvers.

20 Distribution/Availability of Abstract	21 Abstract Security Classification	
__ unclassified/unlimited __ same as report __ DTIC users	Unclassified	
22a Name of Responsible Individual Richard M. Howard	22b Telephone (include Area Code) (408) 656-2870	22c Office Symbol AA/Ho

DD FORM 1473,84 MAR 83 APR edition may be used until exhausted

All other editions are obsolete

Approved for public release; distribution is unlimited.

An Application of Parameter Estimation
to the Stability and Control
of the
BQM-147 Unmanned Aerial Vehicle

by

Patrick J. Quinn
Commander, United States Navy
B.S., Northern Michigan University, 1975

Submitted in partial fulfillment
of the requirements for the degree of

MASTER OF SCIENCE IN AERONAUTICAL ENGINEERING

from the

NAVAL POSTGRADUATE SCHOOL
June 1993

Author: _____
Patrick J. Quinn

Approved by: _____
Richard M. Howard, Thesis Advisor

_____
Isaac I. Kaminer, Second Reader

_____
Daniel J. Collins, Chairman
Department of Aeronautics and Astronautics

ABSTRACT

Parameter estimation methods were used to obtain estimates of stability and control derivatives for the Marine Corps BQM-147 Unmanned Air Vehicle. The results from a simple, PC-based linear model and those from a more robust non-linear model, pEst, were compared. A Cramer-Rao bound was used to assess the accuracy of the estimates for both methods. The bounds were high for both the longitudinal case and the lateral-directional case due to the limited maneuvers tested, high levels of noise in the same general frequency range as the control input, and the lack of body-angle data. The linear model failed to provide estimates for the lateral-directional case. Though the results may be used as starting points for a dynamic model of the aircraft it is recommended that the flight test procedures be modified to address the issues raised concerning noise, recorded signals and the need for repeated maneuvers.

TABLE OF CONTENTS

Nomenclature

A	State-Space System Matrix
An	Normal acceleration
A_Y	Lateral acceleration
b	Span
B	State-Space Control Matrix
c	Reference chord
C	State-Space Output Matrix
C_D	Drag coefficient
C_L	Lift coefficient
C_l, C_m, C_n	Roll, pitch and yaw moment coefficients
$C_{L\alpha}$	Variation in lift coef. with angle of attack
$C_{L\delta e}$	Elevator lift effectiveness
C_{Lq}	Variation in lift coef. with pitch rate
Cm_α	Variation in pitch moment with angle of attack
Cm_q	Pitch damping
$Cm_{\delta e}$	Longitudinal control power
$C_{l\beta}$	Variation in roll moment coef. with sideslip
C_{lp}	Variation in roll moment coef. with roll rate
C_{lr}	Variation in roll moment coef. with yaw rate
$Cl_{\delta a}$	Lateral control power
$Cl_{\delta r}$	Variation in roll moment coef. with rudder angle
Cn_β	Variation in yaw moment coef. with sideslip
Cn_p	Variation in yaw moment coef. with roll rate
Cn_r	Variation in yaw moment coef. with yaw rate
$Cn_{\delta a}$	Variation in yaw moment coef. with aileron angle
$Cn_{\delta r}$	Variation in yaw moment coef. with rudder angle
$C_{Y\beta}$	Variation in side force coef. with sideslip
C_{Yp}	Variation in side force coef. with roll rate
C_{Yr}	Variation in side force coef. with yaw rate
$C_{Y\delta a}$	Variation in side force coef. with aileron angle
$C_{Y\delta r}$	Variation in side force coef. with rudder angle
C_X, C_Y, C_Z	Force coefficients relative to aircrate state
D	State-Space Feed-through Matrix
dt	Time step or sample rate
E	Error term of Trapezoidal Rule
F	Vector force
F_x, F_y, F_z	Component forces

g	Acceleration due to gravity
gw	gross weight
H	Angular momentum
I_x I_y I_z I_{xy} I_{xz} I_{yz}	Moments of inertia (slugs-ft^2)
J	Cost functional or Criterion
JPO	Joint Project Office
K	Kalman Gain
L	Rolling moment component about longitudinal axis
l	Perturbed rolling moment
M	Pitching moment component about lateral axis
m	Perturbed pitching moment
m	Mass
MMLE3	Modified Maximum Likelihood Version 3
N	Yawing moment component about vertical axis
n	Perturbed yawing moment
p	roll rate
PC	Personal Computer
pEst	Murray, Maine parameter estimation code
$\bar{q}$	dynamic pressure
q	pitch rate
R	Innovations covariance matrix
r	yaw rate
RPV	Remotely Piloted Vehicle
s	Reference wing area
T	Thrust component
T_Φ, T_Ψ, T_Θ	Transformation matrices
u	Longitudinal velocity component
u	State-Space control input vector
UAV	Unmanned Aerial Vehicle
v	total velocity vector
v	lateral velocity component
w	Vertical velocity component
W	Weighting matrix

x	Longitudinal axis component
$\mathbf{x}$	State-Space state vector
x_b	Corrected state estimate
$\mathbf{x}^b$	Body-axis vector
$\mathbf{x}_i$	Inertial-axis vector
X_{an} X_{ay} X_{ay} X_{bp}	Sensor location parameters
$\mathbf{y}$	State-Space output vector
y	Lateral axis component
z	Kalman estimate
z	vertical axis component
z_k	Discrete measurement equation
Z_{an} Z_{ay}	Sensor location parameter
α	Angle of attack
β	Sideslip angle
δe δa δr	Elevator, aileron and rudder deflection angles
θ	Pitch angle
ν	Measurement noise vector
ξ	Parameter vector
ϕ	Roll angle
ψ	Heading angle
Ω	Angular momentum vector
ω	State noise vector
$\dot{}$	Dot above, time-rate of change
$\hat{}$	Cicumflex above, corrected estimate
$\tilde{}$	Tilde above, Kalman estimate

ACKNOWLEDGEMENTS

Thesis research cannot begin without first establishing a solid academic foundation. I shall be forever grateful to the faculty of the Department of Aeronautics and Astronautics for their willingness to dedicate countless hours of office time, in addition to classroom time, to assist my efforts in this endeavor. I would especially like to thank the Department Chairman, Dr. Daniel Collins, my thesis advisor, Dr. Richard Howard, and Professor Emeritus Louis Schmidt for providing guidance and inspiration.

This thesis was supported with the kindness and generosity of many people who contributed their time and talents to this effort. I wish to express my sincere thanks to Mr. Stanley Cox of the Johns Hopkins, Applied Physics Laboratory, to Mr. George Mackowiec and Ms. Norma Campbell of the NASA Langley Research Center, and to Captain David Kuechenmeister, USMC, who was so patient in teaching me how to operate the UNIX system. I would like to especially recognize and thank Mr. Albion Bowers of the NASA Ames, Dryden Flight Research Facility, for taking time from his busy schedule to assist me in running the pEst parameter estimation program.

Finally, I would like to thank my dear wife, Marianne, and our four boys, Kevin, Mark, Thomas and Christopher. Without their love and support, none of this would have been possible.

I. INTRODUCTION

Symmetrical-wing, delta-planform (SYMDEL) unmanned air vehicles (UAVs) have been in development and have flown in a variety of mission profiles since the early 1970's. This delta-planform, symmetrical-airfoil configuration was designed to provide equal performance in range, speed and stability in either an upright or inverted attitude [Ref. 1:p. 23]. With this attribute the vehicle can readily accommodate a variety of payloads which makes it ideally suited for specific military applications or as a testbed vehicle for new component technologies.

The EXDRONE UAV was developed in the early 1980's at the Johns Hopkins University, Applied Physics Laboratory (APL). The vehicle design is a descendent of the earlier SYMDEL 4 with a constant-chord section inserted into the middle of the delta planform to provide an accessible avionics bay [Ref. 1:p. 25]. The original APL version of the EXDRONE, referred to as the baseline configuration throughout this document, was intended to meet a United States Marine Corps (USMC) requirement for a UAV to carry an expendable VHF communications jammer. Takeoff, climb out and turn to the desired heading are accomplished by radio control. Once the mission heading is achieved, a radio control command switches control of the vehicle to the autopilot. The autopilot then

controls the vehicle for the duration of the mission. The name EXDRONE implies that the vehicle was intended to be operated autonomously and to be expendable at the end of its mission; however, radio control can be reacquired if necessary and the vehicle can be recovered.

In preliminary flight tests the baseline configuration of the EXDRONE was found to be difficult to handle for less experienced pilots. The vehicle had weak stability and control characteristics in low-speed flight and had a tendency to depart near stall [Ref. 2:p. 1]. The primary mission of the EXDRONE is to dash outbound at a speed of about 100 miles per hour to a predesignated target area and then to loiter in the area and jam enemy VHF communications. With low speed flight being an equally important part of the EXDRONE mission, the USMC UAV Project Office contracted with the NASA Langley Research Center, Flight Dynamics Branch, to conduct exploratory wind tunnel and flight tests in order to determine the aerodynamic characteristics of the vehicle and to provide modifications for aerodynamic improvements [Ref. 2:p. 1]. As a result of the wind tunnel study several modifications were made to the baseline configuration in order to increase pitch control for nose-up trim, improve the stall departure characteristics, minimize the adverse yaw characteristic and reduce the minimum level flight speed as a means of increasing endurance. It was this modified configuration EXDRONE that became the subject of the flight test portion of the NASA

Langley study. A detailed description of the wind tunnel tests on both the baseline and modified configurations can be found in Reference 2.

The modifications to the wing tips and control surfaces that are described in Reference 2 were included in the production contract for the BQM-147A. The following additional modifications are also a part of the production configuration.

1) Position and orientation of the engine
2) Shape of the nose/cowl
3) Number and type of skids

In October of 1991, Developmental Testing (DT) was conducted on the BQM-147A at the Dugway Proving Grounds, Utah. The purpose of the tests was to determine the suitability of the vehicle in the VHF communications jamming mission and to determine the effects of the communications jammer payload on the handling qualities of the airframe. The BQM-147A control surfaces are manipulated by electrical servos that are controlled by an autopilot. The autopilot receives command signals from either a modular radio control unit for direct pilot input or from an onboard microprocessor containing a pre-programmed mission scenario for the autonomous mode. The autopilot processes the error signal from a rate gyro to augment roll damping in flight [Ref. 3:p. 20]. During DT the autopilot had to be fine tuned by hand in a hit or miss

fashion because the vehicle control laws had not been well defined during the pre-production work. It was at this point that the USMC UAV Project Office decided to fund a series of flight tests from which time history data could be used to determine the aerodynamic characteristics of the aircraft.

Research being done at the Naval Postgraduate School (NPS), Department of Aeronautics and Astronautics, using UAV testbeds has been well received by the UAV Joint Project Office. Specifically, aerodynamic parameters obtained by numerical methods and by wind tunnel tests [Refs 4 and 5] have been used by the Target Simulation Lab, Naval Air Warfare Center, Weapons Division (formerly Pacific Missile Test Center), Pt. Mugu, CA., in the development of a math model for the Pioneer UAV flight training simulator. More recent thesis work by U.S. Navy LCDR Robert Graham incorporated a personal computer (PC) based parameter estimation capability into the NPS research program [Ref. 6]. Being advised of this desktop parameter estimation capability, the USMC UAV Project Office expressed an interest in an application of this routine using measured data obtained from the next series of flight tests. The objectives of the application listed in Reference 7 are:

1) To document the performance of the aircraft.

2) To reprogram the autopilot on the production aircraft.

3) To form a basis for suggesting changes to the production aircraft which will improve stability and performance.

4) To develop a PC-based flight simulator which will be used to train operators.

Aircraft parameter estimation routines are used to estimate aircraft stability and control derivatives from actual time history data. The stability and control parameters extracted from these routines provide an accurate model of the actual vehicle and can be used in analyzing the effects of proposed control system changes on aircraft stability and handling qualities. Parameters obtained from observed data can also be used to provide an accurate model of the vehicle for greater fidelity in flight simulators.

The purpose of this study was to use the flight test time history data found in Appendix B in a parameter estimation model to estimate both the longitudinal and lateral-directional stability and control derivatives. Two parameter estimation models were used. The first was an application of a PC-based parameter estimation program by LCDR Robert Graham [Ref. 6]. This model was selected because it is readily available, it operates in a familiar DOS environment and it generally provides good results when compared with more complex mainframe programs [Ref. 8]. The disadvantage of this first parameter estimation routine is that it is a linear, maximum likelihood estimator which assumes that the actual system satisfies the assumptions that were made in the linearization of the model. The second model, named pEst, is an interactive program for parameter estimation in non-linear dynamic systems. Incorporation of the pEst routine into the

ongoing flight test research at NPS provides a capability to model the dynamic behavior of aircraft that cannot be appropriately modeled using the assumptions inherent in the shorter, PC-based MMLE-3 code. Because of suspected non-linearities in the more extreme areas of the flight envelope of the EXDRONE, the linear model may not be sufficient and the pEst routine might better capture the behavior of the system.

II. BACKGROUND

A. HISTORICAL REVIEW

The concept of using remotely piloted vehicles (RPV's) and unmanned aerial vehicles (UAV's) in a tactical combat role had limited acceptance within the military community from the time of its first proposal in 1915 until early in the last decade. The RPV is controlled by a human operator by means of a radio-control guidance link using either direct operator visual contact or onboard video imagery to sense flight parameters. Initial RPV testing was limited by pre-WW II radio-control technology but improvements in guidance technology led to successful developmental flight tests of ordnance carrying RPV's prior to the attack on Pearl Harbor in December 1941. There was limited use of these lethal RPV's throughout the latter stages of World War II and the Korean Conflict. Widespread use of these platforms and full-scale development of follow-on vehicles with greater combat potential were met with opposition by military planners who preferred to use scarce resources on more expensive and ostensibly more technically-challenging guided-missile programs [Ref. 10].

Advancements in radio-control and digital communication technologies coupled with an operational need to defeat more modern military anti-air warfare weapons led to an expanded

role for a new generation of non-lethal UAV's. The UAV differs from the RPV in that the guidance signal, from either a human operator via radio-control uplink or from on-board navigation subsystems, is input to an auto-pilot which generates the appropriate control deflection. UAV's are generally known for their ability to operate autonomously over the entire range of a preprogrammed mission profile. During the Vietnam conflict the Ryan Model 147 Firebee was used for photo reconnaissance, electronic intelligence gathering, communications intelligence and covert psychological warfare missions [Ref. 11:p. 20]. In spite of the tremendous success of UAV's in Southeast Asia, continued support for further UAV development waned in the wake of higher priority military and domestic programs. Not until the unprecedented and highly successful use of UAV's by the Israelis in the Bekaa Valley in 1982 did U.S. military planners become convinced of the tactical usefulness on non-lethal UAV's [Ref. 12].

Recognizing the need for common and interoperable systems, Congress in 1988 directed the Department of Defense (DoD) to consolidate the management of non-lethal UAV programs. The DoD established the UAV Joint Project Office (UAV JPO) and appointed the United States Navy as the executive service. The mission of the Joint Program Office is to expeditiously field quality UAV systems which provide a significant tactical advantage to operational commanders. The objective of the UAV

JPO is to field a family of interoperable systems that optimize commonality [Ref. 13:p. 7].

During Operation Desert Storm, UAV's provided tactical commanders an operational capability that was not previously available. The Marines operated three types of UAV's in various mission roles that included real time reconnaissance, surveillance, target acquisition, spotting and bomb damage assessment. When operation of the Pioneer UAV was jeopardized by parts shortages and while the more fragile Pointer was unable to fly in winds greater than 15 knots, the Marine Corps augmented their UAV operations by reassigning a number of EXDRONE's from a research and development program to be operationally deployed from airfields near the Saudi Arabia-Kuwait border [Ref. 14]. These vehicles were reequipped with color video cameras and were used to find attack routes through enemy defenses.

This demonstrated capability of UAV's to perform multiple functions and the ability to provide near real-time intelligence in a high-threat environment without loss of life has affirmed the commitment by the Services to integrate UAV's into the force structure. The 1992 DoD Unmanned Aerial Vehicles Master Plan [Ref. 13] indicates that the planned procurement of UAV's is in excess of 2300 vehicles. The core strategy of the UAV JPO is the establishment of a family of UAV systems which indicates that these systems must allow for growth in performance and must readily accommodate changing

payloads. As a part of this core strategy the JPO has initiated a Very Low Cost (VLC) UAV program. These VLC systems are used to demonstrate and evaluate the utility of UAV's in tactical units.

In November 1991, the UAV JPO awarded a contract to BAI Aerosystems, Inc. for the production of 110 EXDRONES. At the present time, operational test and production for the Marine Corps Jammer program is not funded and the EXDRONE vehicles are being used in the JPO VLC program [Ref. 13:p. 49]. If the production option in the BAI contract is exercised, it is expected that as a result of the VLC program a new effort to improve range and payload capacity will begin. Having accurate estimates of stability and control derivatives will allow designers to incorporate good flying qualities from the earliest stages of design and avoid repeating errors from earlier versions of the model.

B. PARAMETER ESTIMATION

In Reference 15 Ljung points out that the construction of a model from observed data involves three basic entities:

1) The data record.

2) The set of candidate models.

3) A rule by which candidate models can be assessed using the data.

In an application to aircraft stability and control, the flight test maneuvers should be designed so that the data collected will provide the maximum value to the analyst. Consequently it essential that the flight test program have a clear set of objectives so that the flight test maneuver will cover the area of the envelope that is to be explored. Instrumentation must be considered so that the appropriate parameters are measured to a degree of accuracy that will be suitable to the objectives of the program. The set of candidate models must also be considered. The equations of motion derived from analysis of forces and moments acting on a typical aircraft are well defined. For most applications a linearized set of the equations is adequate for analyzing aircraft stability and control. If a linear model is all that is available for the analysis, then only small- perturbation maneuvers should be included in the flight test. If envelope expansion is the objective of the flight test, then maneuvers that gradually expand the envelope may provide data that indicate a non-linear model is necessary. The rule by which the models are assessed is generally determined by how well the model is able to reproduce the measured data. For example, the modified maximum likelihood program uses an output-error approach that minimizes the difference between the measured parameters and the model estimate of the parameters in successive iterations. This construction of a mathematical model of a dynamic system from observed data is

know as System Identification [Ref. 15:p. 1].

Estimation of aircraft stability and control derivatives from flight test time history data is one of many practical applications of the basic system identification techniques. Of particular note in the aeronautics industry is the work of Lawrence Taylor, Kenneth Iliff, Richard Maine and James Murray of the NASA Ames Research Center, Dryden Flight Research Facility. Their approach to the estimation of aircraft stability and control derivatives through the application of system identification techniques can be found in References 9, 17 and 18. The method of application can be summerized in the following steps:

1) Formulate the dynamic equations that describe the model.

2) Identify from the form of the dimensional derivatives the parameters whose values are unknown.

3) Collect flight test data.

4) Infer the values of the unknown parameters by adjusting the values iteratively until the computed response best matches the measured response.

Throughout the 1980's the most widely accepted aircraft parameter estimation routine was the Modified Maximum Likelihood, version 3, written by Iliff and Maine. The MMLE-3 program evolved from an earlier Newton-Raphson parameter estimation routine by Taylor and Iliff when a more versatile program capable of handling larger amounts of data was required by the industry. When applying system identification

techniques to a real world system, modeling errors are unavoidable since it is likely that the real system does not completely satisfy all of the assumptions on which the model was developed. The existence of unmeasured inputs along with these modeling imperfections perturb the states and to at least some degree invalidate the results of the identification algorithms [Ref. 15]. The advantage of MMLE-3 is that the algorithm is capable of applying the system identification techniques in the presence of state noise and thus produces a more optimistic error bound estimate. Full details of the MMLE-3 program can be found in References 17 and 19. The minimization routines and the criterion used in a personal computer based adaptation of MMLE-3 are discussed in more detail in later sections.

For many aircraft applications the linearized equations of motion provide a reasonably accurate model of the system for small disturbances. For some applications however, the linear model is not sufficient and a more accurate non-linear model is required. Flight testing at the Dryden Flight Research Facility highlighted the limitations of the linear model when applied to maneuvers at extreme flight conditions and with some unique aircraft configurations that exhibited non-linear dynamic behavior. In 1987 Murray and Maine introduced a program for parameter estimation in non-linear dynamic systems. The capabilities of the pEst program are described in Reference 9.

Historically the wind tunnel has served as the primary source of aeronautical data for flight vehicles. The advantage of the wind tunnel is that flow conditions can be accurately controlled, but other influences such as wall interference are difficult to account for. The wind tunnel is also limited in its ability to achieve dynamic similarity with actual flight test conditions. There are numerous reasons why wind tunnel data alone are not sufficient and often the results are validated by flight test. In Reference 18, Maine and Iliff point out that there is a tendency in practice to emphasize positive results and to down play the role of flight test in validating wind tunnel data or analytical predictions. A discussion of the errors that are found and corrected because of the flight test are often omitted from the published reports. Maine and Iliff go on to say that the utility of stability and control parameter estimation can best be evaluated by comparing the predicted data prior to the first flight test with the best estimates from combined flight data and predictions at the conclusion of the flight test program [Ref. 18:p. 4]. The task then is to take maximum advantage of previous information, both analytical and experimental, and to use the estimation routines to fill the gaps. The parameter estimation routines used in this study use a-priori knowledge of the system under investigation to provide to the user the most accurate estimates of aircraft stability and control derivatives.

III. DEVELOPMENT OF THE MATHEMATICAL MODEL

The analysis of a dynamic system begins with the derivation of a mathematical model that is reasonably accurate. Typically the mathematical model is a set of differential equations obtained by the application of physical laws that govern the system. The response of the system to a given input may then be obtained by solving the differential equations.

Development of the equations of motion begins with an application of Newton's second law to a rigid body in a non-rotating inertial-axis system. Motivation is given to make the transformation to a rotating, body-axis reference system. Euler angles are introduced and developed in some detail as a means of referencing body axes to the inertial axes. Finally a brief description of the aerodynamic model is presented in the form of non-dimensional force and moment equations.

A. APPLICATION OF PHYSICAL LAWS

Newton's second law states that the acceleration of an object is proportional to the net force exerted on the object. This law leads directly to the fundamental concepts of the conservation of linear momentum and the conservation of angular momentum [Ref. 20:p. 143]. In a non-rotating inertial reference frame the conservation laws can be expressed in

terms of the vector equations:

$$\sum \boldsymbol{F} = \frac{d}{dt}(m\boldsymbol{v}) \tag{1}$$

$$\sum \boldsymbol{M} = \frac{d}{dt}(\boldsymbol{H}) \tag{2}$$

These equations state that the summation of vector forces (F) acting on a body is equal to the time rate of change of linear momentum (mv) and the summation of external moments (M) acting on a body is equal to the time rate of change of angular momentum (H).

The externally-applied aerodynamic forces and moments acting on an airframe are due primarily to airflow conditions and control-surface deflections. The force and moment equations can be broken down into vector components along the longitudinal (x), lateral (y) and vertical axis (z) of the body with respective velocity components u,v and w.

$$F_x = \frac{d}{dt}(mu) \quad F_y = \frac{d}{dt}(mv) \quad F_z = \frac{d}{dt}(mw) \tag{3}$$

$$L = \frac{d}{dt}H_x \quad M = \frac{d}{dt}H_y \quad N = \frac{d}{dt}H_z \tag{4}$$

Figure 1 illustrates the convention for the forces and moments in a body-fixed reference frame about the center of gravity. The components of the velocity vector **V** are u, v and w aligned

along the x, y and z axes respectively. The moments due to aerodynamic forces are L, M and N.

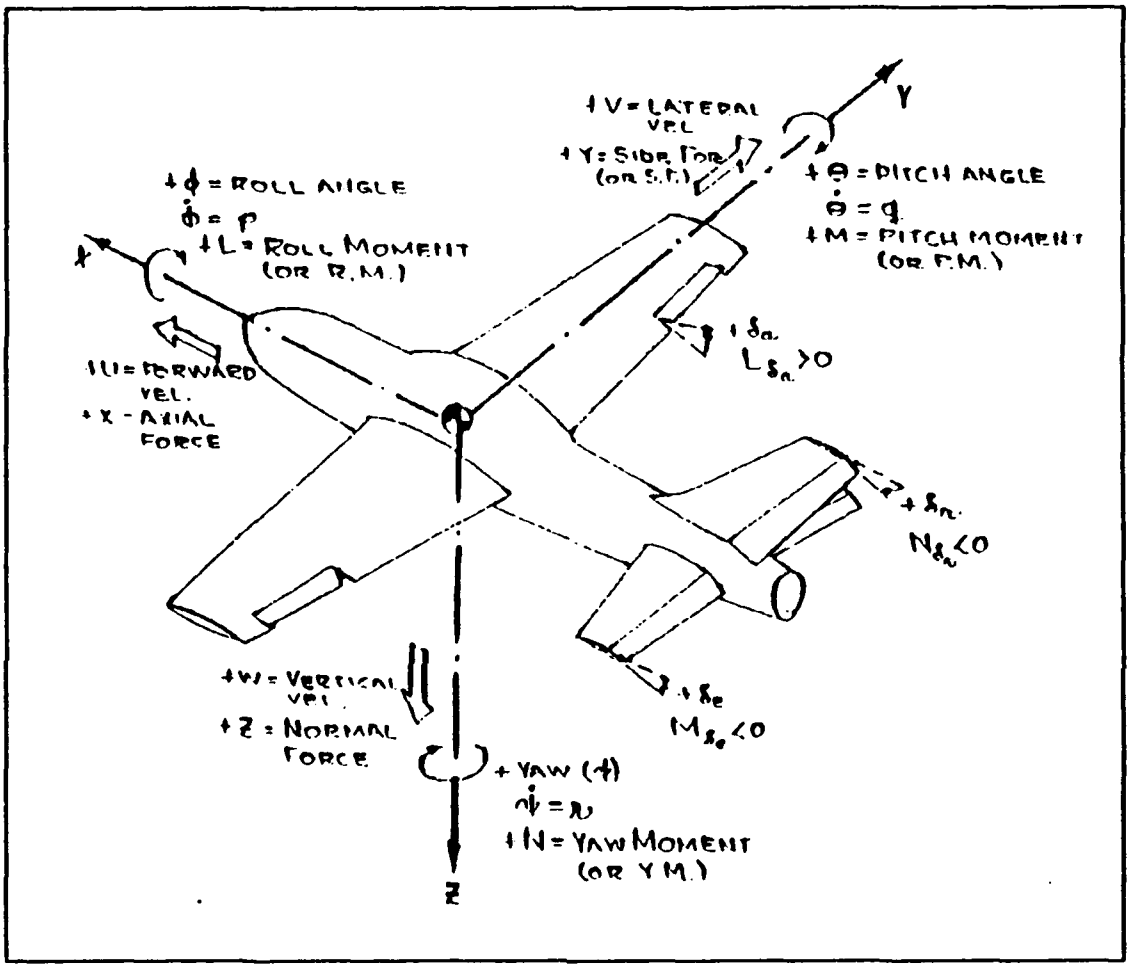

Figure 1 Force and Moment Conventions

References 21 and 22 detail the development of the moment equations referred to a moving center of mass. The result is a vector expression for angular momentum in component form given by:

$$\begin{bmatrix} H_x \\ H_y \\ H_z \end{bmatrix} = \int_{vol} \left(\begin{bmatrix} p(y^2+z^2) \\ q(x^2+z^2) \\ r(x^2+y^2) \end{bmatrix} - \begin{bmatrix} q(xy)+r(xz) \\ p(xy)+r(yz) \\ p(xz)+q(yz) \end{bmatrix} \right) dm \qquad (5)$$

The expression for the angular momentum may then be written as:

$$\boldsymbol{H} = [I_m]\ \boldsymbol{\Omega} \qquad (6)$$

where the vector Ω contains the components of angular velocity p, q and r. The matrix $[I_m]$ is a symmetric matrix of the moments and products of inertia which can be expressed by:

$$[I_m] = \begin{bmatrix} I_x & -I_{xy} & -I_{xz} \\ -I_{xy} & I_y & -I_{xz} \\ -I_{xz} & -I_{yz} & I_z \end{bmatrix} \qquad (7)$$

with components:

$$\begin{aligned} I_x &= \int_v (y^2+z^2)\, dm & I_{xy} &= \int_v (xy)\, dm \\ I_y &= \int_v (x^2+z^2)\, dm & I_{xz} &= \int_v (xz)\, dm \\ I_z &= \int_v (x^2+y^2)\, dm & I_{yz} &= \int_v (yz)\, dm \end{aligned} \qquad (8)$$

With the inertia matrix and angular velocity vector defined, equation (2) can be rewritten as:

$$\sum \boldsymbol{M} = \frac{d}{dt}\boldsymbol{H} = (\boldsymbol{\Omega})\ \frac{d}{dt}[I_m] + [I_m]\frac{d}{dt}\ (\boldsymbol{\Omega}) \qquad (9)$$

Equation (9) indicates that in a fixed reference frame, if the

airframe rotates then the matrix I_m will vary with time. By making the transformation to a rotating coordinate system that is fixed to the airframe, the inertia matrix becomes time invariant and the analysis becomes much simpler [Ref 21].

In making the transformation from the inertial reference to the rotating body reference, the vector equations for **F** and **M** can be expressed as:

$$\boldsymbol{F} = m\frac{d}{dt}(\boldsymbol{v}) + \boldsymbol{\Omega} \times (m\boldsymbol{v}) \tag{10}$$

$$\boldsymbol{M} = \frac{d}{dt}(\boldsymbol{H}) + \boldsymbol{\Omega} \times \boldsymbol{H} \tag{11}$$

The above expressions in terms of the body-axis system assume a constant mass since the mass of the aircraft is not expected to change significantly in the short time during which data are collected. The components of the vector equations (10) and (11) are written as:

$$\begin{aligned} F_x &= m(\dot{u} + qw - rv) \\ F_y &= m(\dot{v} + ru - pw) \\ F_z &= m(\dot{w} + pv - qu) \end{aligned} \tag{12}$$

$$L = \dot{p}I_x - \dot{q}I_{xy} - \dot{r}I_{xz} + qr(I_z - I_y) + (r^2 - q^2)I_{yz} - pqI_{xz} + rpI_{xy}$$
$$M = -\dot{p}I_{xy} + \dot{q}I_y - \dot{r}I_{yz} + rp(I_x - I_z) + (p^2 - r^2)I_{xz} - qrI_{xy} + pqI_{yz} \quad (13)$$
$$N = -\dot{p}I_{xz} - \dot{q}I_{yz} + \dot{r}I_z + pq(I_y - I_x) + (q^2 - p^2)I_{xy} - rpI_{yz} + qrI_{xz}$$

B. EULER ANGLES

The development in the previous section led to a set of six equations of motion derived for a reference system that is fixed to the airframe. Since the position and orientation of the airframe cannot be described relative to its moving reference frame, it is necessary to develop a way of defining the aircraft attitude relative to the earth. The angles that define the rotations that transform the orientation of the body frame to the earth-fixed inertial frame are called the Euler angles [Ref. 22:p. 88].

The transformation begins by aligning the body-axis system with the inertial system (Figure 2). Looking down the Z axis into the X_1Y_1 plane, a vector **R** in that plane can be resolved into x_1 and y_1 components.

$$R = x_1\hat{x} + y_1\hat{y} \quad (14)$$

Rotate an angle Ψ about the Z axis to define a new coordinate plane X_2Y_2. The same resultant vector **R** can be expressed in terms of the components of the new coordinate system.

$$R = x_2\hat{x} + y_2\hat{y} \tag{15}$$

where

$$\begin{aligned} x_2 &= x_1\cos\Psi + y_1\sin\Psi \\ y_2 &= y_1\cos\Psi - x_1\sin\Psi \\ z_2 &= z_1 \end{aligned} \tag{16}$$

In matrix form the new coordinate system can be expressed as a product of the transformation matrix T_Ψ and the vector containing components x_1, y_1 and z_1.

$$\begin{bmatrix} x_2 \\ y_2 \\ z_2 \end{bmatrix} = \begin{bmatrix} \cos\Psi & \sin\Psi & 0 \\ -\sin\Psi & \cos\Psi & 0 \\ 0 & 0 & 1 \end{bmatrix} \begin{bmatrix} x_1 \\ y_1 \\ z_1 \end{bmatrix} \tag{17}$$

With the coordinate system now aligned with the X_2, Y_2, Z_2 coordinate system, the same procedure is applied by looking down the Y_2 axis into the X_2Z_2 plane and observing the **R** vector in terms of components x_2 and z_2 . Rotate an angle Θ about the Y_2 axis to form a new coordinate system X_3, Y_3, Z_3. The vector **R** can now be expressed in terms of components x_3, y_3, z_3 by:

$$R = x_3\hat{x} + z_3\hat{z} \tag{18}$$

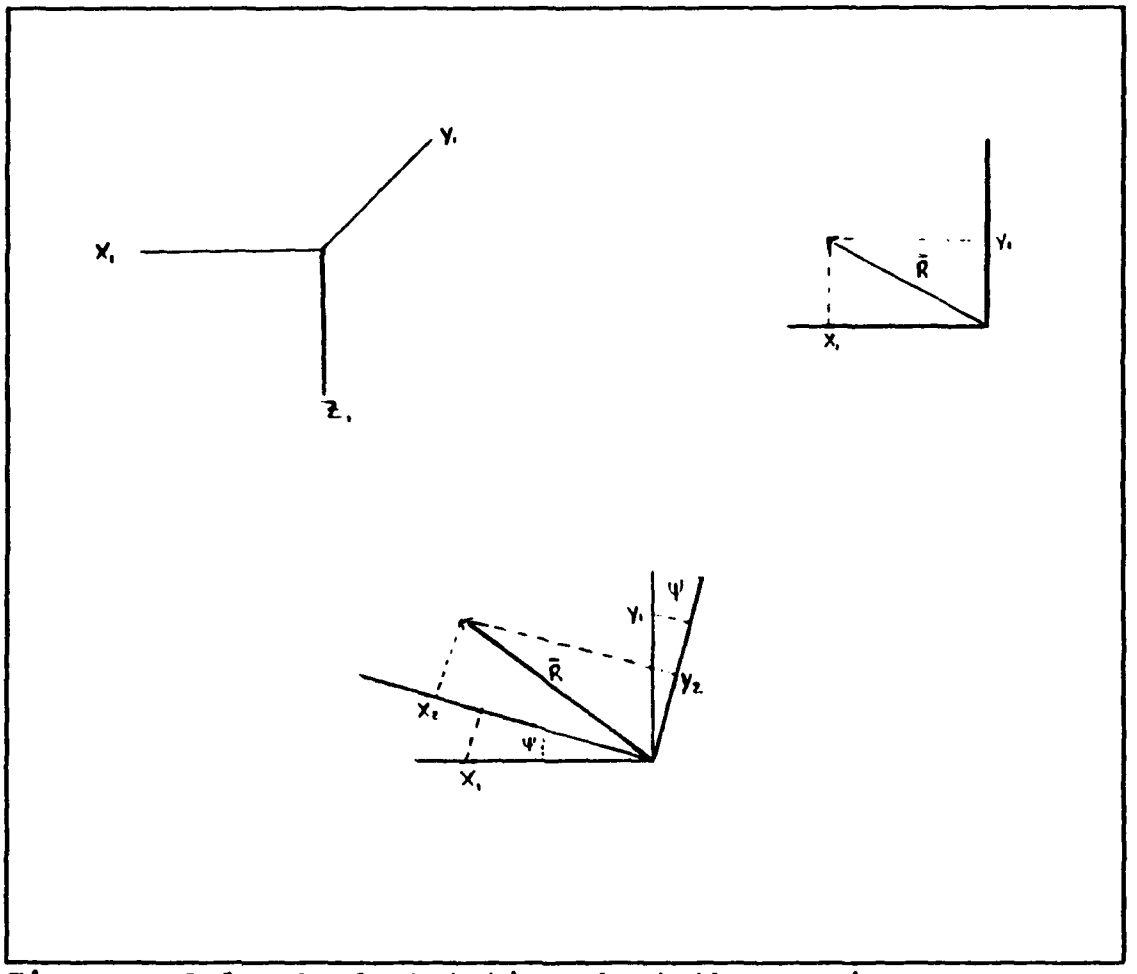

Figure 2 Euler Angle Rotation About the Z axis

where in matrix form the new vector is a product of the transformation matrix T_θ and the vector in the x_2, y_2, z_2 system.

$$\begin{bmatrix} x_3 \\ y_3 \\ z_3 \end{bmatrix} = \begin{bmatrix} \cos\theta & 0 & -\sin\theta \\ 0 & 1 & 0 \\ \sin\theta & 0 & \cos\theta \end{bmatrix} \begin{bmatrix} x_2 \\ y_2 \\ z_2 \end{bmatrix} \qquad (19)$$

A similar procedure is applied to the X_3, Y_3, Z_3 coordinate system by rotating an angle ϕ about the X_3 axis. The

transformation matrix T_Φ is found to be:

$$T_\Phi = \begin{bmatrix} 1 & 0 & 0 \\ 0 & \cos\Phi & \sin\Phi \\ 0 & -\sin\Phi & \cos\Phi \end{bmatrix} \tag{20}$$

A complete transformation from the body axes to the inertial axes by three successive rotations about the Euler angles Ψ, Θ and Φ leads to the expression:

$$X_b = T_\Phi T_\Theta T_\Psi X_i \tag{21}$$

where X_b is a vector of components in the body-axes system and X_i is a vector of components in the inertial-axes system. Figure 3 shows the earth-fixed axis relative to the body- axis system with the three successive rotations about the angles Ψ, Θ and Φ.

Using the relationship in equation 3.21, the inertial velocities can be expressed in terms of the Euler angles and the components of velocity in the body-axis frame. The shorthand notation of References 21 and 22 where C_Θ represents Cos Θ gives:

$$\begin{bmatrix} \dot{x} \\ \dot{y} \\ \dot{z} \end{bmatrix} = \begin{bmatrix} C_\Theta C_\Psi & S_\Phi S_\Theta C_\Psi - C_\Phi S_\Psi & C_\Phi S_\Theta C_\Psi + S_\Phi S_\Psi \\ C_\Theta S_\Psi & S_\Phi S_\Theta S_\Psi - C_\Phi C_\Psi & C_\Phi S_\Theta S_\Psi - S_\Phi C_\Psi \\ -S_\Theta & S_\Phi C_\Theta & C_\Phi C_\Theta \end{bmatrix} \begin{bmatrix} u \\ v \\ w \end{bmatrix} \tag{22}$$

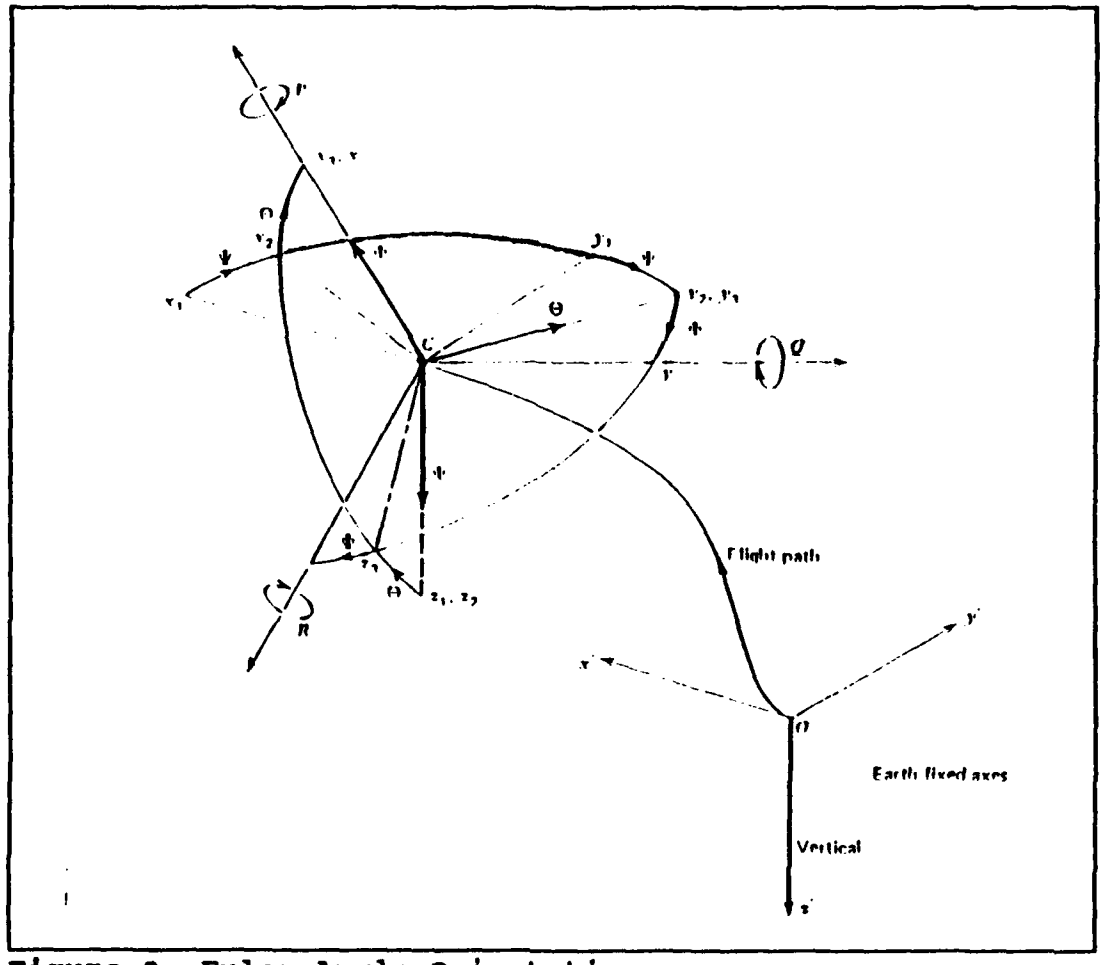

Figure 3 Euler Angle Orientation

The angular rotation rate vector Ω has body-axis components p, q and r where p is the roll rate about the longitudinal axis, q is the pitch rate about the lateral axis and r is the yaw rate about the vertical axis. Using the relationships of the transformation matrices T_ϕ, T_θ and T_ψ given above, the body-axis components of the angular rotation rate vector Ω can be expressed in terms of the Euler-angle rates by:

$$\begin{bmatrix} p \\ q \\ r \end{bmatrix} = \begin{bmatrix} 1 & 0 & -S_\Theta \\ 0 & C_\Phi & S_\Phi C_\Theta \\ 0 & -S_\Phi & C_\Phi C_\Theta \end{bmatrix} \begin{bmatrix} \dot{\Phi} \\ \dot{\Theta} \\ \dot{\Psi} \end{bmatrix} \tag{23}$$

Inverting equation (23) gives the Euler-angle rates in terms of the body-axis rotation rates:

$$\begin{bmatrix} \dot{\Phi} \\ \dot{\Theta} \\ \dot{\Psi} \end{bmatrix} = \begin{bmatrix} 1 & Sin\Phi Tan\Theta & Cos\Phi Tan\Theta \\ 0 & Cos\Phi & -Sin\Phi \\ 0 & Sin\Phi Sec\Theta & Cos\Phi Sec\Theta \end{bmatrix} \begin{bmatrix} p \\ q \\ r \end{bmatrix} \tag{24}$$

C. FORCE AND MOMENT EQUATIONS

The applied forces on the aircraft can be expressed in terms of aerodynamic, gravitational and thrust components. The forces acting on the body of the aircraft relative to the earth are:

$$\begin{aligned} F_x &= \bar{q}sC_x - mgSin\Theta + T \\ F_y &= \bar{q}sC_y + mgSin\Phi Cos\Theta \\ F_z &= \bar{q}sC_z + mgCos\Phi Cos\Theta \end{aligned} \tag{25}$$

where q-bar is the dynamic pressure, s is the reference area, C_x, C_y, C_z are the force coefficients relative to the aircraft state and T is thrust.

The gyroscopic moment due to rotating parts in the engine is ignored and the aerodynamic moments are given by:

$$M_x = \bar{q}scC_l$$
$$M_y = \bar{q}scC_m \qquad (26)$$
$$M_z = \bar{q}scC_n$$

where C_l, C_m and C_n are non-dimensional coefficients of roll, pitch and yaw moments.

D. STABILITY AND WIND AXES

For stability and control analysis it is more convenient to consider the velocity of the aircraft relative to the air [Ref 18:p 8]. Also it is more practical to express equations in terms of angle of attack, α and sideslip angle, ß since these angles are measured directly during wind tunnel testing and flight testing. Angle of attack and sideslip are defined by:

$$\alpha = \tan^{-1}\frac{w}{u} \qquad \beta = \sin^{-1}\frac{v}{V} \qquad (27)$$

where V is the total wind-relative velocity with magnitude given by:

$$V = \sqrt{u^2 + v^2 + w^2} \qquad (28)$$

From Figure 4 the component velocities can be expressed in terms of the angle rotations through alpha and beta and the total wind-relative velocity V by the following process. Rotate about the w axis by an angle ß:

$$\begin{bmatrix} u_2 \\ v_2 \\ w_2 \end{bmatrix} = \begin{bmatrix} C\beta & -S\beta & 0 \\ S\beta & C\beta & 0 \\ 0 & 0 & 1 \end{bmatrix} \begin{bmatrix} u_1 \\ v_1 \\ w_1 \end{bmatrix} \tag{29}$$

Rotate down about the v axis by an angle α:

$$\begin{bmatrix} u_3 \\ v_3 \\ w_3 \end{bmatrix} = \begin{bmatrix} C\alpha & 0 & -S\alpha \\ 0 & 1 & 0 \\ S\alpha & 0 & C\alpha \end{bmatrix} \begin{bmatrix} u_2 \\ v_2 \\ w_2 \end{bmatrix} \tag{30}$$

The component velocities can then be expressed by:

$$\begin{bmatrix} u \\ v \\ w \end{bmatrix} = T_\alpha T_\beta \begin{bmatrix} V \\ 0 \\ 0 \end{bmatrix} \tag{31}$$

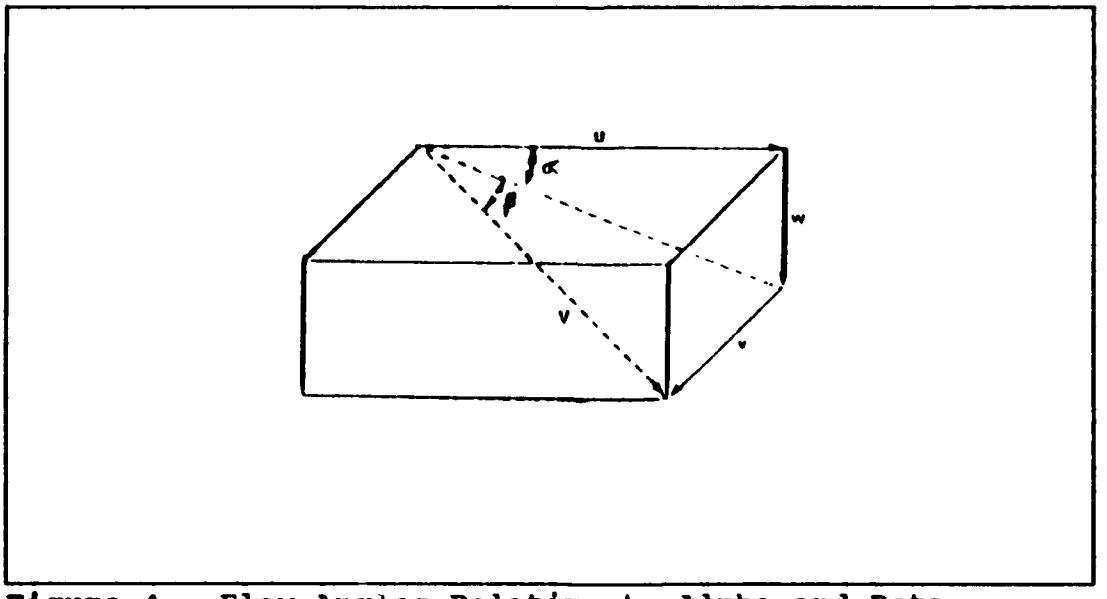

Figure 4 Flow Angles Relative to Alpha and Beta

Through a similar application of the angle relationships the axial forces can be expressed in terms of the non-dimensional coefficients C_D and C_L and related to the stability axes and the wind axes by a transformation matrix.

$$\begin{bmatrix} C_L \\ C_D \end{bmatrix} = \begin{bmatrix} S\alpha & -C\alpha \\ -C\alpha & -S\alpha \end{bmatrix} \begin{bmatrix} C_x \\ C_z \end{bmatrix} \tag{32}$$

$$\begin{bmatrix} C_{D_{wind}} \\ C_{Y_{wind}} \end{bmatrix} = \begin{bmatrix} C\beta & -S\beta \\ S\beta & C\beta \end{bmatrix} \begin{bmatrix} C_D \\ C_Y \end{bmatrix} \tag{33}$$

E. BODY AXIS EQUATIONS OF MOTION

Constructing the body-axis, six-degree-of-freedom equations of motion begins by differentiating equations (27) and (28) to obtain expressions for the time derivatives of V, alpha and beta. Equating equations (12) and (25) yields:

$$\begin{aligned} \dot{u} &= \frac{\bar{q}s}{m} C_x - qw + rv - g\sin\Theta + \frac{T}{m} \\ \dot{v} &= \frac{\bar{q}s}{m} C_y - ru + pw + g\sin\Phi\cos\Theta \\ \dot{w} &= \frac{\bar{q}s}{m} C_z - pv + qu + g\cos\Phi\cos\Theta \end{aligned} \tag{34}$$

Substitute equation (31) for u, v, and w and equation (34) for the time derivatives of u, v, and w. Use equations (32) and (33) to substitute in for the force coefficients Fx, Fy and Fz. The construction is completed by substituting equation

(33) to substitute in for the force coefficients Fx, Fy and Fz. The construction is completed by substituting equation (26) into equation (13). The resulting nine equations can then be expressed as:

$$\dot{V} = -\frac{\bar{q}s}{m} C_{D_{wind}} + g(\cos\Phi\cos\Theta\sin\alpha\cos\beta + \sin\Phi\cos\Theta\sin\beta - \sin\Theta\cos\alpha\cos\beta) - \frac{T}{m}\cos\alpha\cos\beta \tag{35}$$

$$\dot{\alpha} = -\frac{\bar{q}s}{mV\cos\beta} C_L + q - (\tan\beta)(p\cos\alpha + r\sin\alpha) + \frac{g}{V\cos\beta}(\cos\Phi\cos\Theta\cos\alpha + \sin\Theta\sin\alpha) - \frac{T\sin\alpha}{mV\cos\beta} \tag{36}$$

$$\dot{\beta} = \frac{\bar{q}s}{mV} C_{Y_{wind}} + p\sin\alpha - r\cos\alpha + \frac{g}{V}\cos\beta\sin\Phi\cos\Theta + \frac{\sin\beta}{V}(g\cos\alpha\sin\Theta - g\sin\alpha\cos\Phi\cos\Theta + \frac{T}{m}\cos\alpha) \tag{37}$$

$$\dot{p}I_x - \dot{q}I_{xy} - \dot{r}I_{xz} = \bar{q}sbC_l + qr(I_y - I_z) + (q^2 - r^2)I_{yz} + pqI_{xz} - rpI_{xy} \tag{38}$$

$$-\dot{p}I_{xy} + \dot{q}I_y - \dot{r}I_{yz} = \bar{q}scC_m + rp(I_z - I_x) + (r^2 - p^2)I_{xz} + qrI_{xy} - pqI_{yz} \tag{39}$$

$$-\dot{p}I_{xz} - \dot{q}I_{yz} + \dot{r}I_z = \bar{q}sbC_n + pq(I_x - I_y) + (p^2 - q^2)I_{xy} + rpI_{yz} - qrI_{xz} \tag{40}$$

$$\dot{\Phi} = p + q\tan\Theta\sin\Phi + r\tan\Theta\cos\Phi \tag{41}$$

$$\dot{\Theta} = q\cos\Phi - r\sin\Phi \tag{42}$$

$$\Psi = r\cos\Phi\sec\Theta + q\sin\Phi\sec\Theta \qquad (43)$$

The nine equations listed above are valid for a rigid vehicle in a constant wind with the following assumptions.

1) Flat, non-rotating earth
2) Constant mass
3) Thrust vector along the X axis
4) Body axis referenced to the aircraft center of gravity

Singularities occur at $\Theta = \pm 90$ degrees, $\beta = \pm 90$ degrees and at zero velocity.

F. AERODYNAMIC MODEL

Equations (12) and (25) can be combined to give a representation of the forces acting on the aircraft. Changes in the forces from a given reference condition can be represented by a Taylor series expansion as a function of the motion variables. In the development of the aerodynamic model, it is assumed that any change in the longitudinal force is a function of angle of attack, pitch rate and longitudinal control. Changes in the longitudinal forces and moment can then be represented by:

$$\begin{aligned}
\Delta X &= \frac{\partial x}{\partial u}\Delta u + \frac{\partial x}{\partial w}\Delta w + \frac{\partial x}{\partial \delta_e}\Delta\delta_e \\
\Delta Z &= \frac{\partial z}{\partial u}\Delta u + \frac{\partial z}{\partial w}\Delta w + \frac{\partial z}{\partial \dot{w}}\Delta\dot{w} \\
\Delta M &= \frac{\partial M}{\partial u}\Delta u + \frac{\partial M}{\partial w}\Delta w + \frac{\partial M}{\partial \dot{w}}\Delta\dot{w} + \frac{\partial M}{\partial q}\Delta q + \frac{\partial M}{\partial \delta_e}\Delta\delta_e
\end{aligned} \qquad (44)$$

Likewise it is assumed that the lateral-directional aerodynamic forces and moments are functions only of sideslip angle, roll rate, yaw rate and lateral-directional control-surface changes. Expansions for ΔY, ΔL and ΔN can then be expressed in terms of the motion variables Δv, Δp, Δp, Δr and $\Delta\delta$ by:

$$\begin{aligned}
\Delta Y &= \frac{\partial Y}{\partial v}\Delta v + \frac{\partial Y}{\partial p}\Delta p + \frac{\partial Y}{\partial r}\Delta r + \frac{\partial Y}{\partial \delta_r}\Delta\delta_r \\
\Delta L &= \frac{\partial L}{\partial v}\Delta v + \frac{\partial L}{\partial p}\Delta p + \frac{\partial L}{\partial r}\Delta r + \frac{\partial L}{\partial \delta_r}\Delta\delta_r + \frac{\partial L}{\partial \delta_a}\Delta\delta_a \\
\Delta N &= \frac{\partial N}{\partial v}\Delta v + \frac{\partial N}{\partial p}\Delta p + \frac{\partial N}{\partial r}\Delta r + \frac{\partial N}{\partial \delta_r}\Delta\delta_r + \frac{\partial N}{\partial \delta_a}\Delta\delta_a
\end{aligned} \qquad (45)$$

In equations (44) and (45) a conventional three-axis control system consisting of aileron, rudder and elevator is assumed. Additional control terms may be added for non-conventional configurations. Reference 23, Chapter IV clarifies the significance of each of the derivative terms in the expansions and explains the physical significance by relating the longitudinal and lateral-directional forces and moments to the aerodynamic derivatives and motion variables.

Stability and control derivatives in dimensional form are convenient for application of modern control theory methods when solving flight dynamic problems. References 21 and 22 use the dimensional form in the development of the state-space

model. The non-dimensional coefficients, however, provide a convenient means of accounting for aircraft speed and size, and for air density since they are insensitive to dynamic pressure over large ranges [Ref. 24:p. 113]. Table 1 summarizes the longitudinal stability and control derivatives in terms of non-dimensional coefficients and Table 2 summarizes the lateral-directional stability and control derivatives. The derivatives represent the change in an aerodynamic force or moment coefficient due to a change in state or control input.

TABLE 1 LONGITUDINAL STATES AND DERIVATIVES

Longitudinal Stability and Control Derivatives		
State or Control	Normal Force	Pitch Moment
Angle of Attack	CL_{α}	Cm_{α}
Pitch Rate	CLq	Cm_{q}
Elevator Control	$CL_{\delta e}$	$Cm_{\delta e}$

TABLE 2 LATERAL-DIRECTIONAL STATES AND DERIVATIVES

Lateral-Directional Derivatives			
State or Control	Side Force	Roll Moment	Yaw Moment
Sideslip	CY_{β}	Cl_{β}	Cn_{β}
Roll Rate	CY_{p}	Cl_{p}	Cn_{p}
Yaw Rate	CY_{r}	Cl_{r}	Cn_{r}
Aileron Control	$CY_{\delta a}$	$Cl_{\delta a}$	$Cn_{\delta a}$
Rudder Control	$CY_{\delta r}$	$Cl_{\delta r}$	$Cn_{\delta r}$

IV. MAXIMUM LIKELIHOOD ESTIMATION

A. ESTIMATION THEORY

The problem of obtaining unknown aircraft stability and control derivatives through parameter estimation techniques is theoretically straight forward. In the previous chapter it was emphasized that the most important part of this analysis is deriving a reasonable mathematical model that consists of a set of dynamic equations that contains the unknown parameters. The system can then be excited by a pre-determined input specifically designed so that the response of the system will allow the values of the parameters to be determined. The system response to the pre-determined input is measured. Values of the parameters are then determined by the constraint that the computed response of the model match the measured response of the system. This deterministic approach to parameter identification is complicated by the presence of other elements such as process noise and measurement noise that must be considered in real-world systems.

The mathematical model derived in the previous chapter is based on the physical laws that govern the system and is considered to be well defined. In deriving any model of a physical system it is necessary to make some compromise

between simplicity and accuracy. A model that is too complicated will require a higher expenditure of resources and a model that is too simple will not have sufficient accuracy to be useful. The objective is to define a mathematical model that represents the essential aspects of the physical system and will provide reasonably accurate predictions of the dynamic behavior [Ref. 21:p. 67]. The term "reasonably accurate" implies that modeling errors are inevitable. In Reference 17 Maine and Iliff state:

> There is no comprehensive theory of modeling error available. Any modeling error is simply treated as state and/or measurement noise, in spite of the fact that the modeling error may be deterministic rather than random. This procedure has not been rigorously justified, but combined with careful choice of the model, is probably the best approach available.

These unavoidable modeling errors are intentionally accepted in an effort to produce a simplified but practically useful simulation.

The presence of both measurement noise and state noise changes the nature of the problem from a deterministic process to a stochastic process. Measurement noise arises from the realization that the system response cannot be perfectly measured and sensor inaccuracies are certain. State noise is random excitation of the system from external, unmeasured sources. The noise is a disturbance that acts uninterruptedly upon the system making it impossible to predict exactly how the system will behave. Consequently the unknown parameters must be estimated by some statistical criterion [Ref 17:p 8].

The real value of the MMLE3 program is that the algorithm accounts for both state and measurement noise.

B. MODIFIED MAXIMUM LIKELIHOOD VERSION THREE

1. General System Model

In the Modified Maximum Likelihood Estimation (MMLE3) method it is assumed that for the correct values of the unknown parameters, the system is correctly described by the dynamic model developed in the previous chapter. The model can be expressed in state-space format as a function of the states, inputs and unknown parameters represented by $\mathbf{x}$, $\mathbf{u}$ and ξ respectively. The discretized model in state-space form is:

$$\mathbf{x}_{k+1} = A_k \mathbf{x}_k + B_k \mathbf{u}_k + \boldsymbol{\omega}_k \tag{46}$$

where the plant matrix A and the control matrix B contain values of the unknown parameters and ω is the state noise vector. The initial condition is given by:

$$x(t_0) = x_0 \tag{47}$$

Measurements are assumed to be made at discrete time intervals. The measurement equation is:

$$z_k = C x_k + v_k \tag{48}$$

The matrix C is the measurement matrix and v_k is the measurement noise vector. The state noise, ω, and the measurement noise, v_k, are assumed to be zero mean and uncorrelated [Ref. 25:p. 3]. In the presence of white noise the estimation is a stochastic process. For each estimate of the unknown parameters in the vector ξ, there is associated with the estimate a probability that the values in the response history are close to the measured values. The maximum likelihood estimates are the estimates that maximize that probability.

2. Kalman Estimator

A Kalman estimator is used to provide estimates for the states while minimizing the effects of the process and measurement noise. The difference between the measured value and the Kalman estimate at a given time, t(i), is called the residual and is given by:

$$\left[z_k - \tilde{z}_{\xi_k}\right] \tag{49}$$

The subscript ξ indicates that the estimate is a function of the unknown parameters. To maximize the probability that the computed time history is close to the measured time history it is necessary to minimize the criterion given by [Ref 25:p 3]:

$$J(\xi) = \frac{1}{2}\sum_{i=1}^{N}\left[z(t_i) - \tilde{z}_{\xi}(t_i)\right]^T R^{-1}\left[z(t_i) - \tilde{z}_{\xi}(t_i)\right] + \frac{N}{2}\ln|R| \tag{50}$$

Where R is the innovations co-variance matrix. From equation (50) it can be seen that the effect of the state and measurement noise is only to increase the value associated with the criterion $J(\xi)$.

The discrete, stochastic estimation is a recursive process that makes an estimate after each measurement. The new estimate depends upon the prior estimate and the new measurement. In terms of a Kalman estimator equation, the prediction and correction steps can be written as:

$$\begin{aligned} \tilde{x}_k &= A_k \hat{x}_k + B_k u_k \\ \hat{x}_k &= \tilde{x}_k + \dot{K}\left[z_k - \tilde{z}_k\right] \end{aligned} \tag{51}$$

Equation (51) states simply that the corrected value is equal to the old estimate plus a confidence factor times the residual. The gain or confidence factor is chosen by solution of the Riccati equation such that the errors associated with the states are driven towards the convergence criterion as quickly as possible. MMLE3 uses only the steady state solution of the Riccati equation. A complete explanation of the discrete, stochastic process can be found in Chapter 6 of Reference 27.

3. Cramer-Rao Bounds

In any stochastic process some measure of accuracy is necessary. In the MMLE3 estimator the Cramer-Rao bound is a measure of the reliability of the estimate based on the

information obtained from the dynamic maneuver. In simpler terms, the Cramer-Rao bound is an estimate of the standard deviation of the estimates. The measure of reliability is improved when a sufficient number of measurements are provided and the assumptions used in the prediction model are valid. The Cramer-Rao bounds are the square roots of the diagonal elements of the information matrix. A precise mathematical description of the information matrix and the calculation of the Cramer-Rao bound can be found in References 25 and 27. For the purposes of this study it is enough to know that the Cramer-Rao bound is a good indicator of the accuracy of an estimated parameter.

4. A-Priori Information

Wind tunnel data from the study conducted by the NASA Langley Research Center, Flight Dynamics Branch, provide some insight into the aerodynamic characteristics of the BQM-147A. Measurements tabulated in Reference 2 are useful in providing estimates for some of the stability and control parameters. The MMLE3 parameter estimation routine allows the estimation algorithm to consider this a-priori information by adding a quadratic penalty function to the criterion [Ref. 27:p. SR-4]. Equation (50) can then be re-expressed by:

$$J(\xi) = \frac{1}{2}\sum_{i=1}^{N}\left[z(t_i) - z_\xi(t_i)\right]^T R^{-1}\left[z(t_i) - z_\xi(t_i)\right] + \frac{1}{2}(\xi-\xi_0)^T W (\xi-\xi_0) \quad (52)$$

where ξ_0 is the vector of a-priori values and W is the weighting matrix. The a-priori information can be used to speed the convergence; however, the results will be biased towards the weighted estimates [Ref 27:p ST-8]. A good technique to avoid the problems associated with biased estimates is to remove the weighting after initial convergence. The initial weighted values should be close enough to the maximum likelihood estimates to allow rapid convergence to an unbiased estimate when the weighting is removed and additional iterations are allowed.

5. Linearized Equations of Motion

In the analysis of aircraft stability and control it is often more practical to restrict the area of interest to steady-state motion and the response of the aircraft to small perturbations about a steady-state condition [Ref 24:p 33]. Equations (35) through (43) in Chapter 3 are a full set of coupled, non-linear equations that completely describe the dynamic behavior of the aircraft. The simplification of the model by applying small-angle theory significantly reduces the complexity of the model without necessarily compromising

accuracy. For a wide range of practical applications on well-behaved systems, a linear model is sufficient.

References 22 through 25 provide details in applying small-angle theory to the non-linear equations of motion from which the linearized equations used in MMLE3 are derived. From equations (36), (39) and (42), a small angle approximation leads to the simplified longitudinal equations:

$$\dot{\alpha} = -\frac{\bar{q}S}{mV} C_L + q + \frac{g}{V} \tag{53}$$

$$\dot{q} = \frac{\bar{q}S}{I_y} C_m \tag{54}$$

$$\dot{\theta} = q \tag{55}$$

In the approximation, a plane of symmetry about the X-Z plane is assumed, making I_{yz} and I_{xy} equal to zero. The aerodynamic coefficients in the above equations are:

$$C_L = C_{L_\alpha}\alpha + C_{L_\delta}\delta + C_{L_0} \tag{56}$$

$$C_m = C_{m_\alpha}\alpha + C_{m_\delta}\delta + C_{m_q}\frac{qc}{2V} + C_{m_0} \tag{57}$$

From equations (56) and (57) the vector ξ is expressed as a function of the unknown stability and control derivatives by:

$$\xi = \xi\,(C_{L_\alpha}, C_{L_\delta}, C_{m_\alpha}, C_{m_\delta}, C_{m_q}) \tag{58}$$

From the application of the small angle approximation to equations (37), (38), (40) and (41), the simplified lateral-directional equations are:

$$\dot{\beta} = \frac{\bar{q}s}{mV} C_Y + \frac{g}{V}\phi - r \tag{59}$$

$$\dot{p}I_x - \dot{r}I_{xz} = \bar{q}sbC_l + qr\,(I_y - I_z) + pqI_{xz} \tag{60}$$

$$\dot{r}I_z - \dot{p}I_{xz} = \bar{q}sbC_n + pq\,(I_x - I_y) - qrI_{xz} \tag{61}$$

$$\dot{\phi} = p + r\cos\phi\tan\theta + q\sin\phi\tan\theta \tag{62}$$

The aerodynamic coefficients for the lateral-directional equations are:

$$C_Y = C_{Y_\beta}\beta + C_{Y_p}\frac{pb}{2V} + C_{Y_r}\frac{rb}{2V} + C_{Y_\delta}\delta + C_{Y_0} \tag{63}$$

$$C_l = C_{l_\beta}\beta + C_{l_p}\frac{pb}{2V} + C_{l_r}\frac{rb}{2V} + C_{l_\delta}\delta + C_{l_0} \tag{64}$$

$$C_n = C_{n_\beta}\beta + C_{n_p}\frac{pb}{2V} + C_{n_r}\frac{rb}{2V} + C_{n_\delta}\delta + C_{n_0} \qquad (65)$$

The "delta" parameter is a general expression for control input and must be expanded to consider all inputs that contribute to the total force or moment coefficient. The contributions to the total side force coefficient from roll rate and yaw rate are small compared to the other contributing parameters and are usually ignored. The vector of unknown parameters, ξ, can be expressed as a function of the lateral-directional stability and control derivatives by:

$$\xi = \xi\,(C_{Y_\beta}, C_{l_\beta}, C_{N_\beta}, C_{l_p}, C_{N_p}, C_{l_r}, C_{n_r}, C_{l_{\delta_a}} C_{n_{\delta_a}}, C_{Y_{\delta_r}}, C_{l_{\delta_r}}, C_{n_{\delta_r}}) \qquad (66)$$

C. pEst

For many aircraft applications the linearized equations of motion provide a reasonably accurate model of the system for small disturbances. For some applications however, the linear model is not sufficient and a more accurate non-linear model is required. Flight testing at the Dryden Flight Research Facility highlighted the limitations of the linear model when applied to maneuvers at extreme flight conditions. In 1987 Murray and Maine [Ref 9] introduced the pEst program for parameter estimation in non-linear dynamic systems.

1. General System Model

Conceptually, parameter estimation in non-linear dynamic systems is the same as the parameter estimation in linear systems. The general system model is separated into a continuous-time state equation and a discrete response equation represented by [Ref. 9:p. 3]:

$$\dot{\boldsymbol{x}}(t) = f[\boldsymbol{x}(t), \boldsymbol{u}(t), \xi] \tag{67}$$

$$\boldsymbol{z}(t_i) = g[\boldsymbol{x}(t_i), \boldsymbol{u}(t_i), \xi] \tag{68}$$

The cost function is the criterion by which the model's computed response is measured against the measured time history response. The pEst program defines quantitatively the criterion by:

$$J(\xi) = \frac{1}{2 n_z n_t} \sum_{i=1}^{n_t} [z(t_i) - \hat{z}(t_i)]^T W [z(t_i) - z(t_i)] \tag{69}$$

Where n_z and n_t are the number of response variables and the number of measured time history points.

2. Estimator

The feedback process, like that used in the MMLE3 estimator, is recursive. The non-linear equations used in pEst preclude using the discrete-time Kalman estimator

formulation of MMLE3; however, the feedback term is still proportional to the difference between the measured response and the computed response [Ref. 9:p. 3]:

$$\hat{x}(t_i) = \tilde{x}(t_i) + k[z(t_i) - \tilde{z}(t_i)] \tag{70}$$

3. Parameters

The parameters are the values that can be estimated by pEst. Each of the parameters has five attributes: current value, estimation status, predicted value, Cramer-Rao bound and change in value from the previous iteration [Ref 9:p 11]. The initial current value is a best estimate of the parameter entered by the user. Typically the initial current value input is derived from a source such as DATCOM, [Ref. 30] or it may be the result of measured data from either wind tunnel studies or flight tests. The estimation status indicates to the user which parameters are being estimated. A parameter is either active or inactive. The predicted value is the value of the parameter computed by pEst and it is used to update the current value for each successive iteration. The Cramer-Rao bound and the change in parameter value are defined in the estimation process. The Cramer-Rao bound is a measure of the accuracy of the estimate. A list of the names and a description of the parameters available in pEst can be found in Section B.16, Reference 9. For this study, the parameter

vector, ξ, is the same as the parameter vector used in the MMLE3 routine.

4. States and Responses

The attributes of the states are status and integration limit. The attributes of the response variables are status and weighting. If a state is active, the state equation is integrated and its value is used in the equations of motion. If the value of the state exceeds the integration limit, the integration is terminated. If the response variable, or output variable, is active then its time history values are computed and placed in a special output file. The weighting of a response variable specifies the value to be used in the W matrix of the cost function. Weighting the response variables based on a-priori knowledge may help the routine converge more rapidly; however, the results may be biased towards the weighted estimates. Table 4.13 of Reference 24 shows the relative importance and prediction accuracies of the stability derivatives using theoretical methods. The table may be used as a guideline if weighting is desired.

5. Equations of Motion

Equations (35) through (43) define the non-linear equations of motion used in the pEst routine. The assumption of symmetry about the X-Z plane that was used in MMLE3 is not used in pEst; however, the assumptions of fixed aircraft

geometry and constant mass are valid [Ref. 9:p. 17]. In this study, equations (36) through (42) are integrated to obtain the predicted state variables in the vector x-tilde. A list of the 14 response equations can be found in Section 6.1.4 of Reference 9.

V. MMLE3 APPLICATION

Recent thesis work by LCDR Robert Graham [Ref. 6] incorporated a PC-based parameter estimation capability into the NPS research program. The Maine and Iliff MMLE3 code has been used for a number of years for large scale work where the use of mainframe computer systems was justified [Ref. 9:p. 1]. Research by Erickson [Ref. 8] showed that for less demanding work, a PC-based parameter estimation routine for a longitudinal model generally provides comparable results when compared to more complex mainframe programs. The code written by Graham uses the commercially available software package, MATLAB®, to build interactive files for both the longitudinal and lateral-directional models. The MATLAB State-Space Identification Tool, (SSID) [Ref. 28], comprises a main Modified Maximum Likelihood Estimator (MMLE) program, along with several supporting functions for parameter estimation. The supporting functions are used to convert the parameter vector into the state-space model and to arrange the necessary inputs for the MMLE program. A complete listing of the code written by Graham can be found in Appendices E and F of Reference 6. The modifications to the supporting functions in Reference 6 required for this application are discussed in the following sections. Figure 5 [Ref. 9:p. 43], shows how the

various MATLAB files interact in the parameter estimation routine.

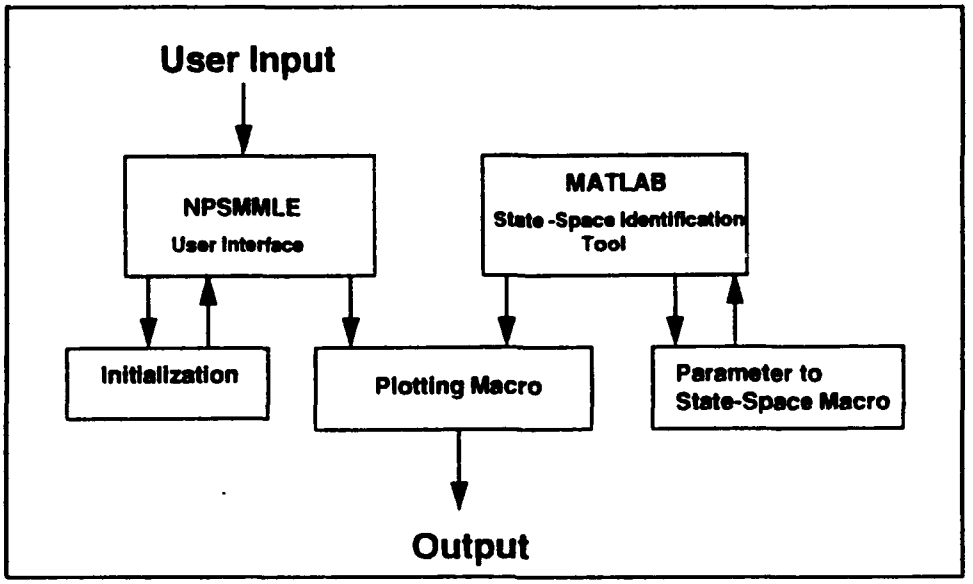

Figure 5 Interactive MATLAB .M Files

A. DATA ACQUISITION

1. Flight Test

The data made available for this study were provided by NASA Langley Research Center and were the result of flight tests conducted at the NASA Langley Plumtree Test Site in March, 1992. This flight test comprised a single set of flight maneuvers consisting of pitch, roll and yaw doublets. A partial sequence of events is listed in Table 3. The roll and yaw doublets were merged into a single input file so that all of the lateral-directional modes would be excited.

Figures 6 and 7 show a typical control input for the doublet maneuvers.

2. Atmospheric Data

Specific atmospheric data for the date and time of the flight tests were unknown. Best estimates of atmospheric conditions for the test site were from a local area weather briefing and were recorded on the flight card by the flight test pilot.

3. Sensor Placement

Twin alpha and beta sensors were symmetrically located about the longitudinal axis and 2.5 feet in front of the vehicle center of gravity (cg). An averaging scheme was used on the two sets of measured data and a single set of data for alpha and beta was provided. Accelerometers for X, Y and Z axes were located on the cg point. A rate sensing gyro was located on the waterline, aft of the cg. Details on sensor characteristics were not available.

The aircraft equations of motion developed in Chapter III assume that the sensors are located at the cg. Since several of the observed signals are functions of the position of the sensors, it is necessary to correct the sensor measurement for the offset. For the longitudinal model the measured variables α_m and A_n are corrected to the cg by [Ref. 18:p. 26]:

$$\alpha_{cg} = \alpha_m + \frac{X_{ap}}{V} q \tag{71}$$

$$A_{n_{cg}} = A_n - \frac{X_{an}}{g}\dot{q} - \frac{Z_{an}}{g}q^2 \qquad (72)$$

For this application, X_{ap} is positive forward of the cg and was given a fixed value of +2.5 feet. Since the X-and-Z axis accelerometers were located at the cg, the value of X_{an} and Z_{an} is zero. For the lateral-directional model, the measured variables β_m and A_y are corrected to the cg by [Ref 18:p 27]:

$$\beta_{cg} = \beta_m - \frac{X_{bp}}{V}r \qquad (73)$$

$$A_{y_{cg}} = A_y - \frac{X_{ay}}{g}\dot{r} + \frac{Z_{ay}}{g}\dot{p} \qquad (74)$$

The X distance to the beta probe was set at +2.5 feet and the value of X_{ay} and Z_{ay} was set to zero.

4. Measured Signals

A total of twenty-four signals were measured and recorded during the flight test. These signals are presented in Table 4. Details of how the data were filtered, digitized, time tagged and recorded were not available.

B. USER FUNCTION

The PC-based MMLE3 application requires a user-written function to convert the parameter vector into a state-space system model [Ref. 28:p. SR-3]. The following two subsections describe the creation of the P2SS.m file for this study.

1. Longitudinal Model

In the general system model given by equation (46), the response of the system is a function of the state vector, **x**, and the control input, **u**. Since the measured flight test data do not include pitch angle and in the short-period approximation forward velocity is assumed to be constant, the simplified longitudinal model can be reduce to equations (53) and (54) for α and q. These two equations contain terms which are neither functions of the state variables or the control inputs. Consequently, the control input was augmented with a unity input to incorporated these terms in the state-space model. The state vector is represented by:

$$\boldsymbol{x} = \begin{bmatrix} \alpha \\ q \end{bmatrix} \tag{75}$$

The control input is represented by:

$$\boldsymbol{u} = \begin{bmatrix} \delta_e \\ 1 \end{bmatrix} \tag{76}$$

In the state-space formulation the vector **p** is the vector of stability and control parameters. This vector is expressed in terms of its elements by:

$$\mathbf{p}=\left[C_{L_\alpha} \quad C_{m_\alpha} \quad C_{m_q} \quad C_{L_{\delta_e}} \quad C_{m_{\delta_e}}\right] \tag{77}$$

The plant matrix can now be expressed in terms of the elements of the parameter vector by:

$$A=\begin{bmatrix} \dfrac{-\bar{q}s}{gwV\cos\alpha_1}p(1) & 1 \\ \dfrac{\bar{q}sc}{I_y}p(2) & \dfrac{\bar{q}sc^2}{2VI_y}p(3) \end{bmatrix} \tag{78}$$

The control matrix is expressed in terms of the elements of the parameter vector by:

$$B=\begin{bmatrix} \dfrac{-\bar{q}s}{gwV\cos\alpha_1}p(4) & \dfrac{\bar{q}s}{gwV\cos\alpha_1}\left(p(1)+p(4)\,\delta_{e_1}\right)-q_1 \\ \dfrac{\bar{q}sc}{I_y}p(5) & \dfrac{-\bar{q}sc}{I_y}\left(p(2)\,\alpha_1+p(5)\,\delta_{e_1}\right)-\dfrac{\bar{q}sc^2}{2VI_y}p(3)\,q_1 \end{bmatrix} \tag{79}$$

In the longitudinal application it is desired to evaluate the dependence of any change in normal acceleration upon longitudinal control input. The equation for normal acceleration in terms of non-dimensional stability and control parameters is derived in Chapter 4 of Reference 22. The general system output equation can be expressed in terms of a

parameters is derived in Chapter 4 of Reference 22. The general system output equation can be expressed in terms of a parameter vector, **y**, that contains the variable A_n in addition to the states α and q. The output and measurement equations of the form given in equation (48) are augmented by a feed-through matrix, D. The output matrix, C, can be expressed by:

$$C=\begin{bmatrix} 1 & 0 \\ 0 & 1 \\ \frac{\bar{q}S}{mg}p(1) & 0 \end{bmatrix} \tag{80}$$

The feed-through matrix, D, is given by:

$$D=\begin{bmatrix} 0 & 0 \\ 0 & 0 \\ \frac{\bar{q}S}{gw}p(4) & \frac{-\bar{q}S}{gw}\left(p(1)\,\alpha_1+p(4)\,\delta_{e_1}\right)+A_{n_1} \end{bmatrix} \tag{81}$$

The subscripted states, α_1 and q_1, are the elements of the initial state vector $\mathbf{x_0}$. The input for the initial vector comes directly from the first element in the measured data file for each of the states.

The longitudinal model given above specifies the state equation in continuous form. In computing the continuous-to-discrete-time conversion, the sample time, dt, is required. Since MATLAB will not allow a global variable to be used in a function argument, the P2SS.m file must be modified to allow

2. Lateral-Directional Model

In the lateral-directional model the state vector, **x**, is represented by:

$$x = [\beta \; p \; r \; \phi]^T \tag{82}$$

The control input vector, **u**, is represented by:

$$u = \begin{bmatrix} \delta_a \\ \delta_r \\ 1 \end{bmatrix} \tag{83}$$

The subscripted variables δ_a and δ_r represent the aileron and rudder control inputs. The input vector is augmented by a unity input to incorporate the additional terms that influence lateral acceleration in the measurement equation. The measurement vector is:

$$y = [\beta \; p \; r \; \phi \; A_y]^T \tag{84}$$

The lateral-directional parameter vector, **p**, is:

$$p = \left[C_{Y_\beta} \; C_{l_\beta} \; C_{n_\beta} \; C_{l_p} \; C_{n_p} \; C_{l_r} \; C_{n_r} \; C_{l_{\delta_a}} \; C_{n_{\delta_a}} \; C_{Y_{\delta_r}} \; C_{l_{\delta_r}} \; C_{n_{\delta_r}} \right] \tag{85}$$

The only change to the NPSP2SS4.M file in Reference 6

was to input the time step, dt, for the sampling rate of the measured data file.

From Table 4 it can be seen that roll-angle was not measured during flight test. Since the spiral mode is dominated by the roll angle component, it was necessary to numerically integrate the roll rate, p, in order to provide a roll angle input estimate. For N intervals with equal spacing, the extended trapezoidal rule can be written as:

$$I = \int_a^b f(x) = \frac{dt}{2}\left[f(a) + 2\sum_{j=1}^{N-1} f(a + j(dt)) + f(b)\right] + E \qquad (86)$$

A complete development of the extended trapezoidal rule and a discussion of the error term, E, can be found in Chapter IV of Reference 29.

C. INITIALIZATION

The initialization macro is a supporting function that imports the measured time history file, prompts the user for the physical dimensions of the aircraft and prompts for the initial values of the parameters that are to be identified.

1. Physical Characteristics

Table 5 presents the aircraft physical characteristics that were input for this study. To be consistent with the physical characteristics used in the NASA static wind-tunnel tests, the theoretical root chord was used as the reference

1. Physical Characteristics

Table 5 presents the aircraft physical characteristics that were input for this study. To be consistent with the physical characteristics used in the NASA static wind-tunnel tests, the theoretical root chord was used as the reference wing chord. Moments of inertia and sensor offset information were provided by the Marine Corps UAV Project Office, Intelligence Systems, Quantico, VA.

2. Initial Estimates

The SSID Modified Maximum Likelihood Estimator requires a set of predicted aerodynamic characteristics to be used as starting values for the iterative algorithms. In this study a combination of wind tunnel data and analytic estimates was used as a source of predicted values. Tables 6 and 7 present the parameter, the predicted value of the parameter and the source of the predicted value for the longitudinal and lateral-directional case studies.

D. MODIFIED MAXIMUM LIKELIHOOD ESTIMATOR

The Modified Maximum Likelihood Estimator is the main program used by the MATLAB SSID tool and it is the only program that is called by the user. MMLE calls the supporting functions to provide the necessary inputs for the estimation algorithm. The primary inputs used by the MMLE macro are:

1) **uydata**: An n-by-m matrix where the m columns are the measured time history inputs of the vector **u** followed by the outputs of the vector **y** and n is the number of time steps.

2) **p2snam:** The name of the P2SS function that converts the parameter vector to the state-space model.

3) **p0:** The initial parameter estimates entered during initialization.

4) **rms0:** A vector containing the standard deviations of a-priori parameter estimates.

5) **gg0:** The initial guess of the innovations co-variance matrix.

6) **linesearch:** An option to help convergence during the Constrained-Newton minimization phase.

7) **opt:** A vector that specifies the number of iterations for the various minimization phases and the convergence criteria that permits termination of each phase.

For this study, **rms0** was a zero vector indicating that initial parameter weighting was not used. The initial innovations co-variance matrix, **gg0**, was set to a small, non-zero diagonal matrix to minimize the effects of the noise.

There are four variations of the Newton method available for the minimization of the weighted error sum. The **opt** vector was set so that minimization begins with a Marquardt, gradient algorithm. The gradient algorithm performs well when the cost function is very steep, but performance tends to deteriorate as a minimum is approached and the cost becomes more flat [Ref. 28:p. SR-8]. When the user-specified **marq** value is reached, the process has been conditioned well enough for a Constrained-Newton minimization algorithm to begin. This algorithm is most accurate near the minimum of a cost function when the cost function is quadratic [Ref. 9:p. 16].

The **linesearch** option is set "true" to help convergence in the Constrained-Newton phase. Reference 28 discusses each of the minimization phases in more detail. For this study the value of **marq** was set at 0.02 and the convergence criteria was set at 0.001. All parameters are identified in both the Marquardt and the Constrained-Newton phases.

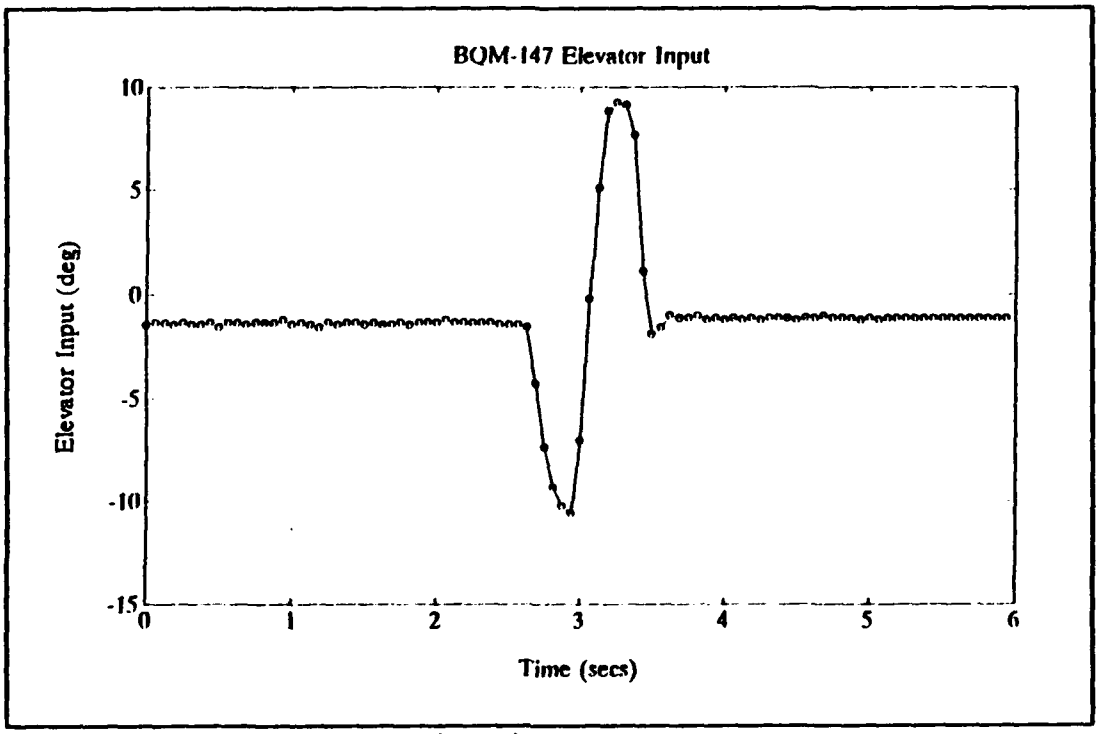

Figure 6 BQM-147 Longitudinal Input

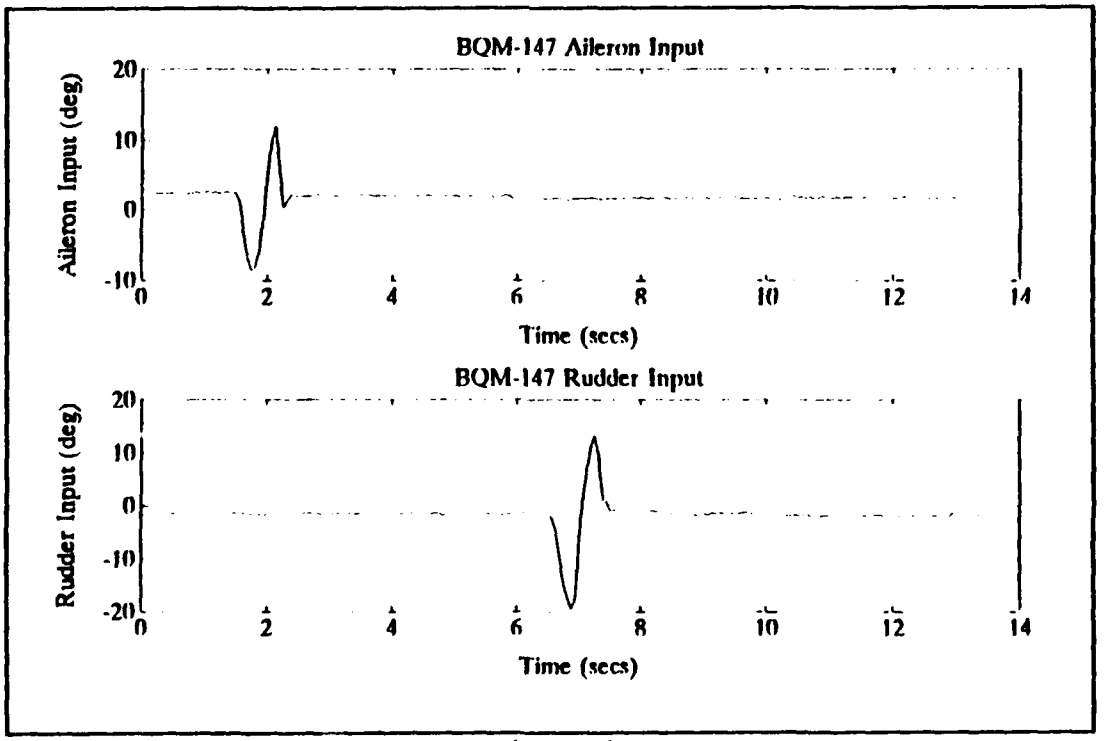

Figure 7 BQM-147 Lateral-Directional Input

TABLE 3 FLIGHT 03-24 FLIGHT CARD

Pre-Flight and Takeoff	
P01	Engine Off Data
P02	Static Measurement (nose up)
P03	Static Measurement (right wing up)
P2A	Takeoff Data
Stability and Control Maneuvers (100%)	
P2B1	Pitch-Up Doublet
P2B2	Pitch-Down Doublet
P2B3	Roll-Right Doublet
P2B4	Roll-Left Doublet
P2B5	Yaw-Right Doublet
P2B6	Yaw-Left Doublet
Trim Flight Data	
P2E1	20% Throttle
P2E2	50% Throttle
P2E3	100% Throttle

TABLE 4 FLIGHT 03-24 MEASURED SIGNALS

Columns 1 through 4			
ALPHA	BETA	VELOCITY	RPM
Columns 5 through 8			
RUDDER	AIL_LEFT	ELEV_LEFT	AIL_RIGHT
Columns 9 through 12			
ELEV_RIGHT	THROTTLE	PITCH_RATE	ROLL_RATE
Columns 13 through 16			
YAW_RATE	AX	AY	AZ
Columns 17 through 20			
AIL_CMD	RUDDER_CMD	ELEV_CMD	ALTITUDE
Columns 21 through 24			
SERVO_VOLT	SERVO_AMP	BLANK	BLANK

TABLE 5 BQM-147 PHYSICAL CHARACTERISTICS

Reference Area (S)	21.24 ft^2
Reference Chord (c-bar)	4.458 ft
Wingspan (b-bar)	8.167 ft
Gross Weight (w)	65 lb
Moment of Inertia (Iy)	3.443 $slug\text{-}ft^2$
Moment of Inertia (Ix)	3.648 $slug\text{-}ft^2$
Moment of Inertia (Ixz)	0
Moment of Inertia (Iz)	5.965 $slug\text{-}ft^2$
Sensor Offset (Xap)	+2.5 ft
Sensor Offset (Xbp)	+2.5 ft
Sensor Offset (Zan)	0
Sensor Offset (Zay)	0
Sensor Offset (Xan)	0
Sensor Offset (Xay)	0

TABLE 6 INITIAL PARAMETER ESTIMATES, LONGITUDINAL

Parameter	Value	Source
$C_{L\alpha}$	2.4350	Wind Tunnel [Ref 2:p 20]
Cm_{α}	1.6900	Wind Tunnel [Ref 2:p 20]
Cm_{q}	-0.1089	DATCOM [Ref 30]
$C_{L\delta e}$	-0.6670	DATCOM [Ref 30]
$Cm_{\delta e}$	-0.4060	DATCOM [Ref 30]

TABLE 7 INITIAL PARAMETER ESTIMATES, LATERAL-DIRECTIONAL

Parameter	Value	Source
$C_{Y\beta}$	-.2005 /rad	Wind Tunnel [Ref 2:p 24]
$C_{l\beta}$	-.0325 /rad	Smetana [Ref 31:p 108]
$C_{n\beta}$	.0430 /rad	Wind Tunnel [Ref 2:p 24]
C_{lp}	-.3525 /rad	Smetana [Ref 31:p 122]
C_{np}	.0027 /rad	Smetana [Ref 31:p 122]
C_{lr}	.0729 /rad	Smetana [Ref 31:p 133]
C_{nr}	-.0230 /rad	Smetana [Ref 31:p 135]
$C_{l\delta a}$	.1377 /rad	Smetana [Ref 31:p 124]
$C_{n\delta a}$	-.0194 /rad	Smetana [Ref 31:p 136]
$C_{Y\delta r}$	.1130 /rad	Smetana [Ref 31:p 145]
$C_{l\delta r}$	.0023 /rad	Smetana [Ref 31:p 147]
$C_{n\delta r}$	-.0138 /rad	Smetana [Ref 31:p 149]

VI. pEst APPLICATION

For many aircraft applications the linearized equations of motion provide a reasonably accurate model of the system for small disturbances about an equilibrium condition. For some applications, however, the linear model is insufficient and a more accurate non-linear model is required. Flight testing at the Dryden Flight Research Facility highlighted the limitations of the linear model when applied to maneuvers at extreme flight conditions and with some unique aircraft configurations that exhibited non-linear dynamic behavior. In 1987 Murray and Maine introduced a program for parameter estimation, pEst, in non-linear dynamic systems. A full description of the pEst program can be found in Reference 9.

The pEst program interfaces directly with two other programs. The GetData program, Reference 32, is a FORTRAN utility program that is used to extract selected signals from a time-history input file and to write the selected signals in a user specified format to an output file. The second program interfacing with pEst is XPLOT, Reference 33. The XPLOT program is a plotting utility that is used to plot selected signals from the measured time-history file and the computed time-history file. The following sections describe how the pEst program was set up for the estimation of the BQM-147 stability and control derivatives.

A. MEASURED TIME-HISTORY DATA

The twenty-four signals that comprise the recorded time-history data from the flight test, Table 4, were re-formatted so that they could be read into the GetData program. The FORTRAN utility used for re-formatting is listed in Table 8.

TABLE 8 DATA CONVERSION PROGRAM

```
      program data
      dimension dat(20)
      open(1,file='data01',status='old')
      k=0.
      read(1,*)
 20   read(1,30,end=97) (dat (i),i=1,24)
 30   format(f6.0,2f7.0,f8.0,5f7.0,3x,f4.0,9f7.0,
     # 1x,f7.0,f6.0,3f7.0)
      t=k/16.
      write(2,60) t,(dat(j),j=1,24)
 60   format(f10.3,10x,3g20.14/5(4g20.14/),g20.14)
      k=k+1
      goto 20
 97   write(6,120)
120   format(///'      **** Normal Termination ***'///)
 99   stop
      end
```

The GetData program was used to select the desired signals from the available time-history data. The signals not applicable to the pEst program were deleted. Those signals specifically required for the computation of the estimates were renamed so that the signal names on file matched the

signal names expected by pEst. One new signal was added to provide an input for dynamic pressure. The GetData output file was saved in a compressed format for use by the pEst program.

B. OPERATIONAL STATUS

The pEst program uses a file named *current* to store the operational status of the program. The *current* file is used to provide initial values for program variables, to store the status of the program for recovery and to store the results at the end of each run. The primary elements of the *current* file are parameters, states, outputs and constants. A listing of the *current* parameter status for the longitudinal and lateral-directional applications can be found in Tables 9 and 10.

1. Parameters

The parameters are variables that can be estimated by pEst. The five attributes of each parameter are:

1) Current value: Typically entered by the user
2) Predicted Value: Computed by pEst
3) Estimation Status: Active (T) or Inactive (F)
4) Cramer-Rao bound
5) Change in value from previous iteration

The current values of active parameters were the same as those used in the MMLE3 routine multiplied by a constant to reflect the change in units required for use in pEst. The

active parameters were those that are listed as elements of the parameter vectors given by equations (77) and (85). Only those parameters with an estimation status of "true" are estimated by the program.

The parameter list also allows for a sensor placement input. In the MMLE3 routine the sensor offset was corrected to give a signal that simulated a measurement at the cg. In pEst, the effects of the sensor position are included in the observation equations. A list of the observation equations can be found on page 20 of Reference 9. A description of the available parameters can be found in Section B of Reference 9.

2. States

The status of the state variables in the *current* file is used to determine which of the state equations are to be integrated. The state equations used by pEst are equations (35) through (43). The state vectors for the longitudinal model and the lateral-directional model are given by equations (75) and (82). Since roll angle was not measured, the state, phi, was set inactive for the lateral-directional application.

3. Outputs

The attributes of the outputs are status and weighting. Default weighting was used in the initial *current* file in order to avoid biasing the solution in a particular direction. The outputs are the elements of the output vector, **y**, of the form given by equation (48).

4. Constants

The constants are variables that cannot be estimated by pEst. In this application, constants were used to input the physical characteristics of the BQM-147. The constants and their respective values are the same as those listed in Table 5 for the MMLE3 application.

C. MINIMIZATION ALGORITHMS

The pEst program has several minimization algorithms available. In this application a default Newton-Raphson minimization routine was used. After each iteration the active parameters, the current values and the change in current value from the previous iteration are displayed. The Cramer-Rao bound is computed with the Newton-Raphson algorithm only. The Cramer-Rao bounds are displayed at the user's discretion.

D. COMPUTED TIME-HISTORY

For each output whose status is active a variable time-history is computed. The 'write' command is used to write the time history into a user specified output file. The signals written to the output file are the computed states, the computed responses and the residuals. The output file can be read by the XPLOT program and user selected signals can then be called for display.

TABLE 9 pEst INITIAL STATES; LONGITUDINAL

File Name: Current.p2b1	
Active Parameters	**Value**
cNorm0	1.637171976
cNorma	0.046710000
cNormde	0.029500000
cm0	0.0
cma	-0.001900000
cmq	-0.677000000
cmde	-0.007100000
alpha0	0.0
q0	0.0
ka	1.0
Constants	**Value**
mass	2.0300
ix	3.6480
iy	3.4430
iz	5.9650
ixy	0.0
iyz	0.0
ixz	0.0
area	21.2400
span	8.1670
chord	4.4580
States	**Status**
V	F
alpha	T
q	T
theta	F
Outputs	**Status**
V	F
alpha	T
q	T
theta	F
an	T

TABLE 10 pEst INITIAL STATUS; LAT-DIR

File Name: Current.uav	
Active Parameter	**Status**
cy0	0.0
cyb	-0.00349900
cydr	0.00197210
cl0	0.0
clb	-0.00056719
clp	-0.35248000
clr	0.07290000
clda	0.00240300
cldr	0.00007888
cn0	0.0
cnb	0.00075044
cnp	-0.00270000
cnr	-0.02300000
cnda	0.00033857
cndr	-0.00055497
kb	1.0
States	**Status**
beta	T
p	T
r	T
phi	T
Outputs	**Status**
beta	T
p	T
r	T
phi	T
ay	T
Note: Constants are the same for both Longitudinal and Lateral-Directional	

VII. RESULTS AND DISCUSSION

A stated purpose of this study was the practical application of parameter estimation for estimating stability and control derivatives from BQM-147 flight test data. Previous information from a wind-tunnel study was made available; however, the results of that study did not provide estimates of all the required parameters, and changes in the production configuration would be expected to have some influence on the value of the parameters. Consequently, parameter estimation was not used to validate wind-tunnel or analytical predictions because there was no way to look for consistency between the data sets, nor was there sufficient flight-test data for a valid comparison. The complete aerodynamic data-base was required to be built using flight test data only. The wind-tunnel and analytical predictions were used only to provide starting values for the iterative algorithms and to provide a reasonable range for flight test results.

When a complete data base must be built using flight data only, extensive coverage of the flight envelope is needed. The flight test data made available for this study comprised a single set of flight maneuvers consisting of pitch, roll and yaw doublets. For the longitudinal case, the short-period mode was excited by an elevator doublet. Table 3 shows that

data from only two maneuvers, a pitch-up doublet (P2B1) and a pitch-down doublet (P2B2), were available for exciting the short-period mode. The lateral-directional model included the roll, dutch-roll and spiral modes. The best way to excite all three of these modes is to have both aileron and rudder control inputs. Since the lateral-directional maneuvers were performed under similar flight conditions, the individual roll (P2B3) and yaw (P2B4) doublets were paired into a single maneuver. The measured data describing the maneuvers and the responses are found in Appendix B.

A. MMLE3

The PC-based MMLE3 routine used in this application relies on the locally linearized aerodynamic model presented in Chapter V. The results of the wind-tunnel study [Ref. 2] show that the behavior of the vehicle is approximately linear for angles of attack up to about 15 degrees. The linearized model is valid only when the assumptions made in the linearization process are valid. Thus, the model is ideally suited for small angle perturbation maneuvers and it can be expected that as the magnitude of the maneuver increases, the locally linearized model loses its validity and the estimates from the model are a less accurate representation of the aircraft dynamics.

The process noise option was used in the MMLE3 routine. The risk in using the process noise option is that the Kalman

gains tend to become high, giving the high-frequency modeling errors more opportunity to influence parameter values.

1. Model Validation

In Chapter III, the changes that were necessary to Graham's routine [Ref. 6] to reduce the order of the model were discussed. In order to validate the changes, the modified model was run using the same F-14A data that were presented in Reference 6. The results of the run shown in Figures 8 through 11 compare well with Graham's results.

2. Longitudinal Model

The computations in the MMLE3 routine were limited by the working precision of MATLAB. Prior experience showed that the PC-based routine was highly sensitive to the initial input derivatives. After several adjustments to the initial parameter vector, the run using the P2B1 maneuver converged successfully. The run using the P2B2 maneuver did not converge because of a singularity due to working precision. The results of the P2B1 maneuver are shown in Figures 12 through 15. The MATLAB output listing showing the input and determined derivatives, per radian, is found in Table 11.

The estimated response for α appears to lag the measured response by a time step at the beginning of the maneuver and is unable to keep up with the amplitude of the measured response in the pitch-down portion of the maneuver. This behavior could have been predicted since pitch angle, which

was not measured, is an important term in the α state equation when the maneuver is not restricted to small perturbations from a stable flight condition. The estimated q response generally correlates well with the measured q response though it does not pick up the high rates at the extreme ends of the maneuver. The differences in q may be due to the ignored terms in the state equation in the linearization process. The estimated normal acceleration response appears to correlate well.

3. Lateral-Directional Model

Inspection of the data in Appendix B indicates that the data were exceptionally noisy in the absence of any control input. Noise in the general frequency range of the system response was a problem. When the P2B3 and P2B5 maneuvers were paired for the lateral-directional run, the process noise was too large and the Gauss-Newton iteration was terminated. Consequently there were no results for the lateral-directional model in the MMLE3 routine.

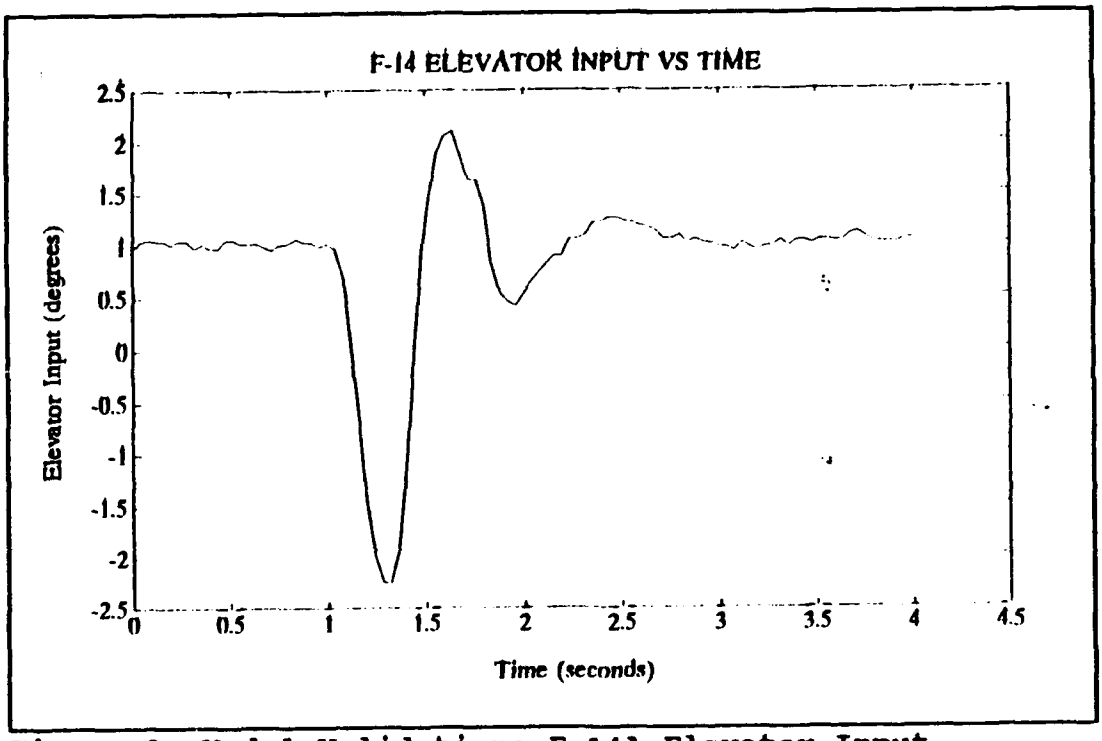

Figure 8 Model Validation: F-14A Elevator Input

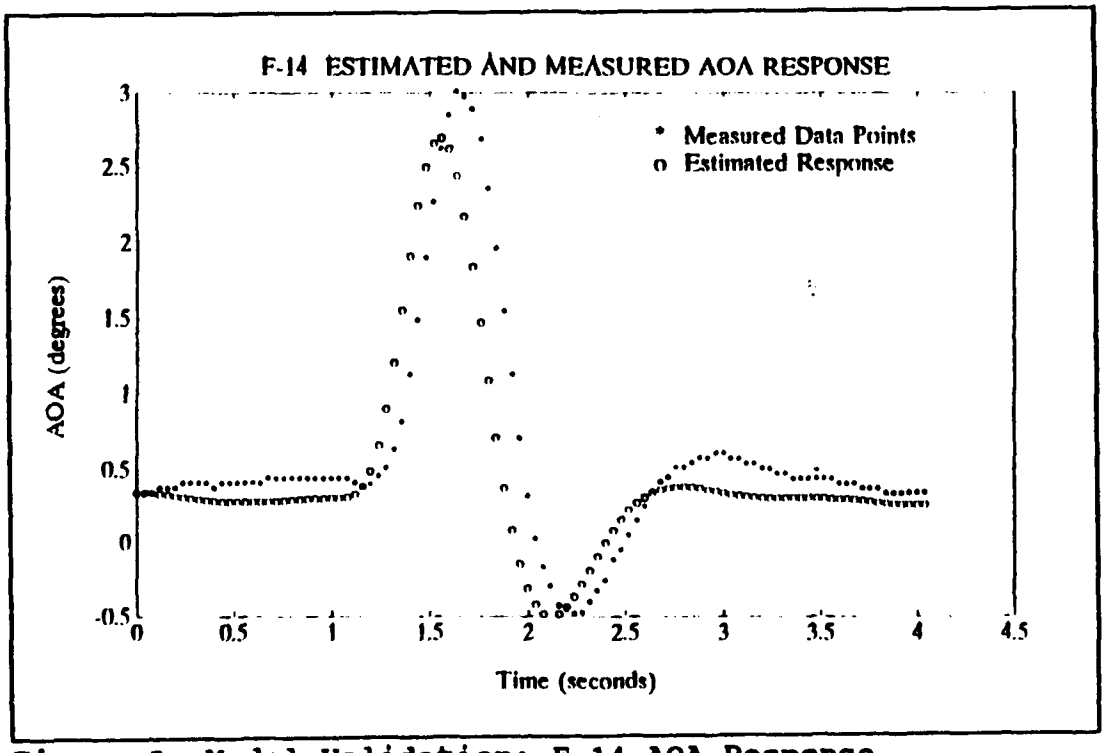

Figure 9 Model Validation: F-14 AOA Response

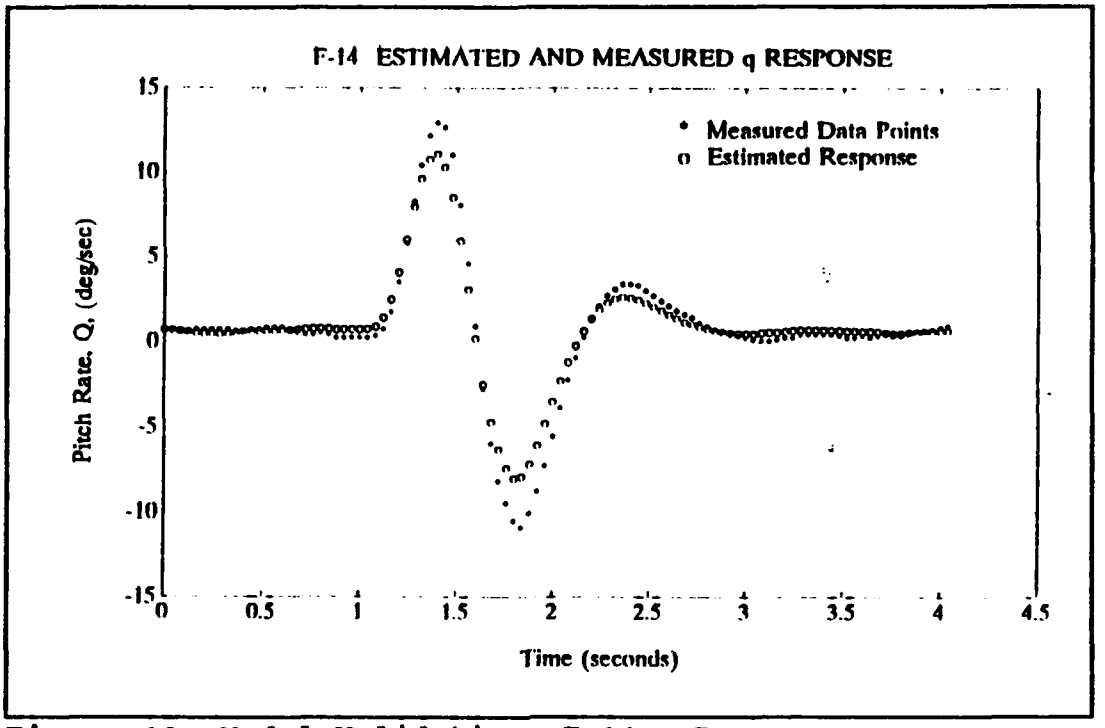

Figure 10 Model Validation: F-14 q Response

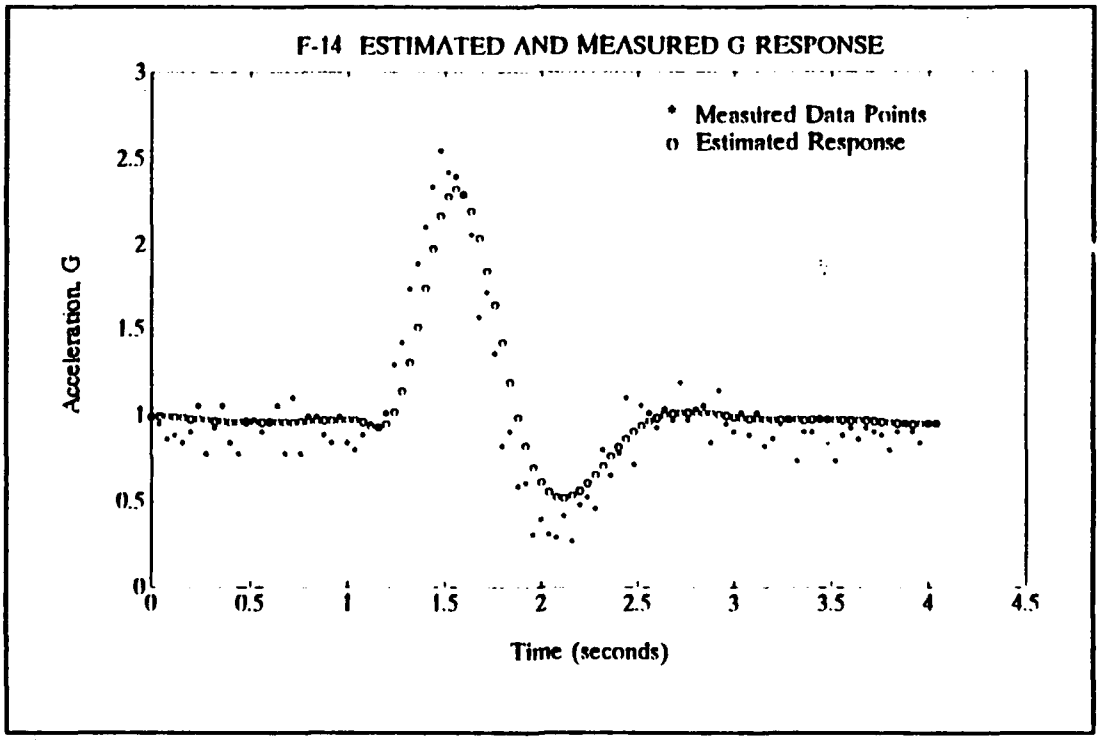

Figure 11 Model Validation: F-14 g Response

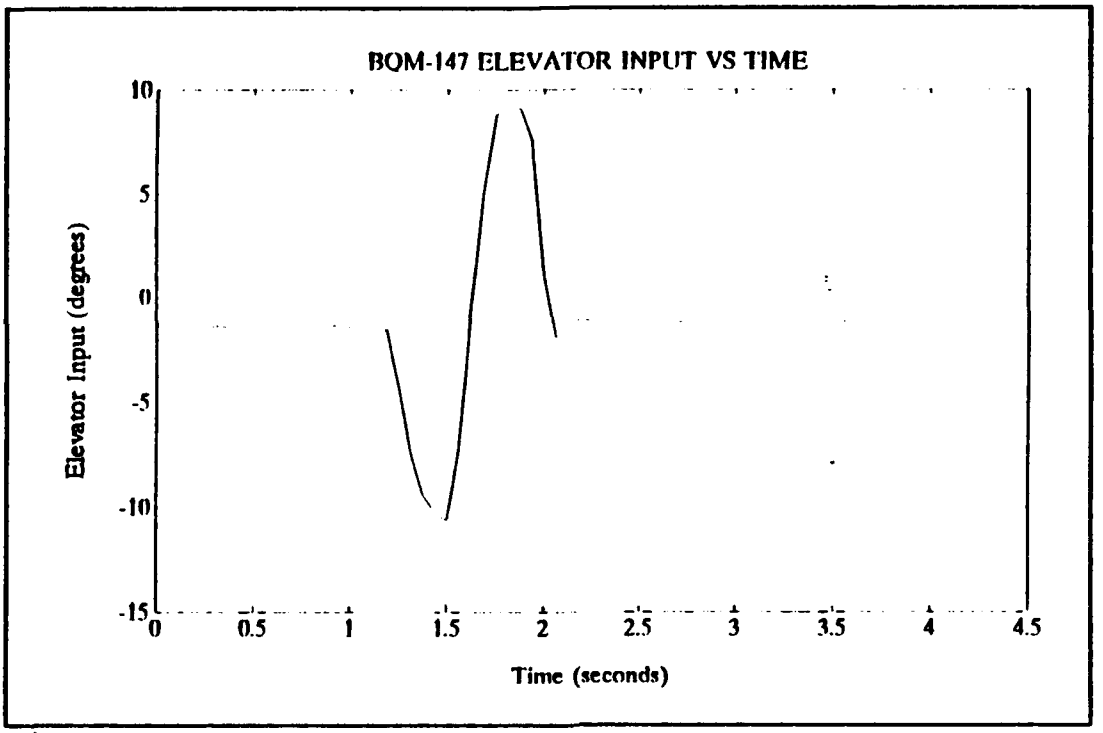

Figure 12 BQM-147 Elevator Input (P2B1)

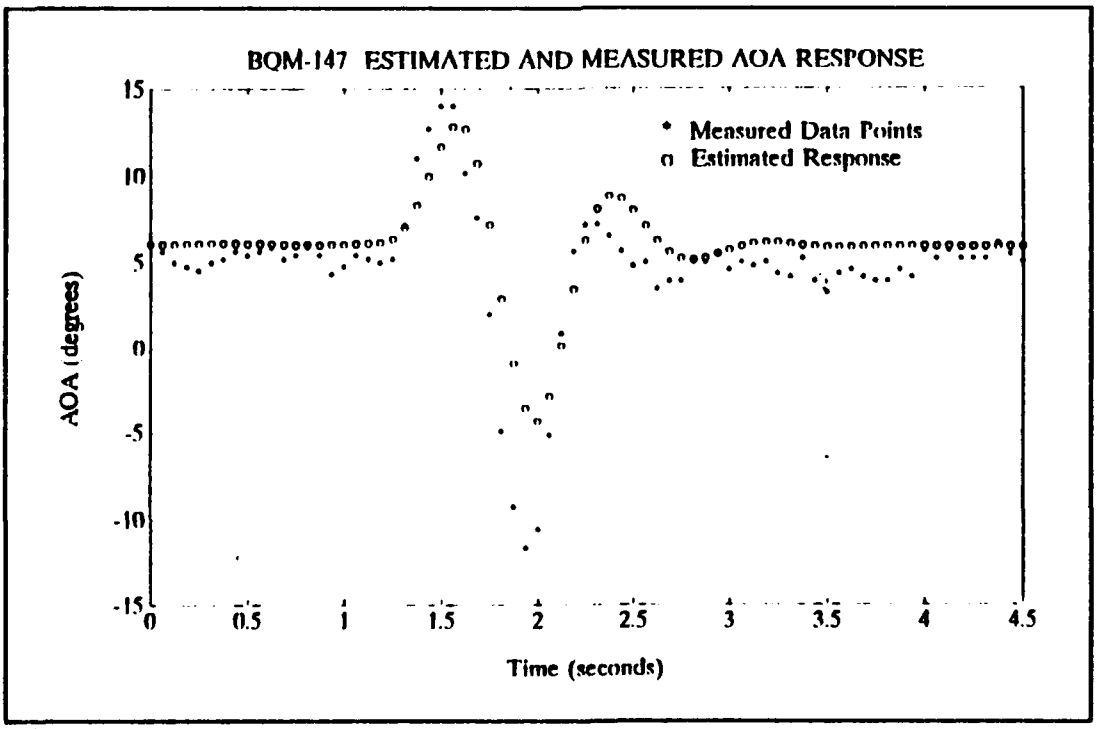

Figure 13 BQM-147 α Response (P2B1)

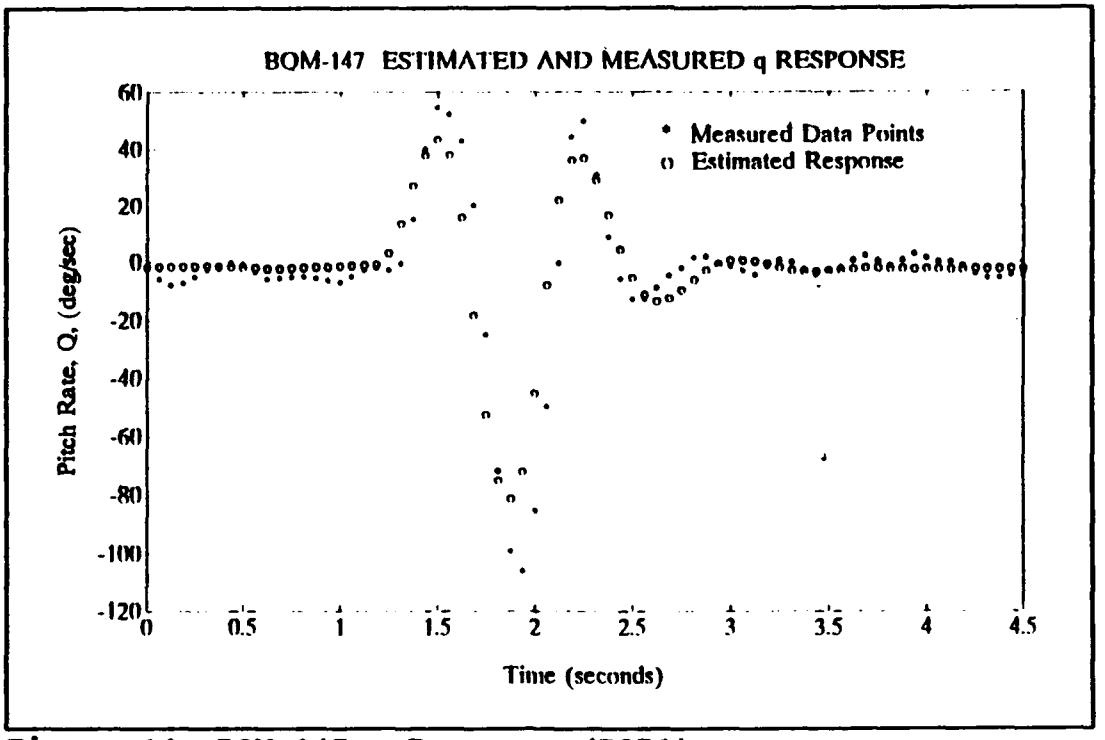

Figure 14 BQM-147 q Response (P2B1)

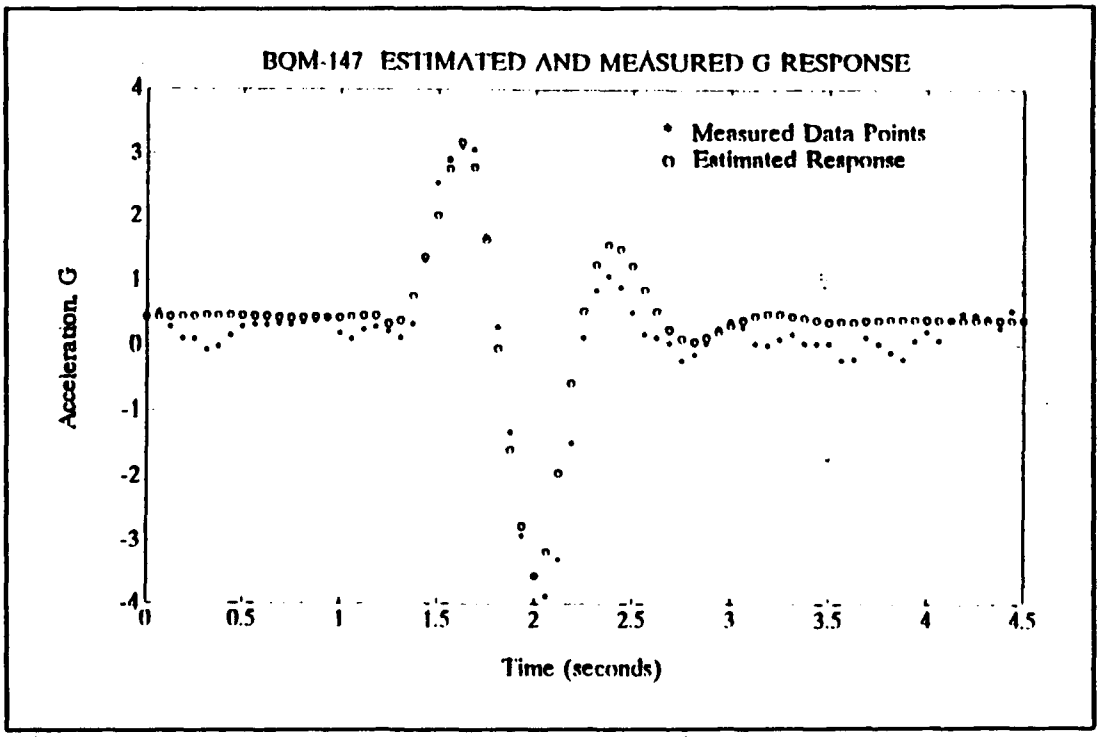

Figure 15 BQM-147 Normal Acceleration Response (P2B1)

TABLE 11 MATLAB RESULTS FOR P2B1

NPS PARAMETER IDENTIFICATION MACRO FILE

FOR ACTUAL FLIGHT TESTS USING SIMPLFIED SHORT PERIOD

LONGITUDINAL STABILITY AND CONTROL DERIVATIVES

----------RESULTS

pid	p(pid)	pref	cramer	2fcramer	insens	gdop
1.0	2.7391	2.4350	0.1084	0.3085	0.0780	1.3902
2.0	-0.0887	-0.1089	0.0028	0.0079	0.0018	1.5088
3.0	-0.1078	-0.6770	0.0414	0.1178	0.0159	2.6088
4.0	0.5015	1.6900	0.0763	0.2171	0.0666	1.1457
5.0	-0.0683	-0.4060	0.0042	0.0120	0.0017	2.4701

MMLE STABILITY & CONTROL DERIVATIVES

CLA	CMA	CMQ	CLDE	CMDE
2.7391	-0.0887	-0.1078	0.5015	-0.0683

INITIAL INPUT DERIVATIVES

2.4350	-0.1089	-0.6770	1.6900	-0.4060

B. pEst

1. Model Validation

A secondary purpose of this study was to integrate the pEst parameter estimation routine into the ongoing research program at the Naval Postgraduate School, Department of Aeronautics and Astronautics. Successful test cases for both the longitudinal and lateral-directional models were run to validate the model. The pEst parameter estimation routine should provide greater capability to the Department because it can be used to model the dynamic behavior of aircraft that cannot be appropriately modeled using the shorter PC-based routine.

2. Longitudinal Model

The longitudinal case was validated using a T-37 time history file received from NASA Dryden. The results of the validation are presented in Figures 16 through 19. The initial set up for the BQM-147 longitudinal model was presented in Table 9 in Chapter VI. The same *current* file was used for both the P2B1 and P2B2 maneuvers.

a. P2B1

The results of the P2B1 maneuver are shown in Figures 20 through 23 and the pEst output listing is shown in Table 12. The estimated response for α correlates well except at the extreme edge of the pitch-down part of the maneuver. The measured data shows a sinusoidal response at the beginning

of the window prior to any control input. This may be an accentuation of the process noise due to the low sample rate. On the initial run, the Cramer-Rao bound for $C_{L\alpha}$ was unacceptably high. Rather than accept the high bound, weight estimates based on discussions with NASA Dryden personnel, were applied to the outputs and subsequent runs showed improved results. The adjustment gave a better estimated response fit for α and a more reasonable Cramer-Rao bound, but the tradeoff was an increase in the pitch-damping coefficient which is evident in the q response. The response presented for both α and q represents the best possible fit achieved from multiple combinations of output weighting. The estimated response for normal acceleration correlates well, though it seems to lead the measured response by a time step. No time skewing was attempted.

b. P2B2

The results of the P2B2 maneuver are shown in Figures 24 through 27, and the pEst output listing is shown in Table 13. The final output weighting values used in the P2B1 case were used for the P2B2 case because they appeared to give the best combination of results. The estimated α response does not keep up with the magnitude of the measured response in the pitch-down part of the maneuver and tends to dampen more quickly at the end of the maneuver. Again, this may be due to ignoring the Θ term in the α state equation. The

measured data show the same sinusoidal response in the absence of control input at the beginning of the time window and again at the end. The estimated q response correlates well. The damping on q tended to increase as weight on α was increased indicating a corellation between the α term and the q term. Normal acceleration fits well though it does not pick up the peaks at the edges of the maneuver.

3. Lateral-Directional Model

The lateral-directional case was validated using a PA-30 time history file received from NASA Dryden. The results of the validation are shown in Figures 28 through 33. The results of the combined P2B3-P2B5 lateral-directional maneuver are shown in Figures 34 through 39. The pEst output listing is presented in Table 14. The ß response correlates well at the onset of the aileron input and follows the measured response through the rudder doublet. The r response fits well at the onset of the aileron input; however, the computed response appears to dampen more quickly than the measured response at the end of the rudder doublet. The p response does not follow the rate through the roll-left portion of the aileron doublet. The estimated response fits well during the rudder input but dampens more rapidly than the measured response. The roll angle response does not correlate well with the approximated angle data obtained through numerical integration of the roll rate. The lateral acceleration

response seems to match in phase but not in amplitude. The measured response shows better damping at the completion of the rudder doublet.

4. Summary

A summary of the longitudinal parameters is presented in Table 15. The columns labeled P2B1 and P2B2 contain the results of the pEst parameter estimation runs. The Cramer-Rao bounds represent an approximation to the standard-deviation and are consistently one order of magnitude less than the value of the parameter. The large perturbation input maneuver and subsequent responses should lead one to suspect that the linear, PC based MMLE3 routine would be an insufficient model for this case study. The plots shown in Figures 12 through 15 support this suspicion. The pEst results provide a better fit between the measured and estimated data. The confidence level is higher for the parameters $C_{L\delta e}$, Cm_{α} and $Cm_{\delta e}$, which have lower relative Cramer-Rao bounds. The values for $C_{L\alpha}$ differ by a factor of 2 and the sign on Cm_q was expected to be negative, indicating a restoring moment for positive pitch rate. The positive Cm_q may indicate that there is a strong correlation between the α term and the q term. More data points are required to improve the confidence level for these two parameters.

The lateral-directional case is summarized in Table 16. Running the lateral-directional case in the non-linear PC

based routine was unsuccessful because the process noise was too high. Only the pEst results are shown. The ß derivatives and the p derivatives have reasonable Cramer-Rao bounds. The variance in the r derivatives is unacceptably high and indicates a low confidence level in the value of the parameters. A sign change in some of the control derivatives indicates a strong correlation with damping terms, a noted problem with parameter estimation methods. More flight data are required for any further analysis.

Three options are available to correct for the high Cramer-Rao bound.

1) Fix the value of the parameter
2) Weight the estimate
3) Use a better input stimuli

Without a-priori knowledge of the parameters, fixing the value of the parameter was not a practical option. The weighting option did not help to improve the overall results because of the tradeoffs in the values of other parameters. A more reasonable approach to output weighting could have been made only if there were data other than the single flight test supporting the aerodynamic data base. With the limited maneuvers, better input stimuli were not available. Without any of the options available, the only choice is to accept the high Cramer-Rao bound with the understanding that the confidence level in the value of the parameter is very low.

There were three limitations in the data that affected the outcome of the lateral-directional results. Signal coverage is very important and unless the flight test maneuvers are restricted to small perturbations about a stable flight condition, the body angles should be included in the signal set. Noise in the same general frequency range as the response is a problem. The flight data were sampled at 16 Hz and nothing is known about the sensor accuracies, filtering, digitizing and time-tagging the data. The low sample rate may have distorted the response signal by accentuating the process noise. To excite the lateral-directional modes, rudder and aileron doublets should be included in a single input maneuver, separated by sufficient time to allow for the first response to dampen. In Flight 03-24, the maneuvers were independent and combining the data sets together may have induced additional error in the response estimates.

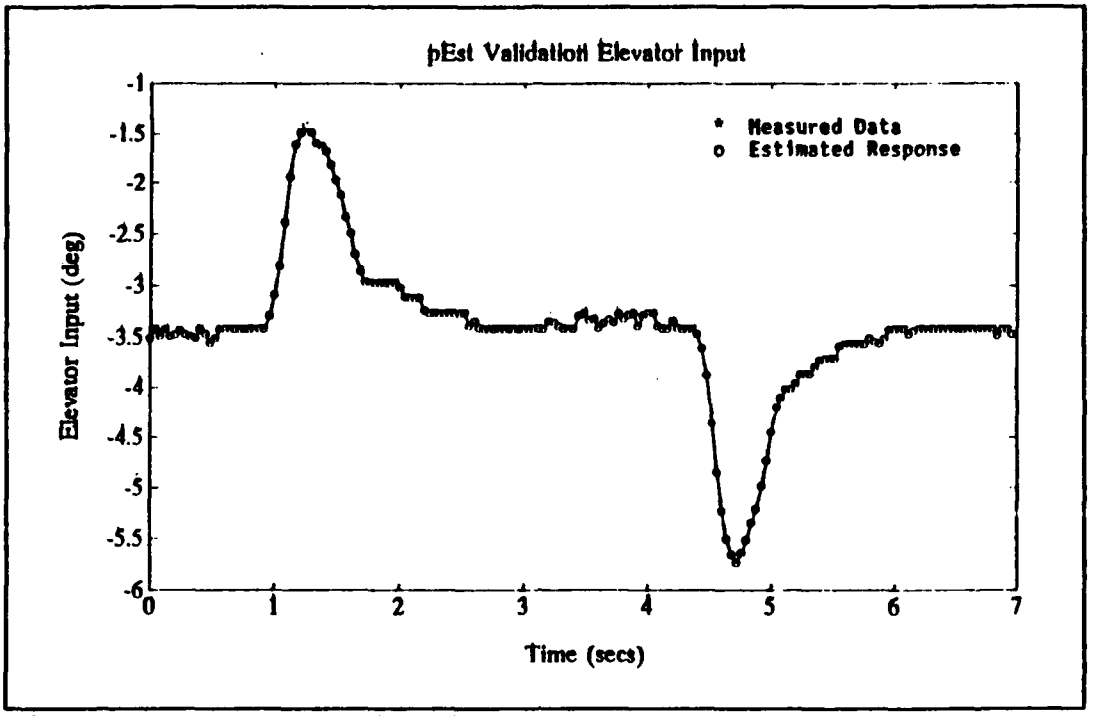

Figure 16 pEst Validation: Elevator Input

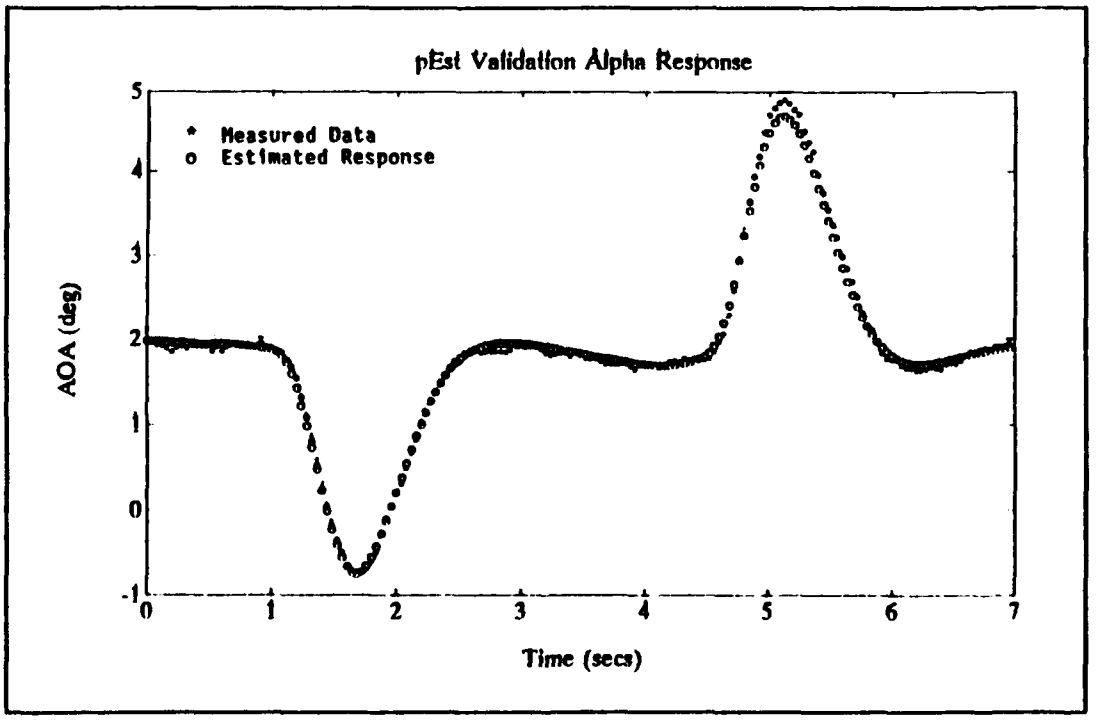

Figure 17 pEst Validation: α Response

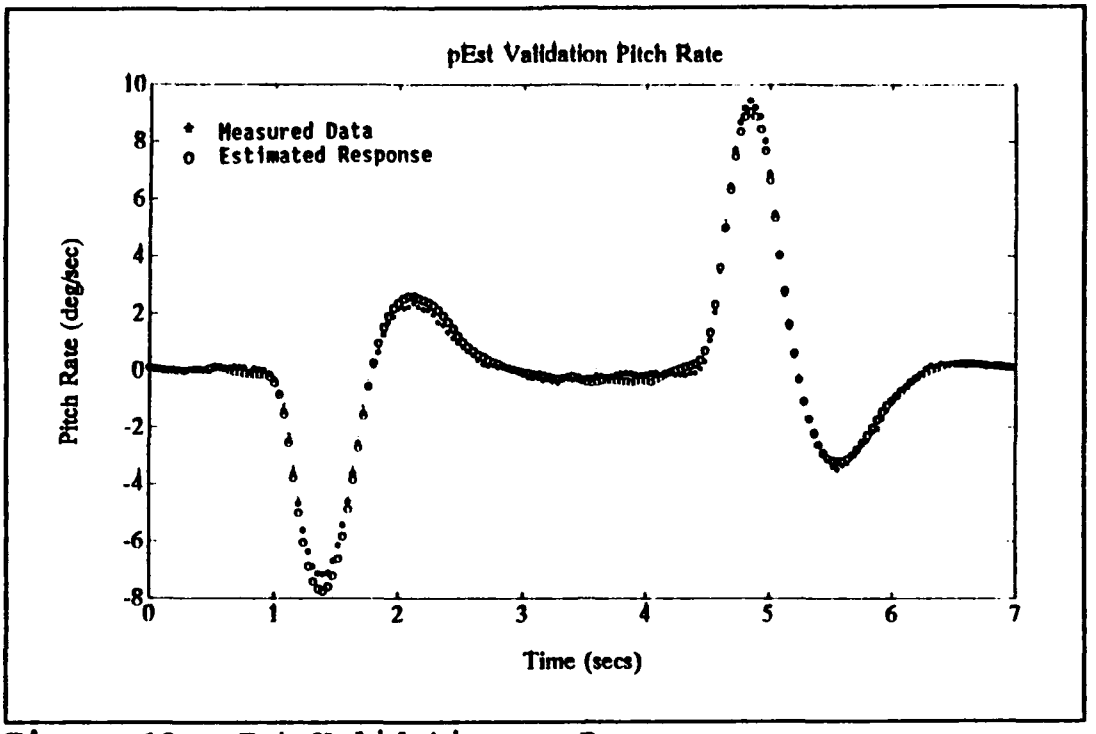

Figure 18 pEst Validation: q Response

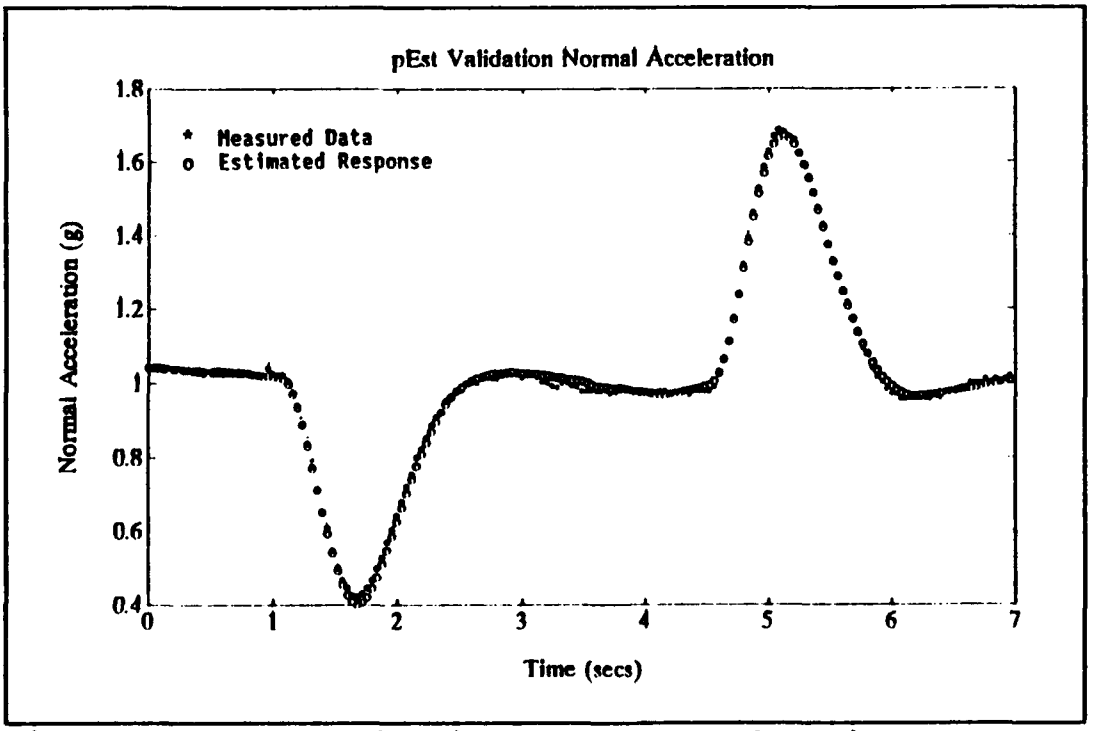

Figure 19 pEst Validation: Normal Acceleration

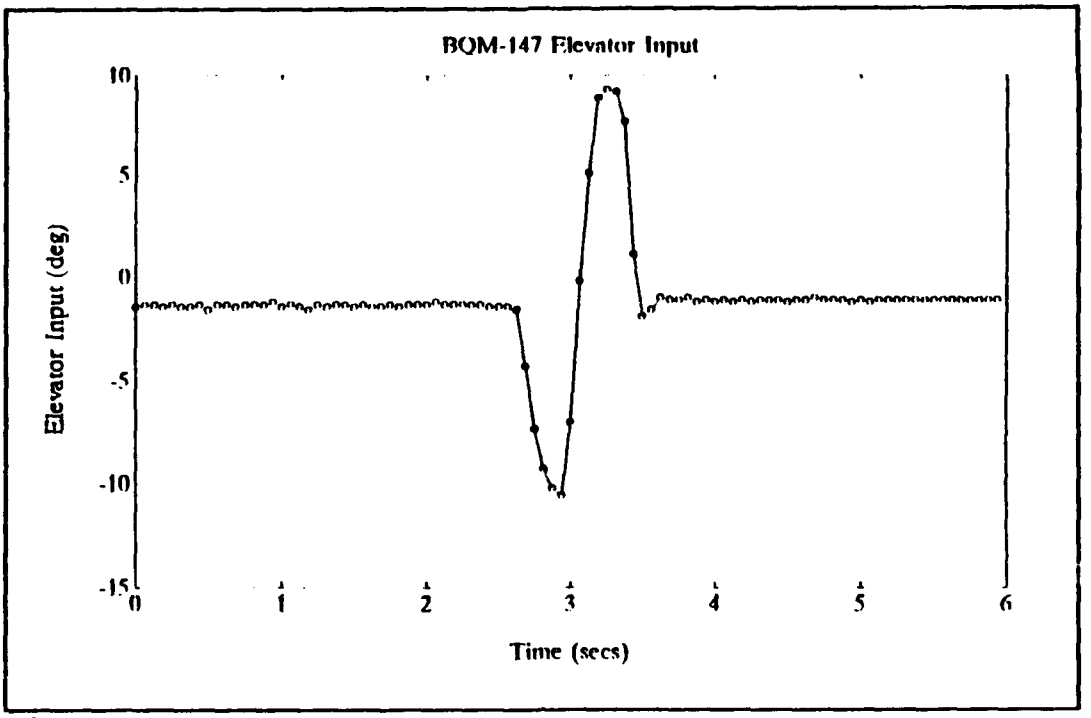

Figure 20 BQM-147 Elevator Input (P2B1)

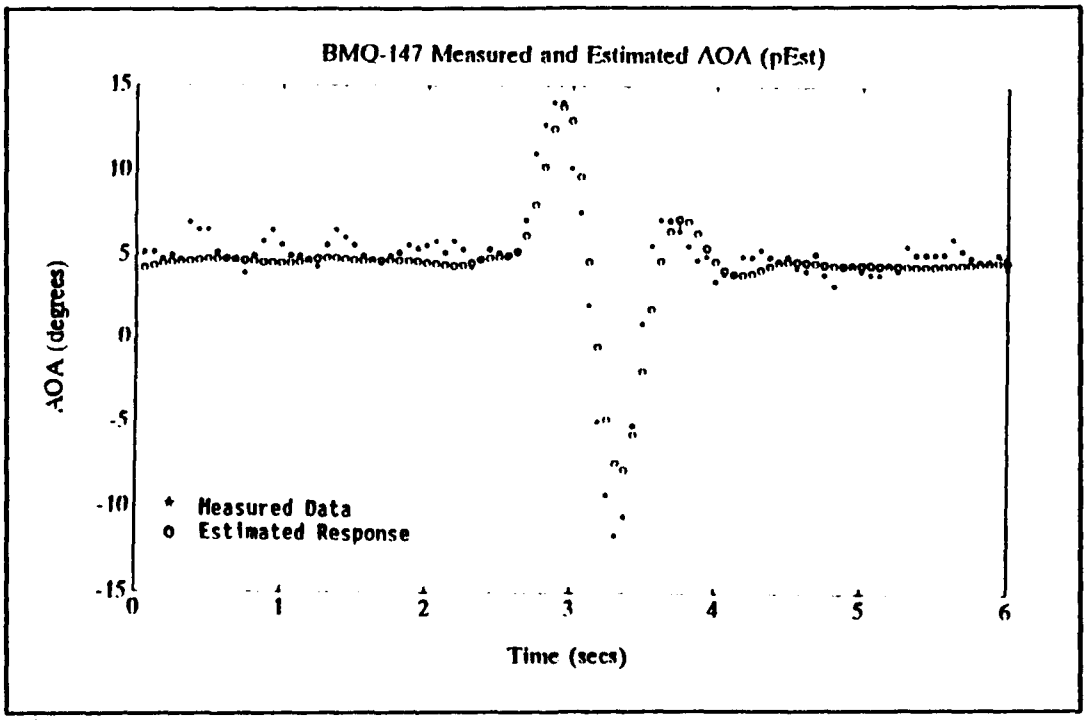

Figure 21 BQM-147 α Response (P2F1)

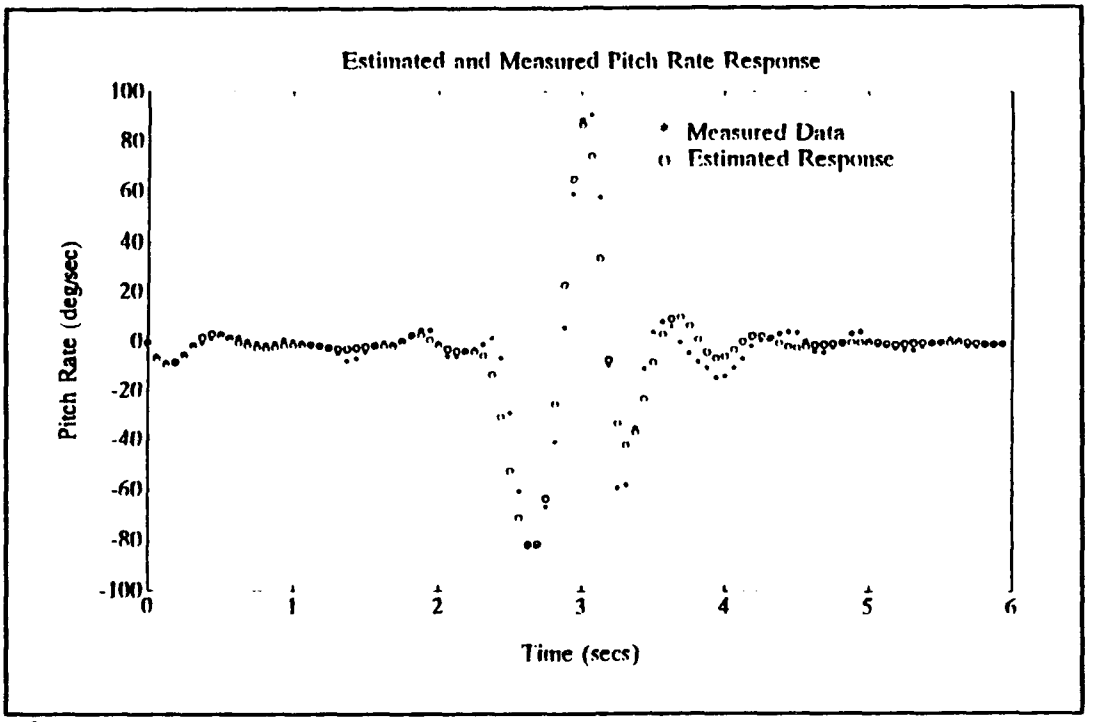

Figure 22 BQM-147 q Response (P2B1)

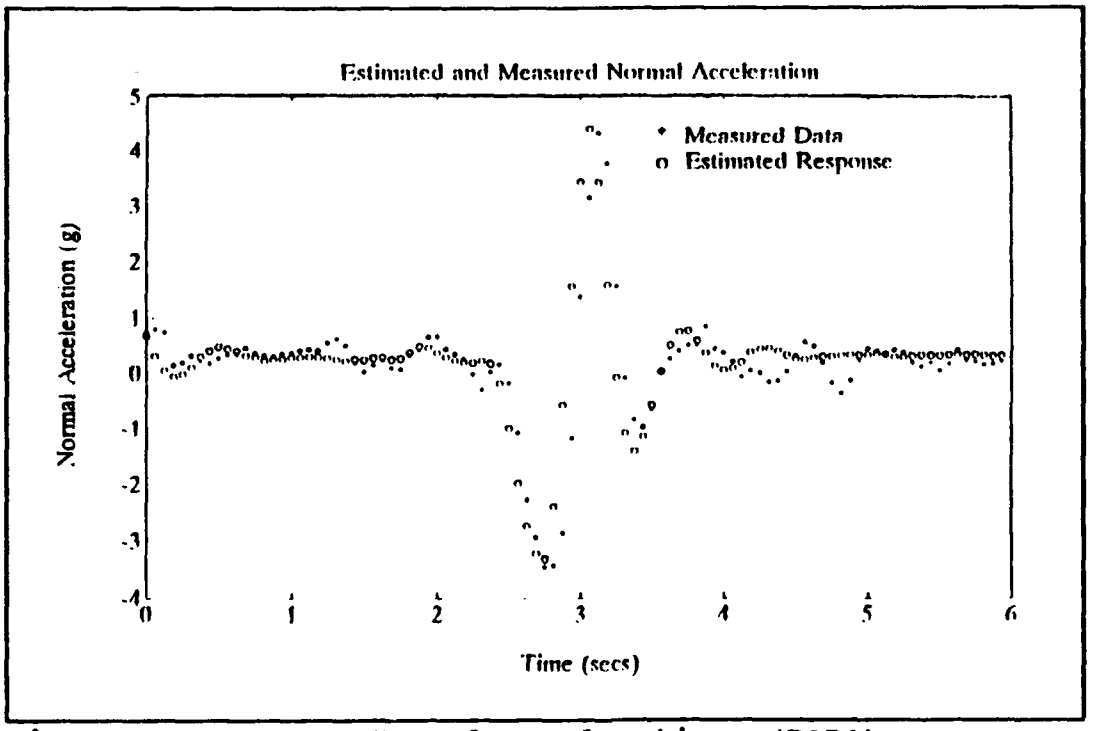

Figure 23 BQM-147 Normal Acceleration (P2B1)

TABLE 12 pEst OUTPUT LISTING

```
Iteration   17
   Lev-Marq used   1 trials. v =     0.     len =  3.150     cost =  37.65
   name         value   on?  delta        name         value   on?  delta

   cNorm0        1.173      T -.4573E-02   cmq          0.3234     T 0.2962E-02
   cNorma      0.8794E-01 T 0.1699E-03    cmde         -.1466E-02 T 0.4741E-05
   cNormde     0.2389E-01 T -.3282E-03    alpha0       -.5625     T -.1678E-02
   cm0         -.3865E-01 T -.1539E-05    ka            1.663     T 0.8075E-02
   cma         -.2951E-02 T -.1587E-04

   total cost =  37.65
  cost per response :
       alpha       q           an
        35.5       69.5        7.88
  iteration   17 used   12 integrations
  *** iteration converged
  estimate used   209 integrations

 pEst: par +cr
   name         value   on?  cr bound     name         value   on?  cr bound

   cNorm0        1.173      T 0.4632E-01   cmq          0.3234     T 0.2749E-01
   cNorma      0.8794E-01 T 0.3379E-02    cmde         -.1466E-02 T 0.4138E-04
   cNormde     0.2389E-01 T 0.2481E-02    alpha0       -.5625     T 0.1954
   cm0         -.3865E-01 T 0.1263E-02    ka            1.663     T 0.6568E-01
   cma         -.2951E-02 T 0.1338E-03

 pEst:
```

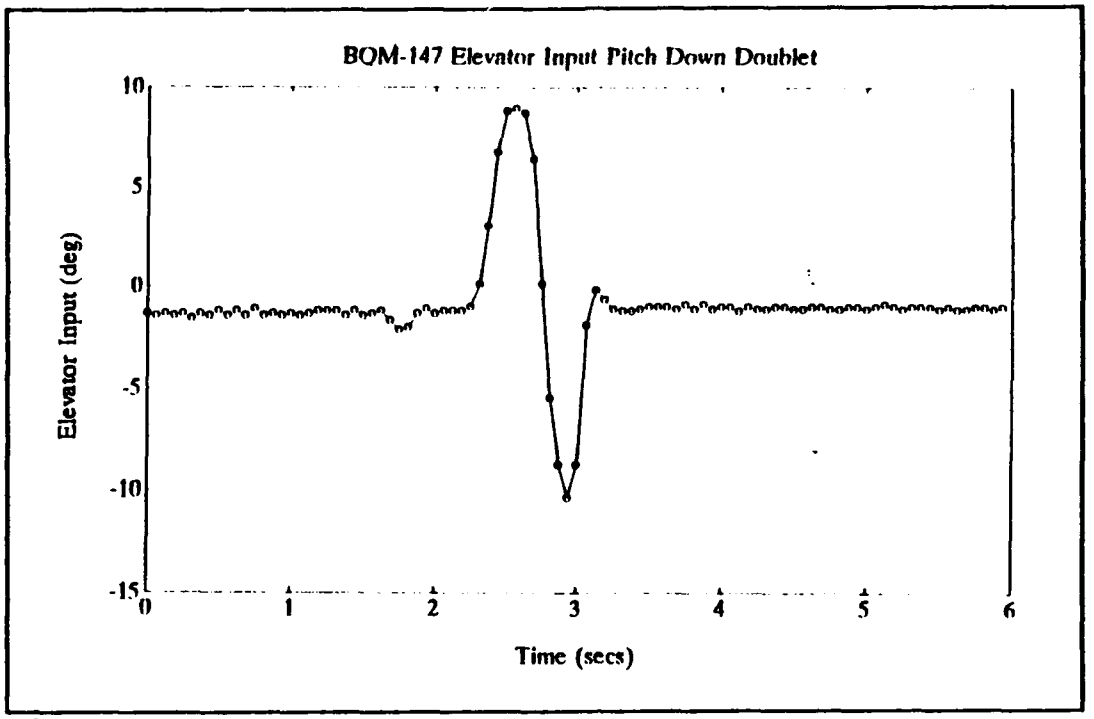

Figure 24 BQM-147 Elevator Input (P2B2)

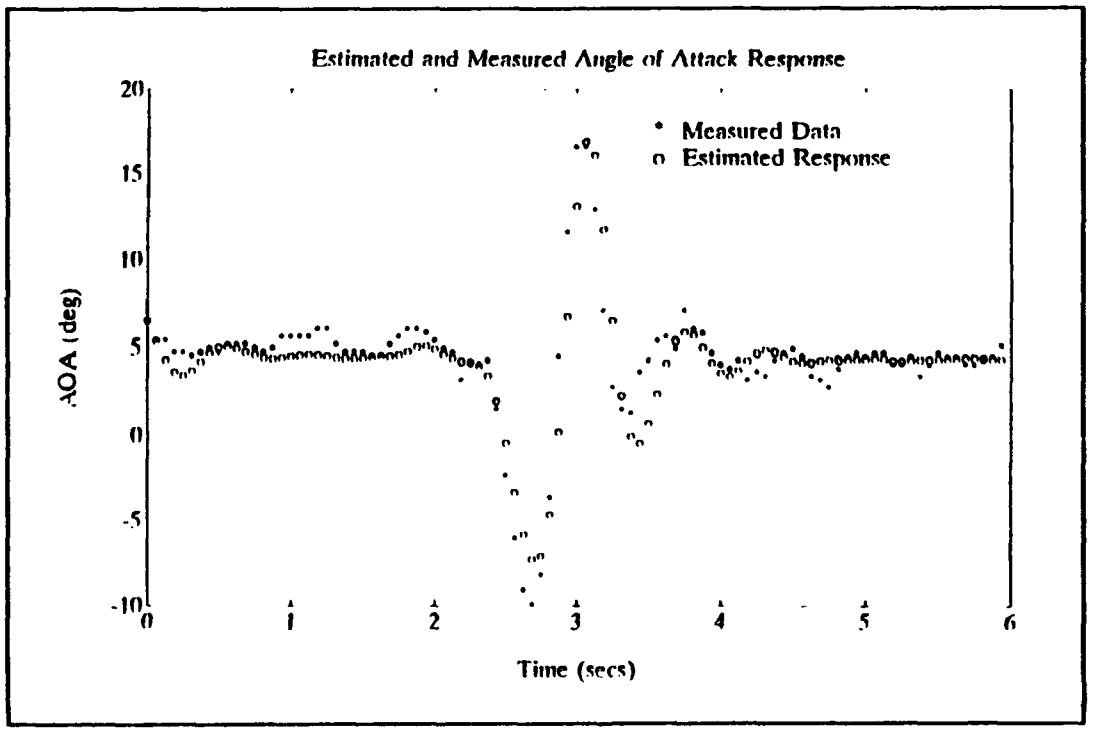

Figure 25 BQM-147 α Response (P2B2)

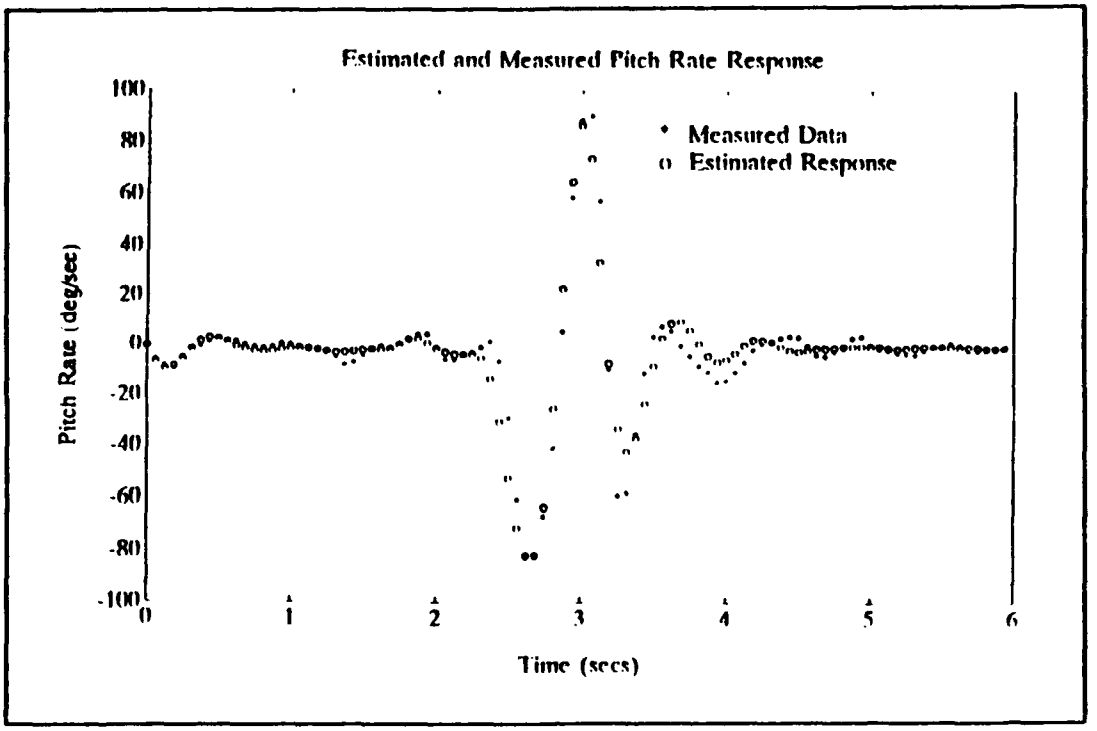

Figure 26 BQM-147 q Response (P2B2)

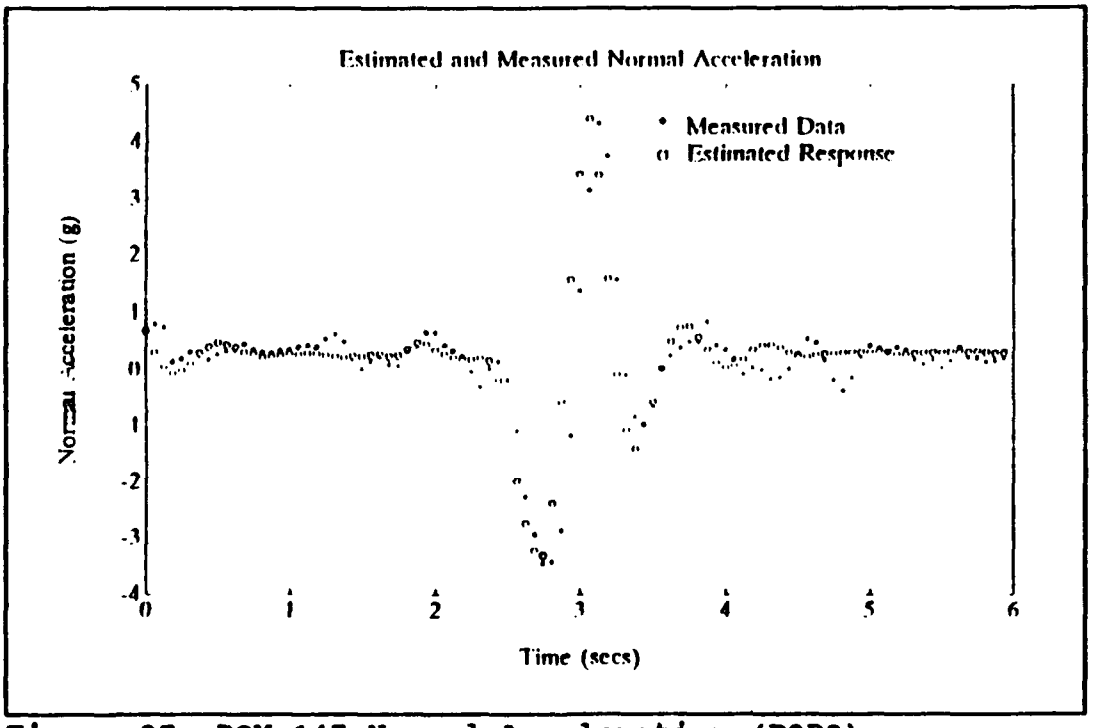

Figure 27 BQM-147 Normal Acceleration (P2B2)

TABLE 13 pEst OUTPUT LISTING (P2B2)

```
Iteration   14
   Lev-Marq used   1 trials. v =     0.     len =  1.637     cost =  103.0
   name        value   on?  delta       name        value   on?  delta

   cNorm0     0.6941     T -.1956E-02   cma        -.2266E-02 T -.3263E-05
   cNorma     0.4120E-01 T -.1341E-03   cmq        0.1355     T 0.3866E-02
   cNormde    0.2149E-01 T -.5021E-04   cmde       -.1600E-02 T 0.1210E-04
   cm0        -.3293E-01 T 0.2963E-05   ka          1.573     T -.4011E-04

   total cost =  103.0
  cost per response :
       alpha       q          an
        66.9       223.       19.5
  iteration   14 used   11 integrations
  *** iteration converged
  estimate used   157 integrations

 pEst: write out2.p2b2

writing computed time history to file 'out2.p2b2'

 pEst: par +cr
   name        value   on?  cr bound    name        value   on?  cr bound

   cNorm0     0.6941     T 0.2587E-01   cma        -.2266E-02 T 0.8947E-04
   cNorma     0.4120E-01 T 0.1786E-02   cmq        0.1355     T 0.1741E-01
   cNormde    0.2149E-01 T 0.1869E-02   cmde       -.1600E-02 T 0.4203E-04
   cm0        -.3293E-01 T 0.1119E-02   ka          1.573     T 0.3094E-01
```

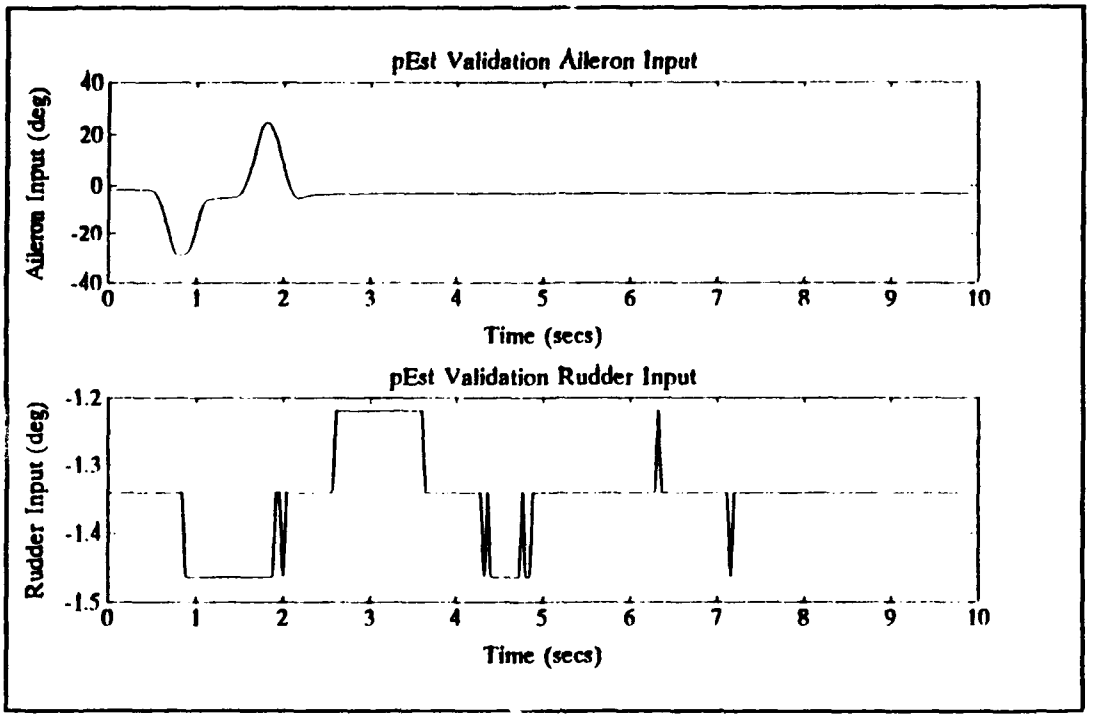

Figure 28 pEst Validation: Lateral-Directional Input

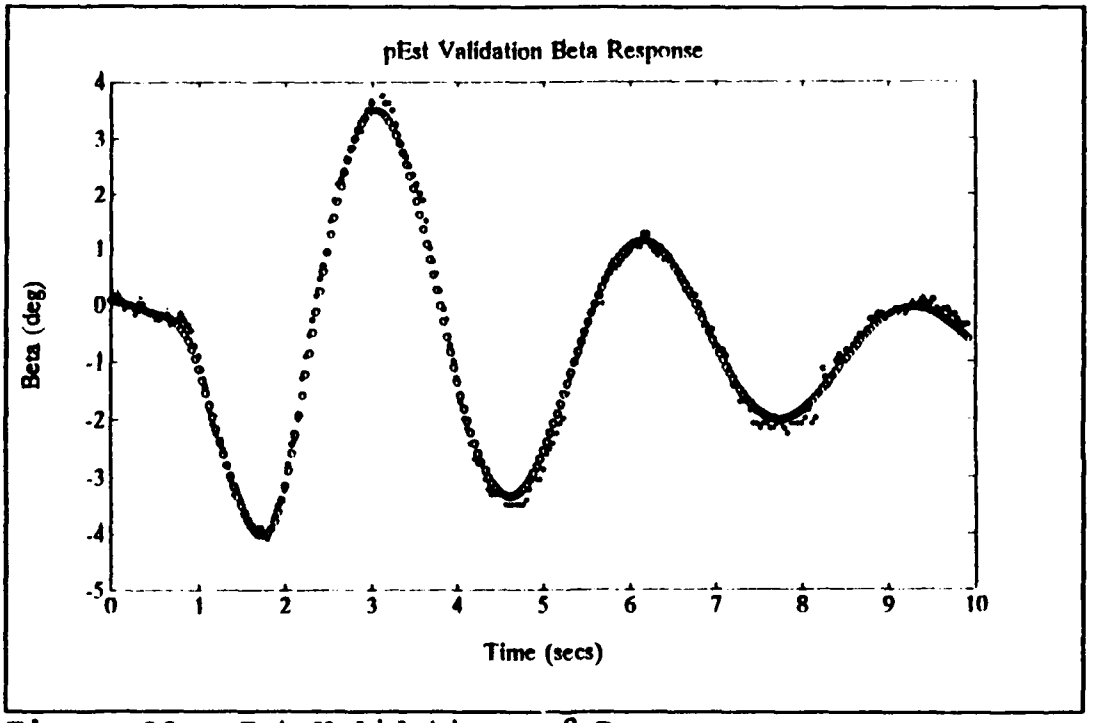

Figure 29 pEst Validation: ß Response

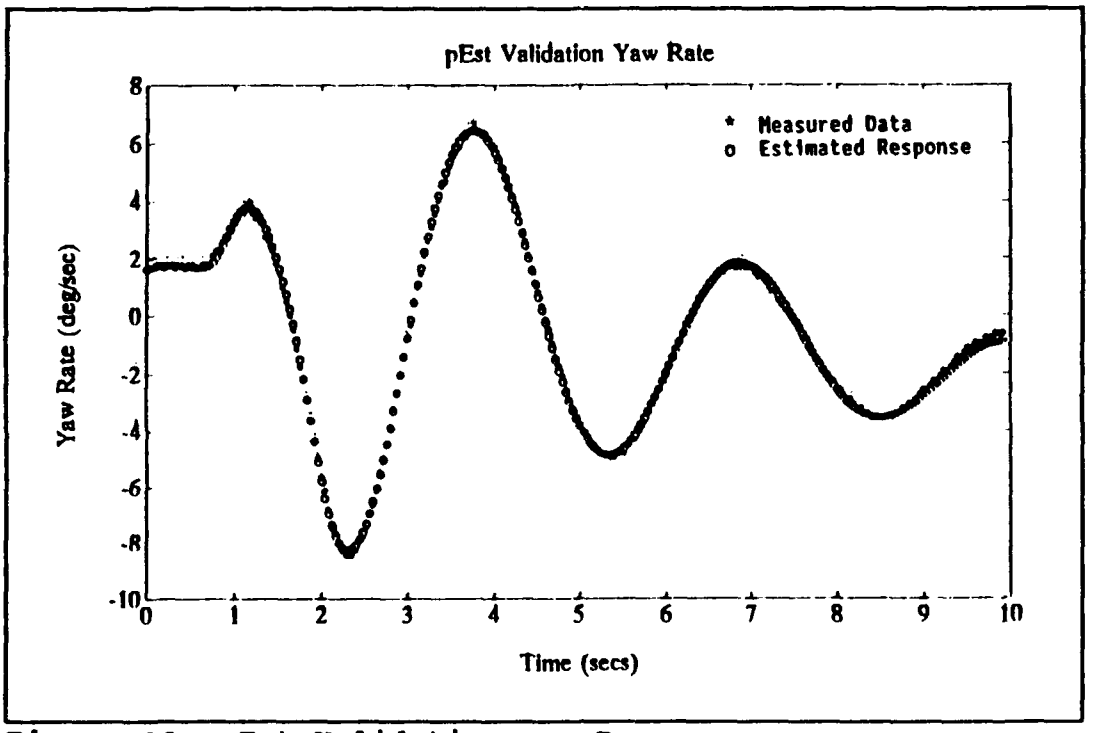

Figure 30 pEst Validation: r Response

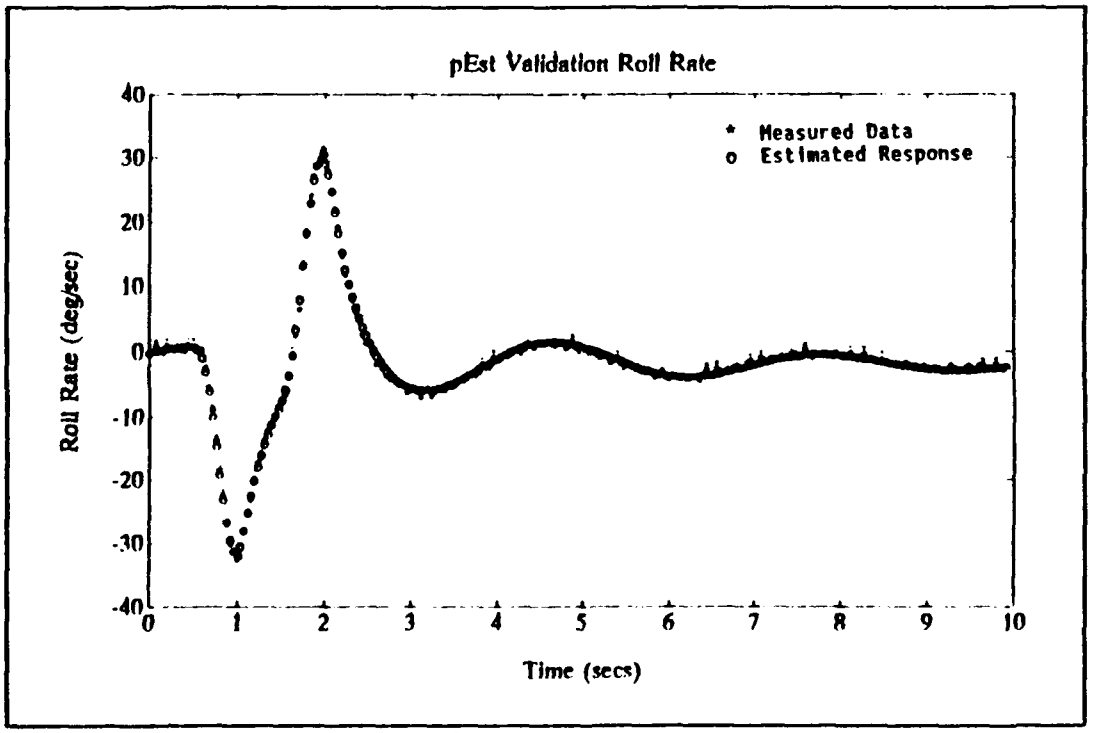

Figure 31 pEst Validation: p Response

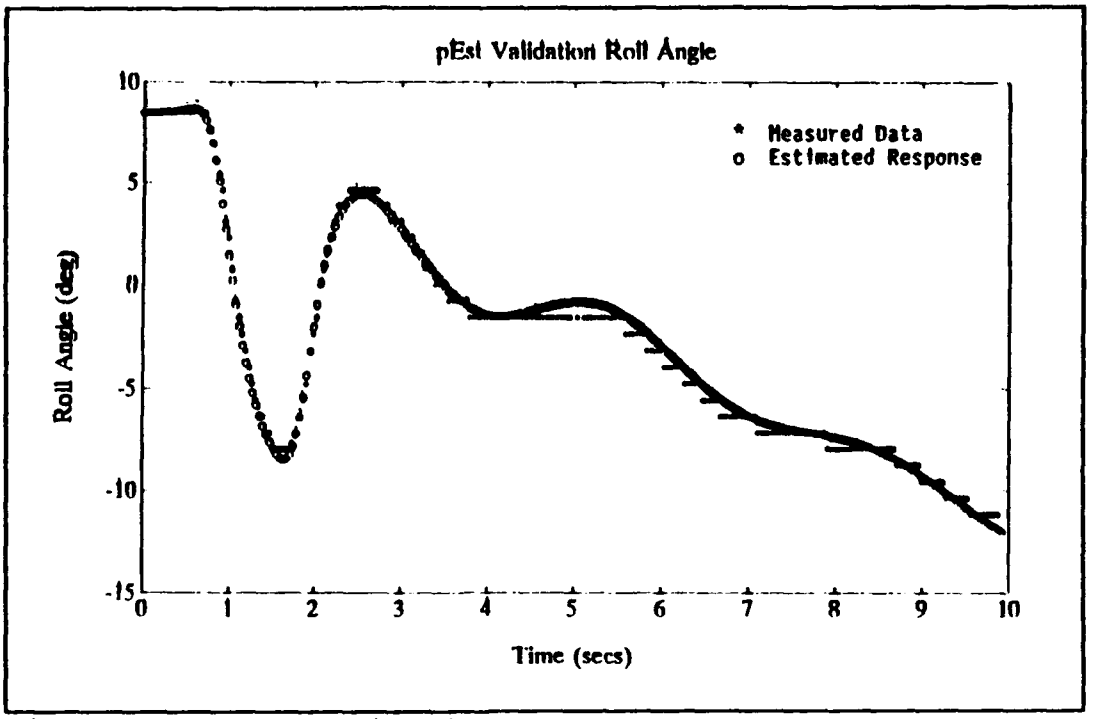

Figure 32 pEst Validation: ϕ Response

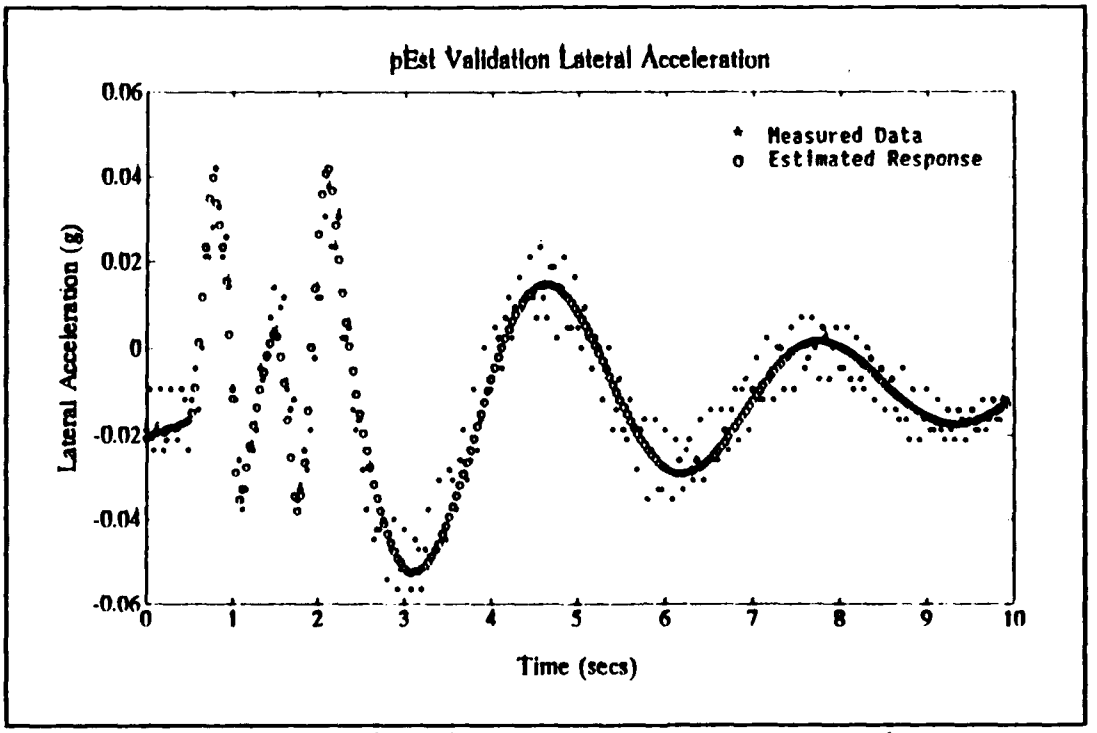

Figure 33 pEst Validation: Lateral Acceleration

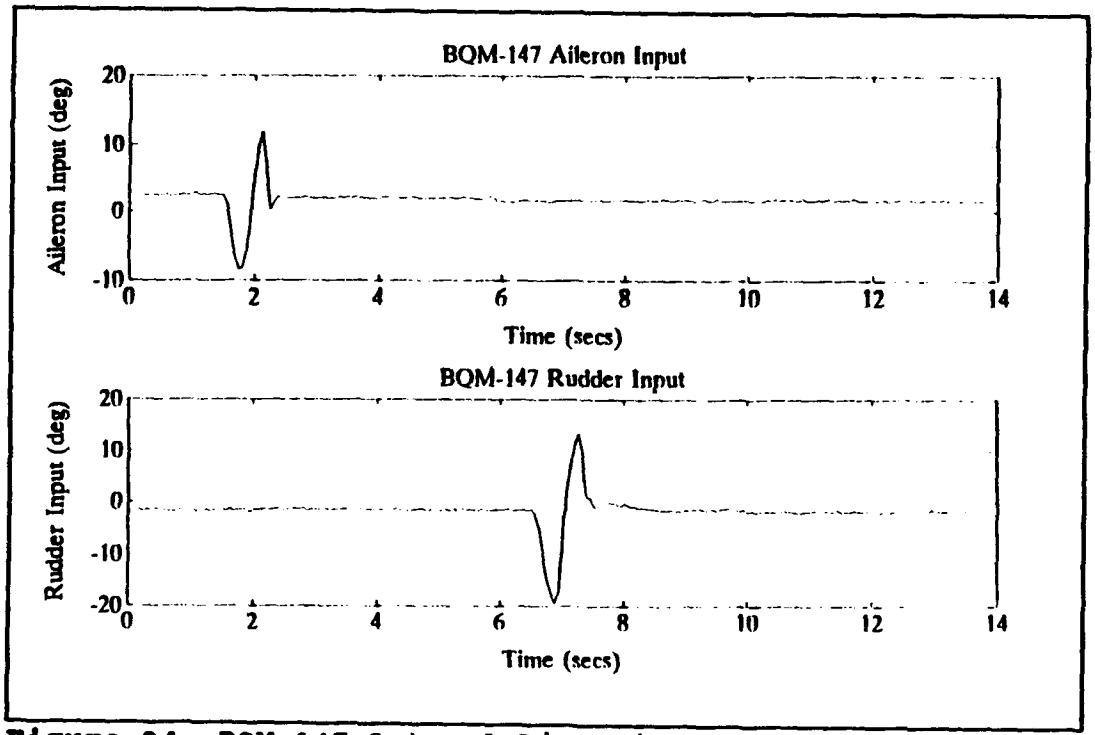

Figure 34 BQM-147 Lateral-Directional Input

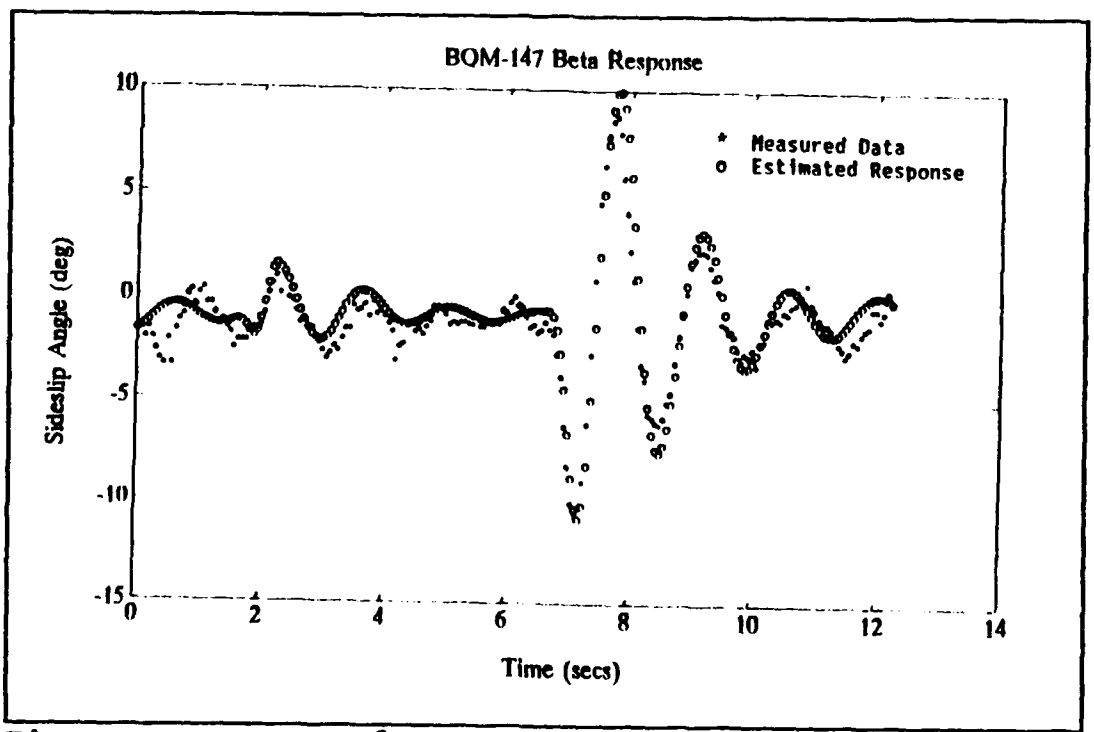

Figure 35 BQM-147 ß Response

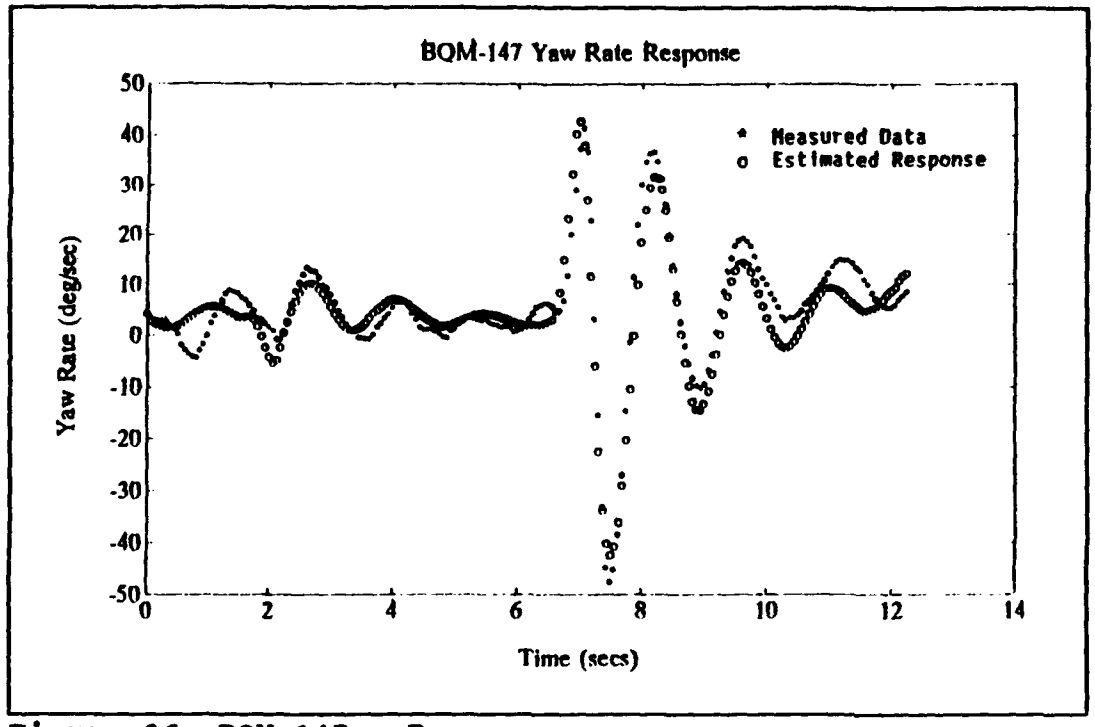

Figure 36 BQM-147 r Response

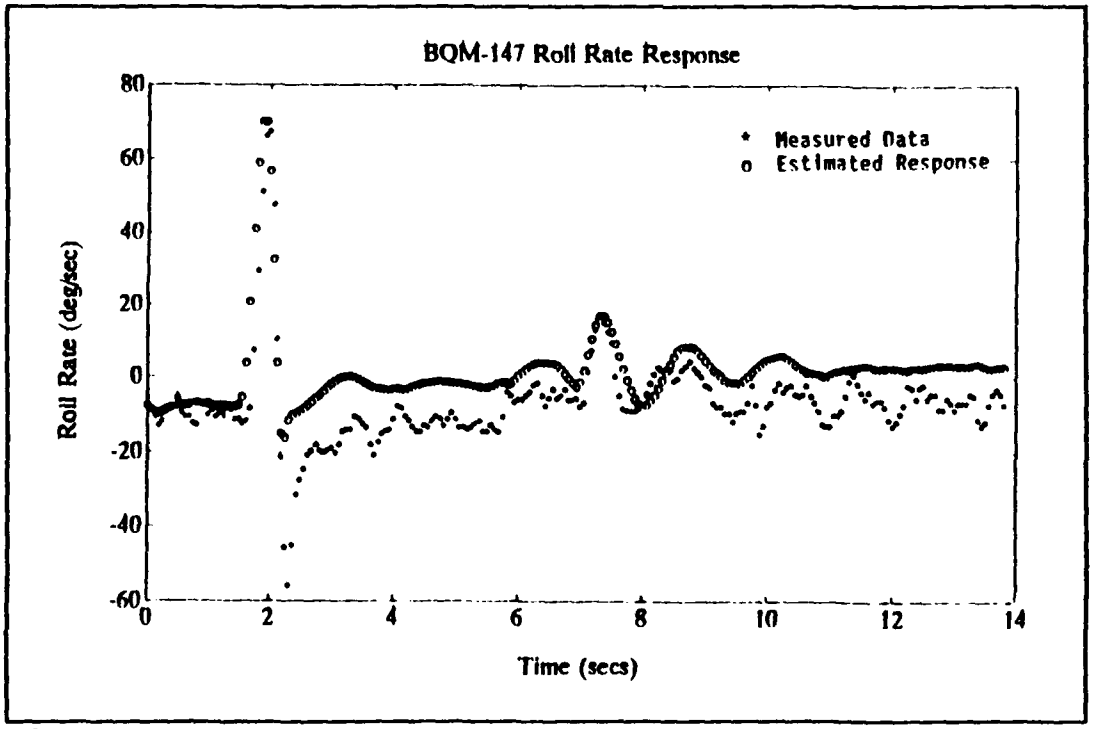

Figure 37 BQM-147 p Response

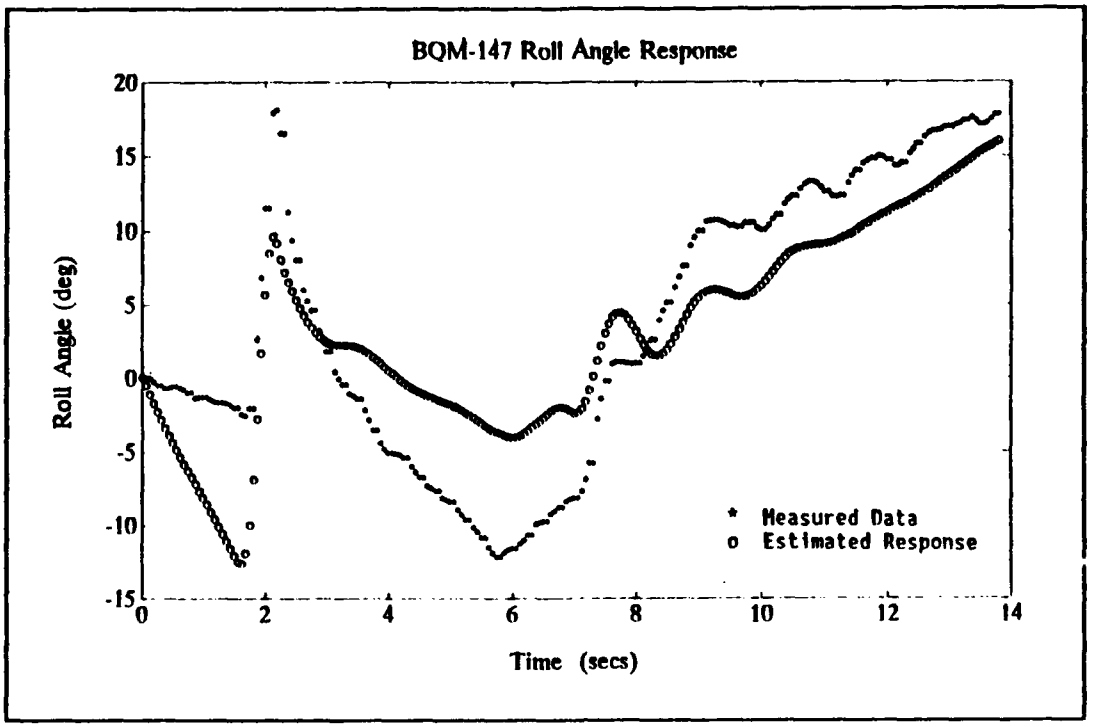

Figure 38 BQM-147 ϕ Response

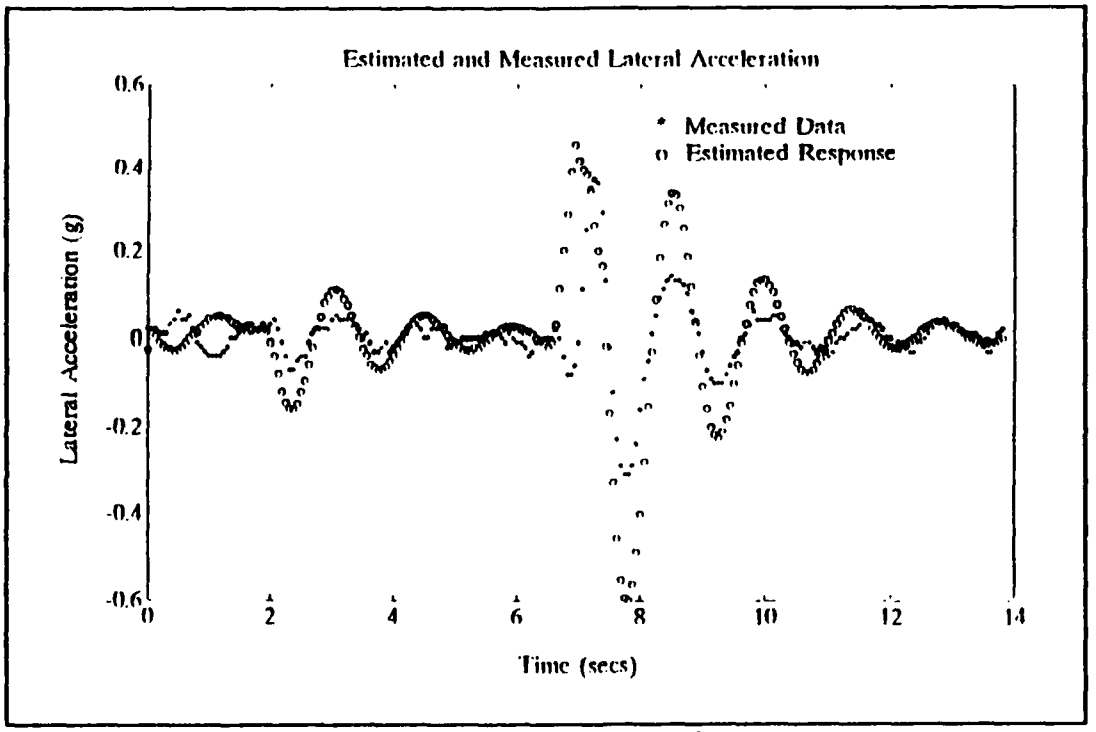

Figure 39 BQM-147 Lateral Acceleration

TABLE 14 pEst OUTPUT: LATERAL-DIRECTIONAL

```
 Lev-Marq used   1 trials. v =     0.     len =  3.436     cost =  1003.
 name         value   on?  delta        name         value   on?  delta

 cy0        0.4222E-02 T -.5625E-06    cldr       0.3856E-04 T -.2546E-06
 cyb        -.8251E-02 T -.1725E-04    cn0        0.3708E-03 T -.2122E-05
 cydr       -.1882E-02 T 0.2043E-05    cnb        0.4335E-03 T 0.3397E-06
 cl0        0.1080E-02 T 0.3836E-05    cnp        -.1212E-01 T 0.1558E-03
 clb        -.9698E-04 T 0.2407E-07    cnr        -.7893E-03 T 0.1786E-03
 clp        -.5860E-01 T -.2733E-03    cnda       -.7178E-04 T 0.3820E-06
 clr        -.3279E-02 T -.1693E-03    cndr       -.2109E-03 T 0.2517E-06
 clda       -.6099E-03 T -.1818E-05    kb          1.067     T 0.2492E-02

 total cost =  1003.
cost per response :
      beta        p           r          phi         ay
      51.2      3.714E+03    322.        817.        109.
iteration   8 used   19 integrations
*** iteration converged
estimate used   155 integrations

pEst: par +cr
 name         value   on?  cr bound     name         value   on?  cr bound

 cy0        0.4222E-02 T 0.2725E-02    cldr       0.3856E-04 T 0.8644E-05
 cyb        -.8251E-02 T 0.1162E-02    cn0        0.3708E-03 T 0.8765E-04
 cydr       -.1882E-02 T 0.6809E-03    cnb        0.4335E-03 T 0.1105E-04
 cl0        0.1080E-02 T 0.4500E-04    cnp        -.1212E-01 T 0.3082E-02
 clb        -.9698E-04 T 0.9580E-05    cnr        -.7893E-03 T 0.6030E-02
 clp        -.5860E-01 T 0.2814E-02    cnda       -.7178E-04 T 0.1808E-04
 clr        -.3279E-02 T 0.2653E-02    cndr       -.2109E-03 T 0.1095E-04
 clda       -.6099E-03 T 0.2033E-04    kb          1.067     T 0.9169E-01

pEst: write outlat7
```

TABLE 15 LONGITUDINAL SUMMARY

Parameter	Initial	MMLE3	P2B1	P2B2
$C_{L\alpha}$	2.4350	2.7391	5.0367	2.3600
$CL_{\delta e}$	1.6900	0.5015	1.3689	1.2314
Cm_{α}	-0.1089	-0.0887	-0.1691	-0.1298
Cm_{q}	-0.6670	-0.1078	0.4997	0.1355
$Cm_{\delta e}$	-0.4060	-0.0683	-0.0840	-0.0917
Cramer-Rao Bounds				
$C_{L\alpha}$		0.1084	0.1936	0.1023
$CL_{\delta e}$		0.0763	0.1422	0.1071
Cm_{α}		0.0028	0.0077	0.0051
Cm_{q}		0.0414	0.0275	0.0174
$Cm_{\delta e}$		0.0042	0.0024	0.0024

TABLE 16 LATERAL DIRECTIONAL SUMMARY

Parameter	Initial	pEst	Cramer-Rao
$C_{Y\beta}$	-0.2005	-0.4728	0.0665
$C_{l\beta}$	-.0325	-0.0056	0.0005
Cn_{β}	0.0430	0.0248	0.0006
Cl_{p}	-0.3525	-0.0586	0.0028
Cn_{p}	0.0027	-0.0121	0.0031
Cl_{r}	0.0729	0.0033	0.0026
Cn_{r}	-0.0230	-0.0008	0.0060
$Cl_{\delta a}$	0.1377	-0.0349	0.0012
$Cn_{\delta a}$	-0.0194	-0.0041	0.0010
$C_{Y\delta r}$	0.1130	-0.1078	0.0390
$Cl_{\delta r}$	0.0023	0.0022	0.0005
$Cn_{\delta r}$	-0.0138	-0.0121	0.0006

VIII. CONCLUSIONS AND RECOMMENDATIONS

A. CONCLUSIONS

Based on the results presented in Chapter 7, the following conclusions are made.

1) The PC-based parameter estimation routine is ideally suited for small maneuvers on stable platforms. The magnitude of the maneuvers in Flight 03-24 exceeded the range of validity for the linear model.

2) The pEst routine was successfully integrated into the NPS Department of Aeronautics and Astronautics flight research program.

3) Noise in the same general frequency range as the system response constitutes a major problem.

4) Body angles should be included in the signal set unless the maneuvers are restricted to small perturbations about a stable flight condition.

5) Improving the confidence level in the values of the parameters presented in Tables 15 and 16 will require modifications to the flight test program.

B. RECOMMENDATIONS

Based on the conclusions presented above and the problems encountered during the course of this study, the following recommendations are made.

For the Marine Corps UAV Project Office, Intelligence Systems (C2IU), Marine Corps Research, Development and Acquisition Command, Quantico, VA. :

1) Evaluate the current status of the BQM-147 Program and determine if additional flight testing to provide higher confidence values of stability and control parameters is warranted.

2) If higher confidence values are desired, formulate a clear set of objectives and modify the flight test program to include a series of multiple maneuvers designed specifically to meet those objectives. The maneuvers should include repeated data points, and roll and pitch angles should be measured.

For the NPS, Department of Aeronautics and Astronautics:

1) Update the Department PC Lab to include MATLAB version 3.5j or higher. As a part of the update, add the State-Space Identification Tool to the current inventory of MATLAB toolboxes. The update will allow instructional use of the PC-based routine in the flight dynamics and systems courses and practical application of a desk-top routine at the NPS UAV Flight Research Lab.

2) Incorporate pEst as an instructional tool in the Flight Dynamics courses at NPS.

3) Investigate modification of the user-modifiable subroutines in pEst to include helicopter dynamics and missile dynamics.

4) Investigate the feasibility of offering a course in non-linear flight dynamics or non-linear control of aerospace vehicles.

5) Suggest as a potential project for the Avionics System Design or Aircraft Design courses, the design of an instrumentation package for a UAV Flight Test Program that would respond to a real-world DoD requirement.

LIST OF REFERENCES

1. Hill, Maynard L., "Delta Wing Mini-UAV's", *Unmanned Systems*, pp 23-31, Spring 1989.

2. NASA Technical Memorandum 4200, *Static Wind-Tunnel and Radio-Controlled Flight Test Investigation of a Remotely Piloted Vehicle Having a Delta Wing Planform*, by Long P. Yip, David J. Fratello, David B. Robelen and George M. Makowiec, July 1990.

3. The Johns Hopkins University, Applied Physics Laboratory, *EXDRONE Flight Manual*, by P.J. Kirsch, July 1987.

4. Lyons, Daniel F., *Aerodynamic Analysis of a U.S. Navy and Marine Corps Unmanned Air Vehicle*, Masters Thesis, Naval Postgraduate School, Monterey, CA., June 1989.

5. Bray, Robert M., *A Wind Tunnel Study of the Pioneer Remotely Piloted Vehicle*, Masters Thesis, Naval Postgraduate School, Monterey, CA., June 1991.

6. Graham, Robert G., *Implementation of a Personal Computer Based Parameter Estimation Program*, Masters Thesis, Naval Postgraduate School, Monterey, CA., March 1992.

7. Marine Corps UAV Project Office, Intelligence Systems (C2IU), Memorandum, Paul Heinhold to Professor R. Howard, 16 January 1992.

8. Erickson, Mark S., *Development of a Personal Computer Based Approach to Aircraft Parameter Identification*, Masters Thesis, AFIT, Wright-Patterson AFB, Ohio, 1991.

9. NASA Technical Memorandum 88280, *pEst Version 2.1 Users Manual*, by James E. Murray and Richard E. Maine, September 1987.

10. Siuru, Bill, *Planes Without Pilots: Advances in Unmanned Flight*, Tab/Aero Books, 1991.

11. Taylor, John W.R. and Munson, Kenneth, *Janes Pocketbook of Remotely Piloted Vehicles*, Collier Books, 1977.

12. Davis, Edward E., "The United States Unmanned Aerial Vehicles Program, The Way Ahead", paper presented at Eigth International Conference, Remotely Piloted Vehicles, Bristol, U.K. 2-4 April, 1990.

13. UAV Joint Project Office, Department of Defense Unmanned Aerial Vehicles Master Plan, 1992.

14. Fulghum, David A., "UAV's Pressed Into Action To Fill Intelligence Void", *Aviation Week & Space Technology*, pp 59-60, 19 August 1991.

15. Ljung, Lennart, *System Identification: Theory for the User*, Prentice-Hall Inc., 1987.

16. Taylor, Lawrence W. and Iliff, Kenneth W., "A Modified Newton-Raphson Method for Determining Stability Derivatives From Flight Data", paper presented at the Second International Conference on Computing Methods in Optimization Problems, San Remo, Italy, 9-13 September, 1968.

17. NASA TP-1563, *User's Manual for MMLE-3, A General FORTRAN Program for Maximum Liklihood Parameter Estimation*, Maine, Richard E. and Iliff, Kenneth W., 1980.

18. NASA Reference Publication 1168, *Application of Parameter Estimation to Aircraft Stability and Control*, Maine, Richard E. and Iliff, Kenneth W., June 1986.

19. NASA Reference Publication 1077, *The Theory and Practice of Estimating the Accuracy of Dynamic Flight-Determined Coefficients*, Maine, Richard E. and Iliff, Kenneth W., 1981.

20. Halliday, David and Resnick, Robert, *Fundamentals of Physics*, First Edition, John Wiley & Sons, Inc., 1970.

21. Ogata, Katsuhiko, *Modern Control Engineering, Second Edition*, Prentice-Hall, 1990.

22. Schmidt, Louis V., Introduction to Flight Mechanics, Class Notes, AE-3340, Naval Postgraduate School, Monterey, CA., July 1992.

23. Nelson, Robert C., *Flight Stability and Automatic Control*, McGraw-Hill Book Company, 1989.

24. Roskam, J., *Airplane Flight Dynamics and Automatic Flight Controls, Part I*, University of Kansas, 1982.

25. Etkin, Bernard, *Dynamics of Flight Stability and Control, Second Edition*, John Wiley & Sons, 1982.

26. Iliff, Kenneth W. and Maine, Richard E., *More Than You May Want to Know About Maximum Liklihood Estimation*, AIAA 84-2070, 1984.

27. Kwakernaak, H. and Sivan, R., *Linear Optimal Control Systems*, Wiley-Interscience, 1972.

28. Milne, Garth, *State Space Identification Tool, For Use With MATLAB*, The Math Works, Inc., March 1988.

29. Nakamura, S., *Applied Numerical Methods With Software*, Prentice Hall, 1991.

30. USAF Stability and Control Handbook, USAF, Wright-Patterson AFB, Ohio, October 1961.

31. Smetana, Frederick O., *Computer Assisted Analysis of Aircraft Performance, Stability and Control*, McGraw-Hill Book Company, 1984.

32. NASA Technical Memorandum 88288, *Manual for GetData Version 3.1, A FORTRAN Utility Program for Time History Data*, Richard E. Maine, October 1987.

33. Vernon, T., *XPLOT, A Utility for Plotting X-Y Data, User Manual Version 3.03*, PRC Inc, 23 January 1992.

APPENDIX A VEHICLE DESCRIPTION

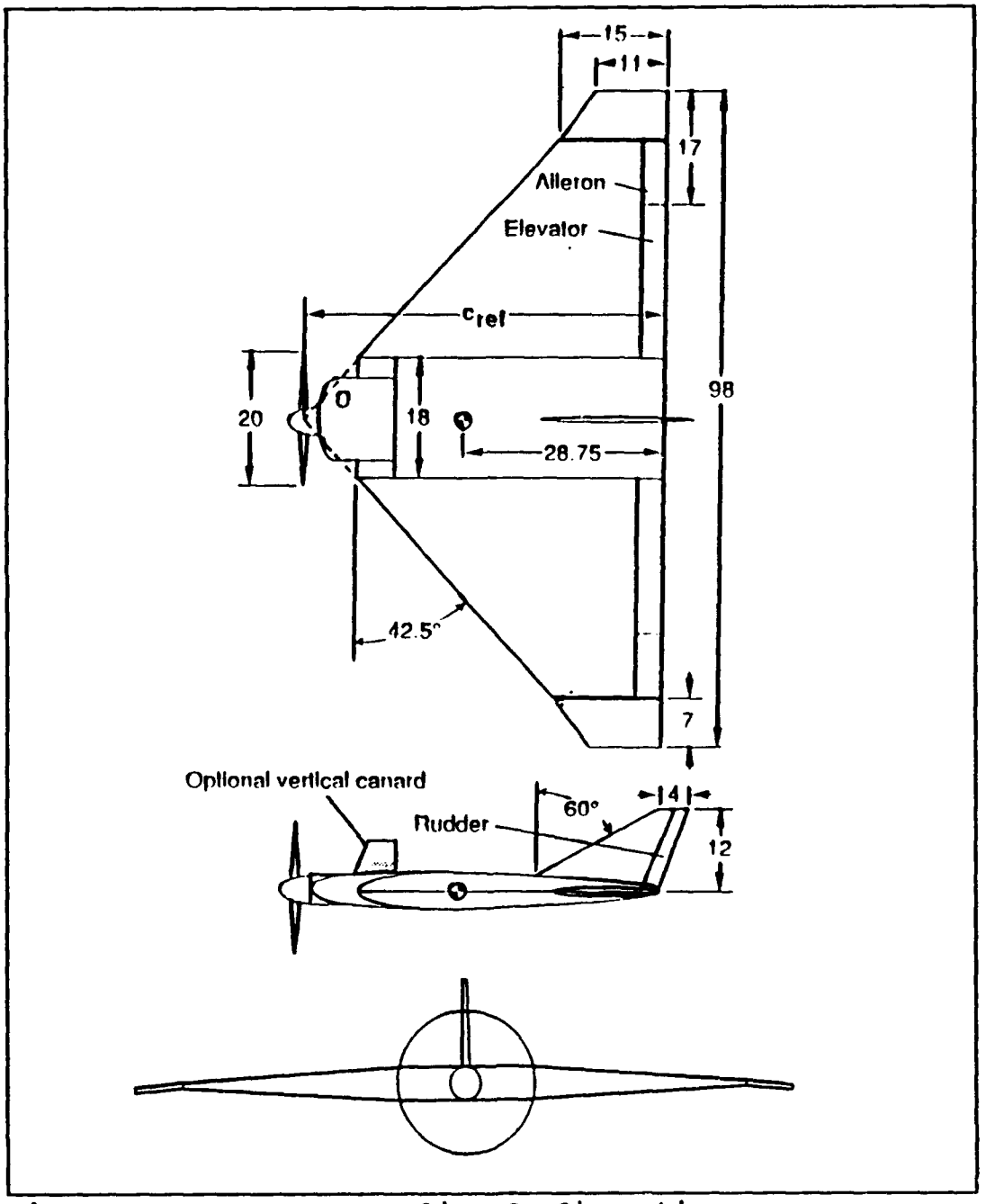

Figure A-1 EXDRONE Baseline Configuration

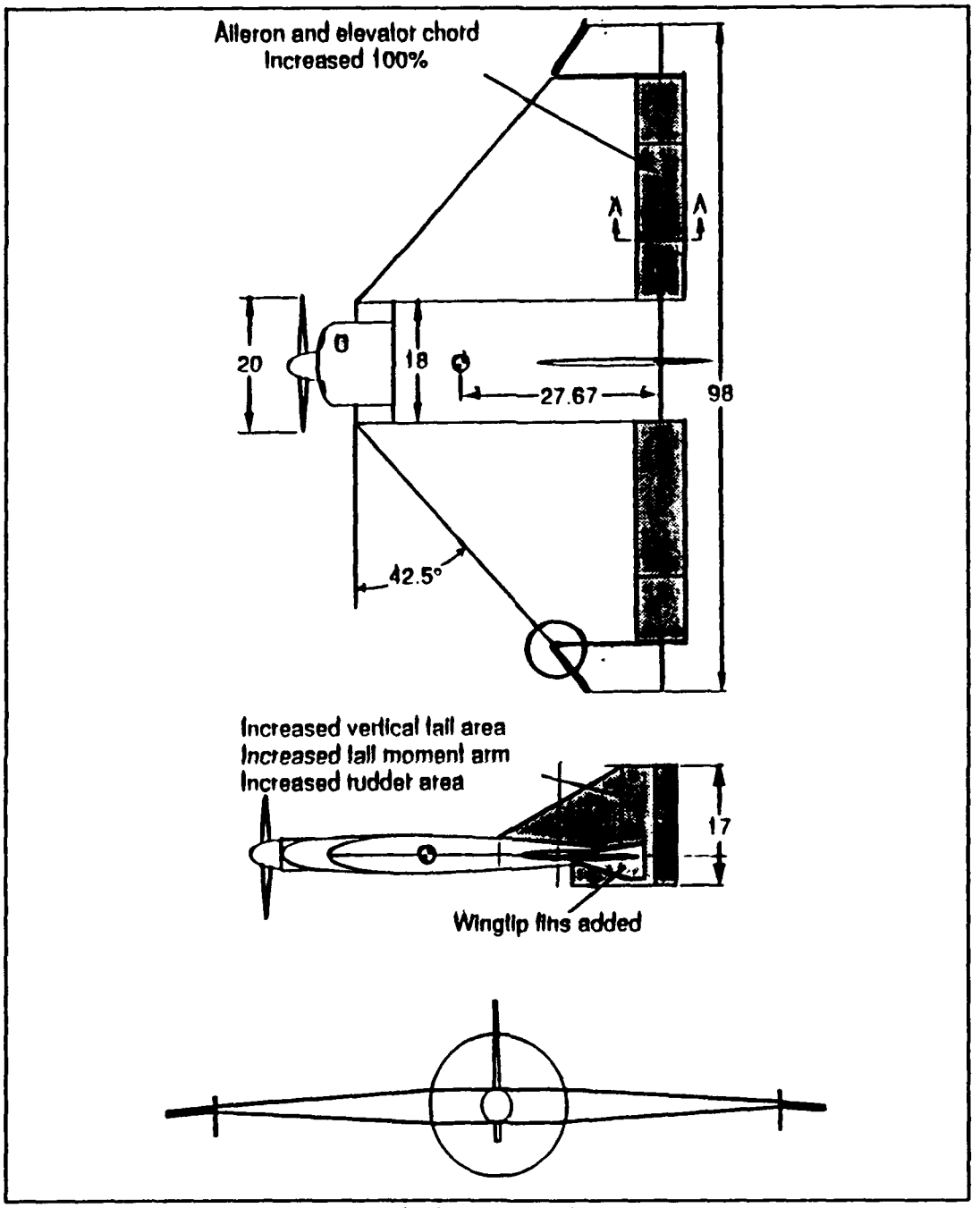

Figure A-2 EXDRONE Modified Configuration

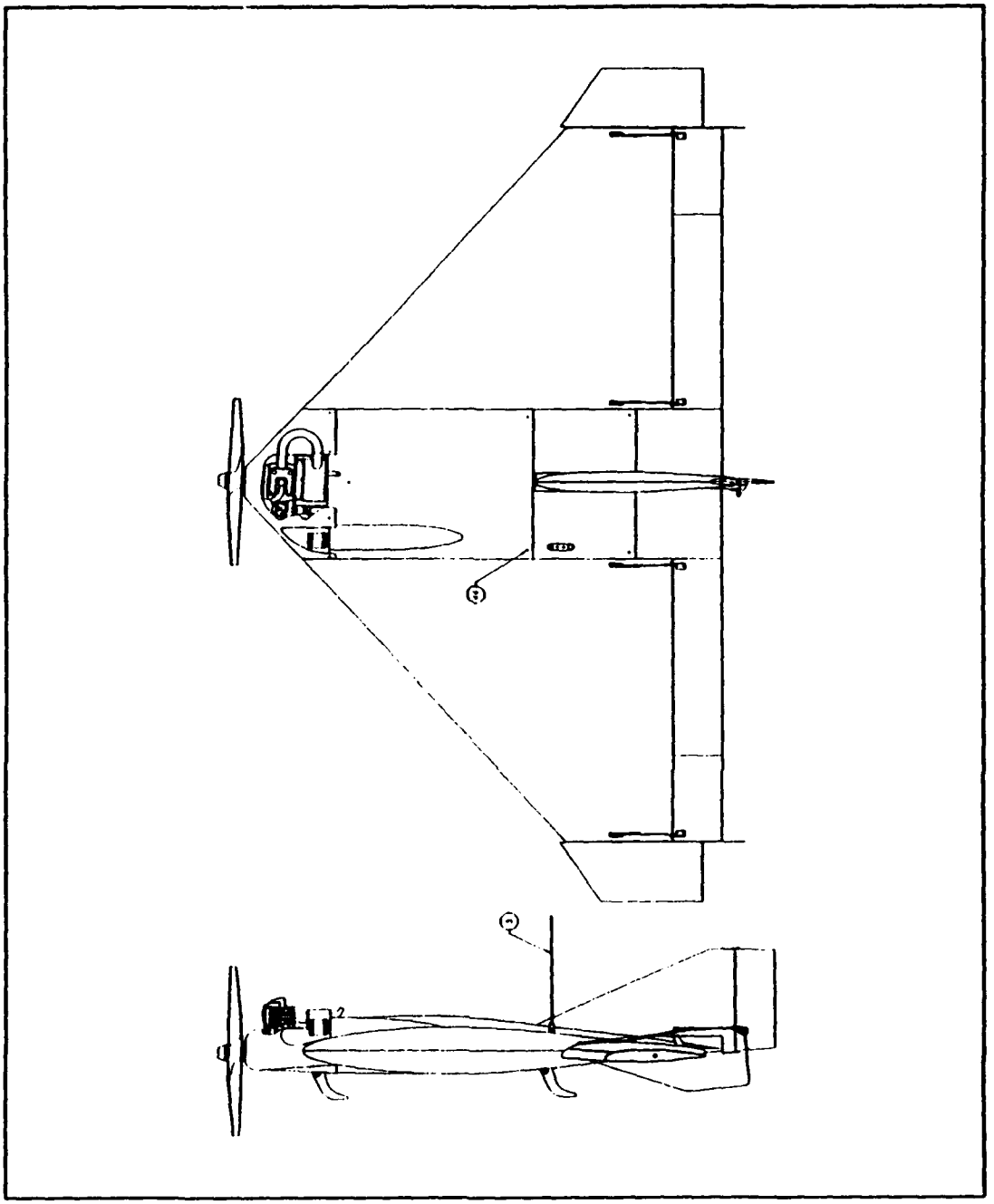

Figure A-3 BQM-147 Production Configuration

APPENDIX B FLIGHT 03-24 TIME HISTORY DATA

A. PITCH-UP DOUBLET (P2B1)

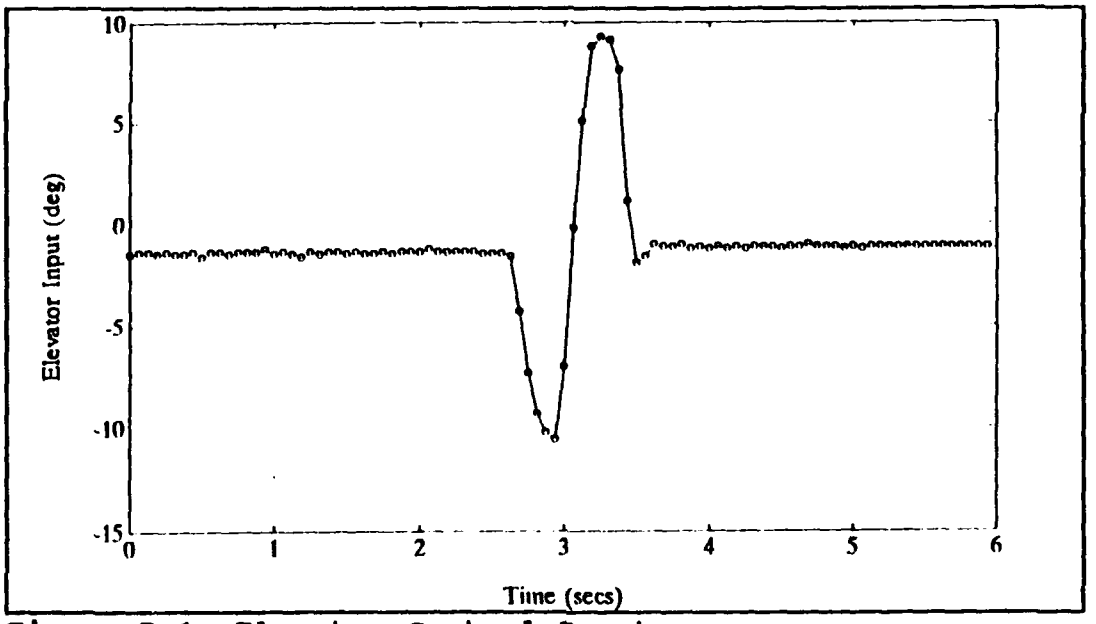

Figure B-1 Elevator Control Input

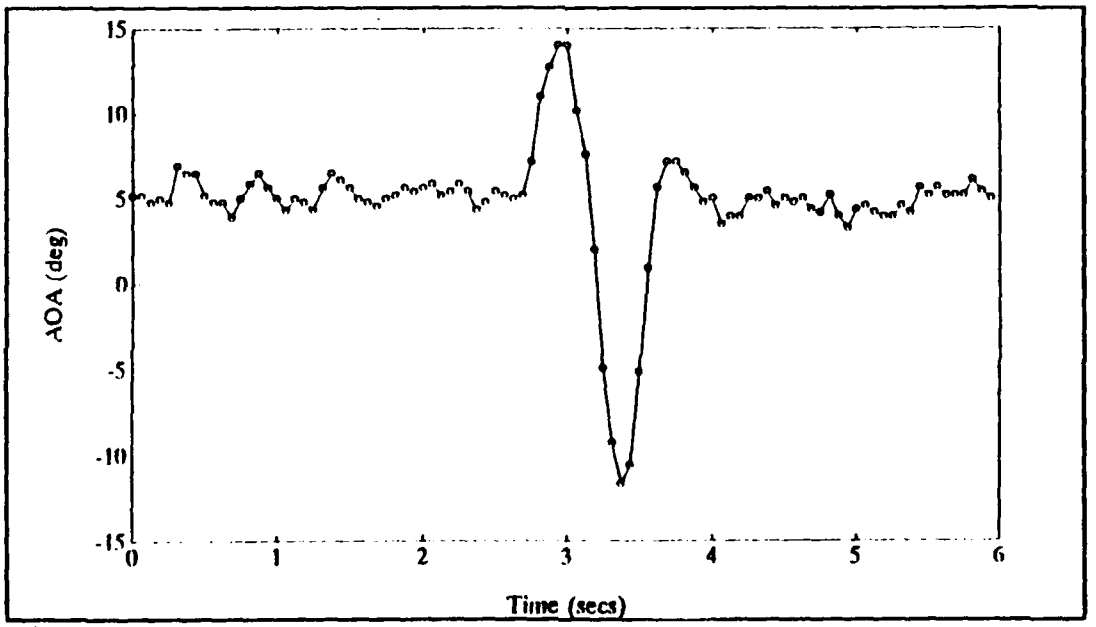

Figure B-2 Angle of Attack Response

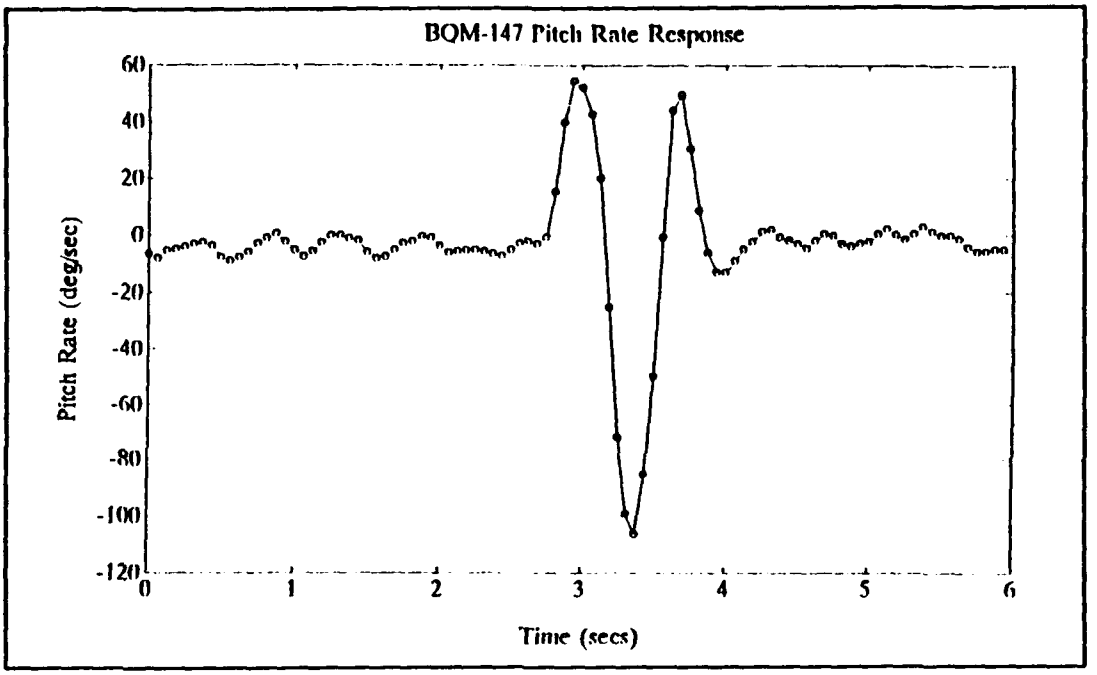

Figure B-3 Pitch-Rate Response

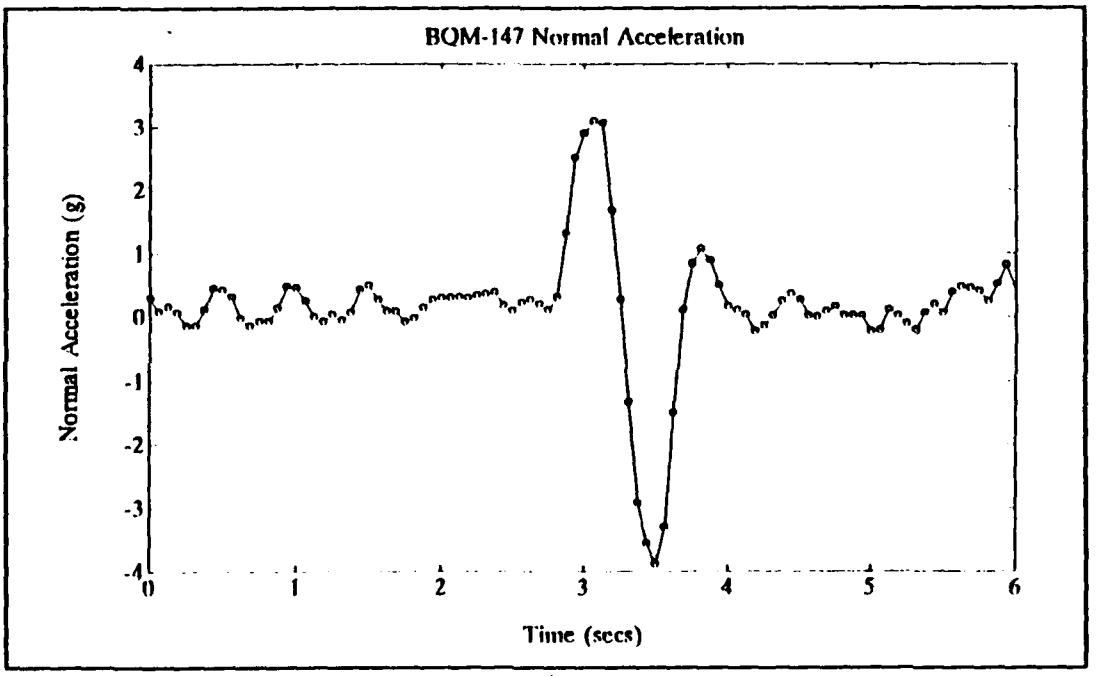

Figure B-4 Normal Acceleration

B. PITCH-DOWN DOUBLET

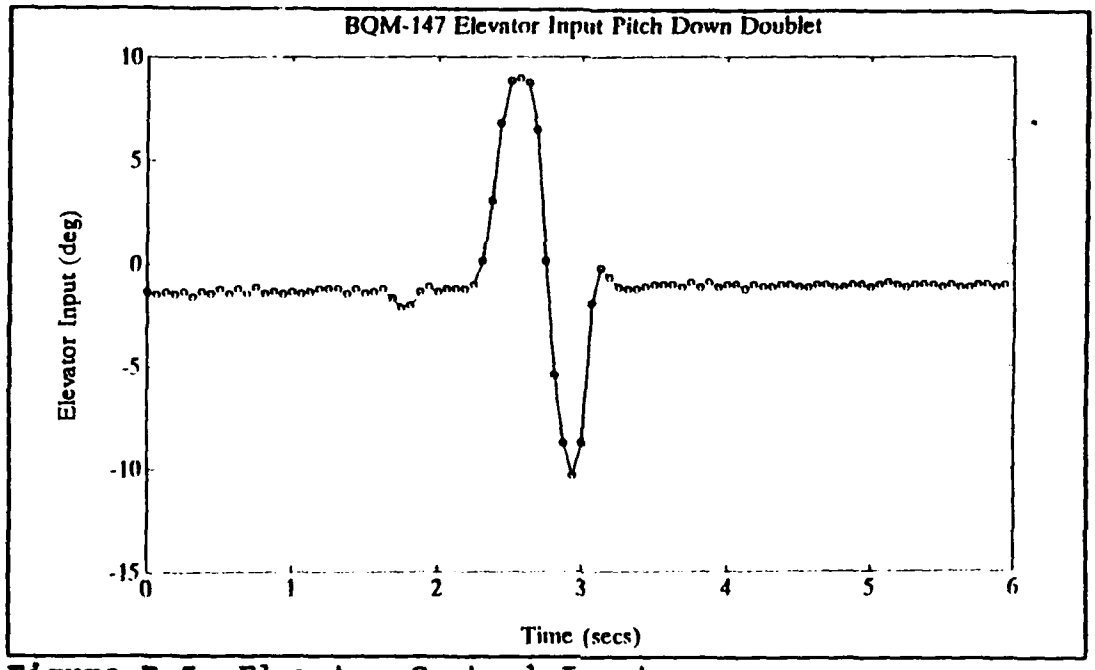

Figure B-5 Elevator Control Input

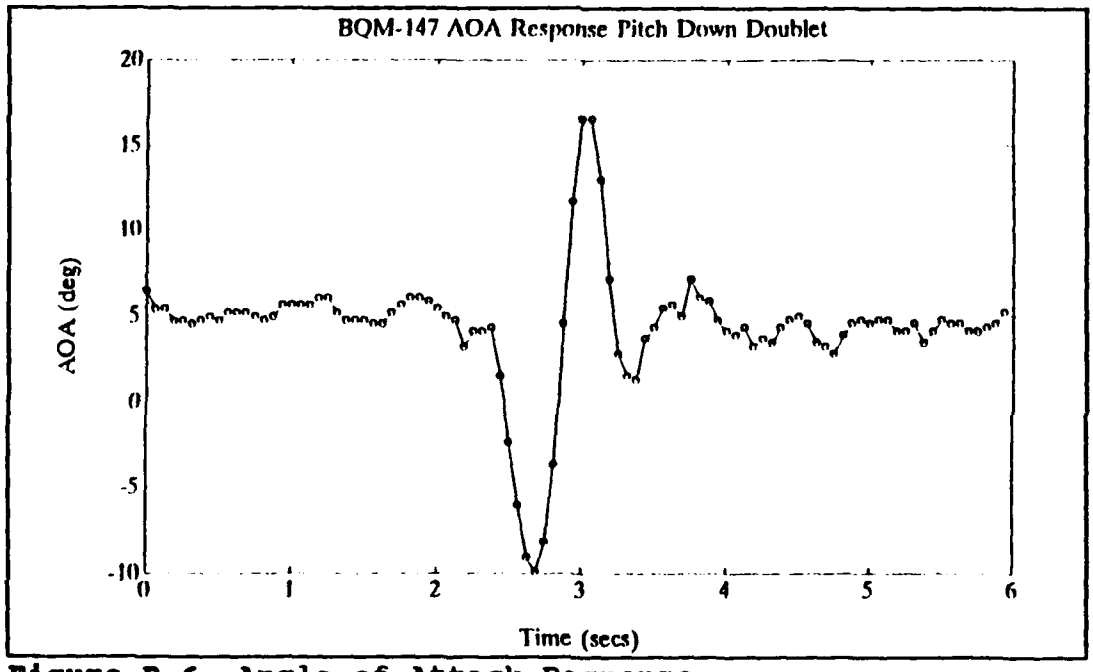

Figure B-6 Angle of Attack Response

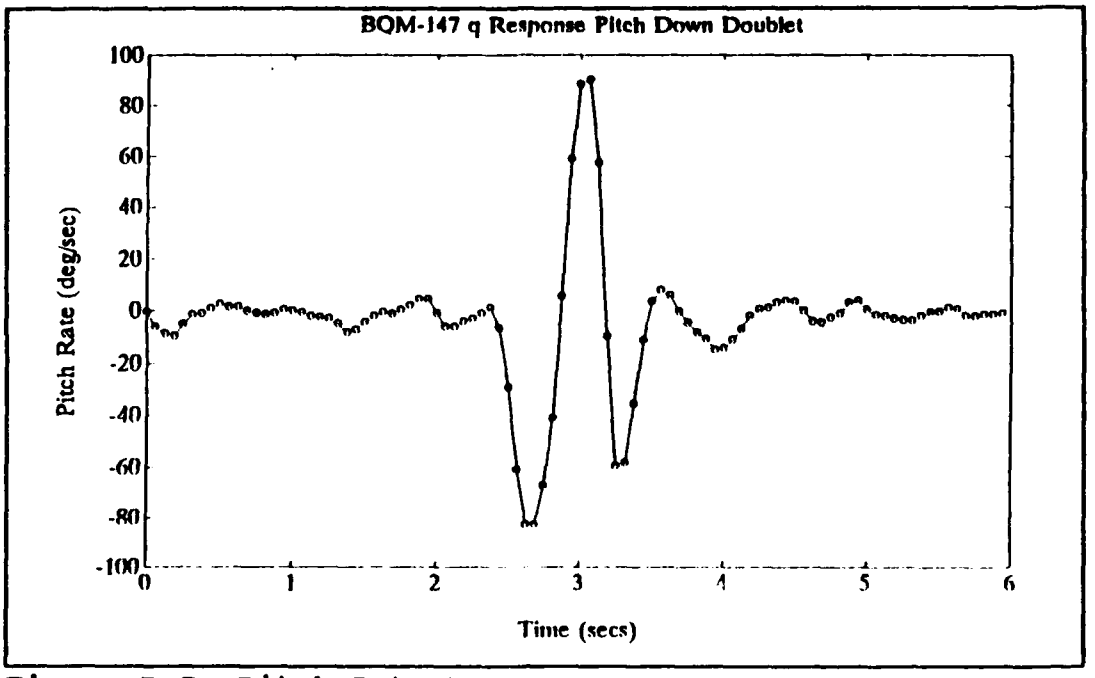

Figure B-7 Pitch-Rate Response

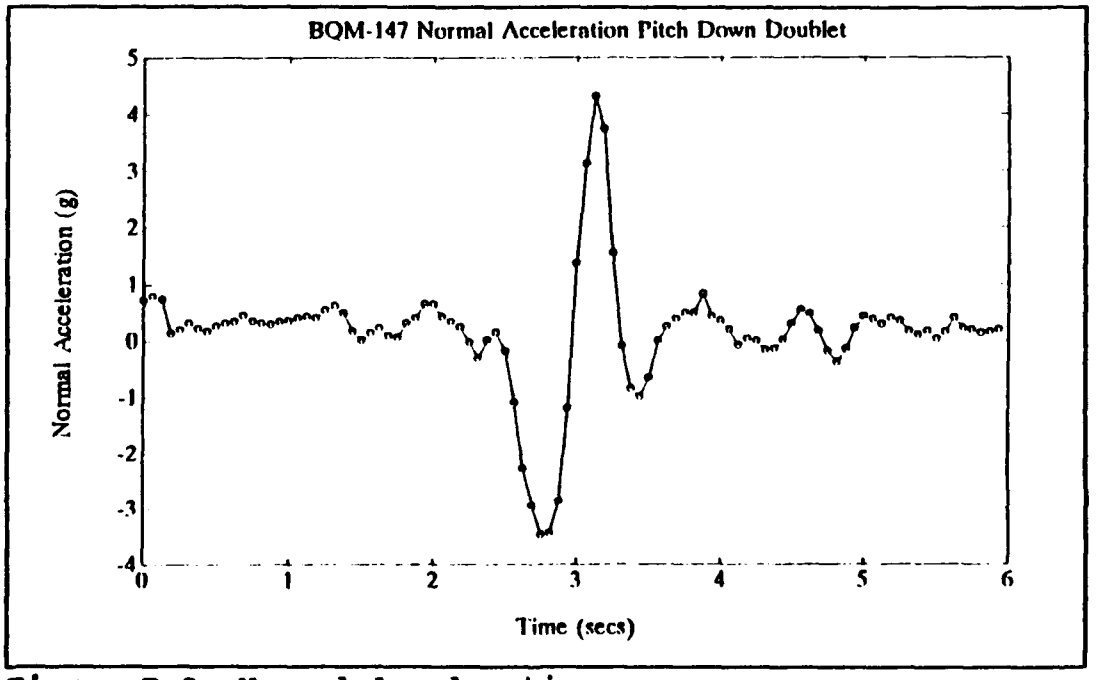

Figure B-8 Normal Acceleration

C. COMBINED ROLL AND YAW DOUBLET (P2B3-P2B5)

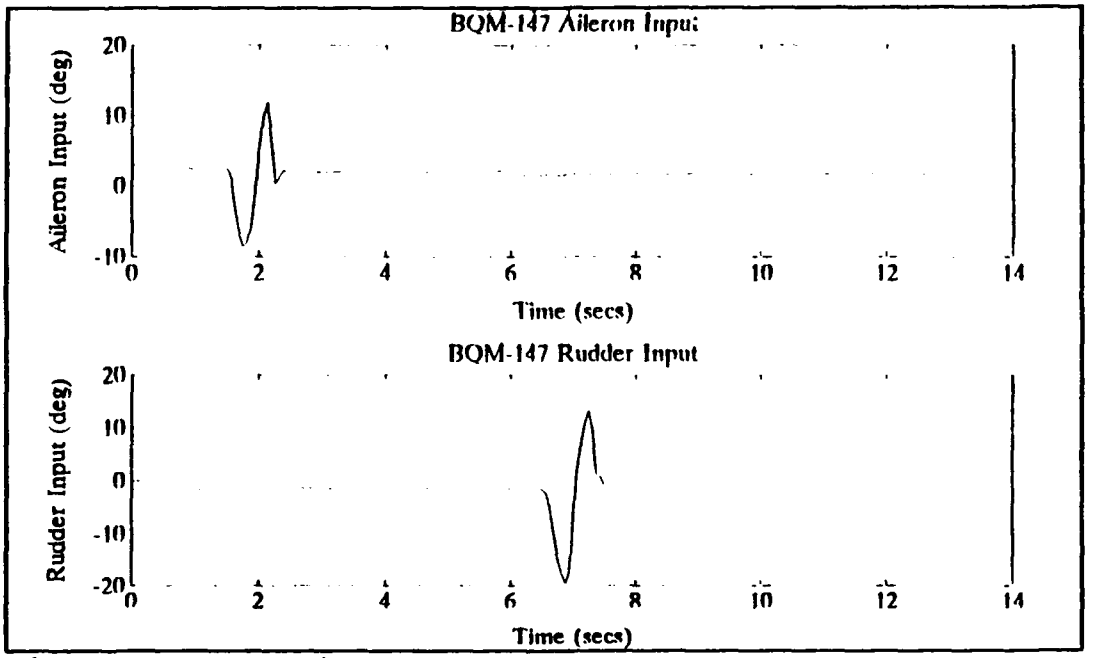

Figure B-9 Combined Control Input

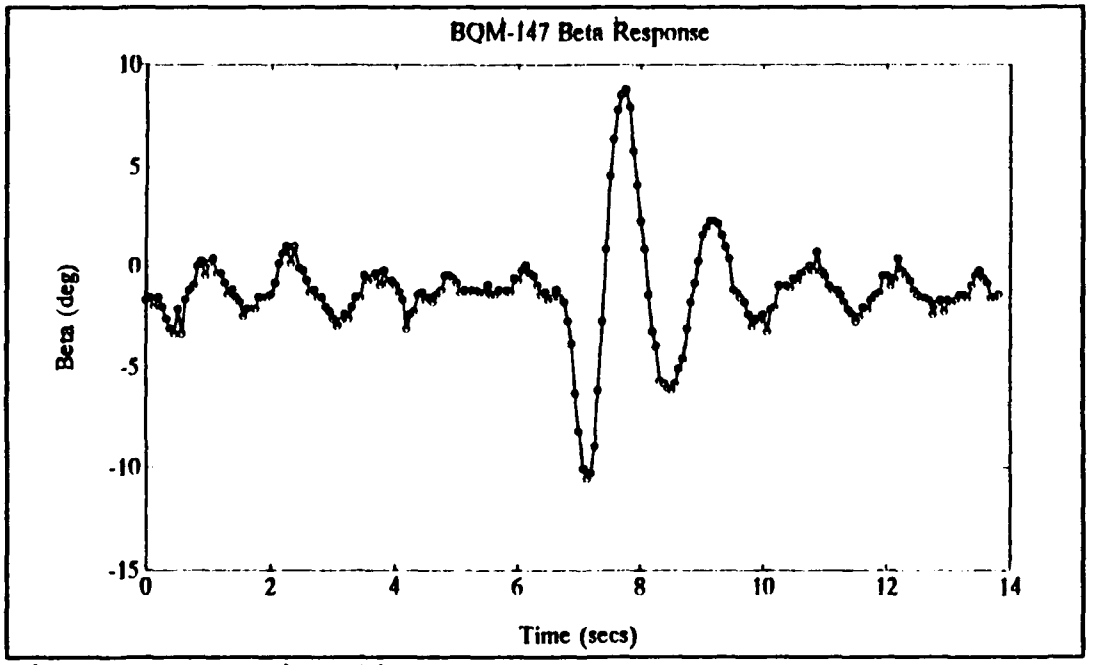

Figure B-10 Sideslip Response

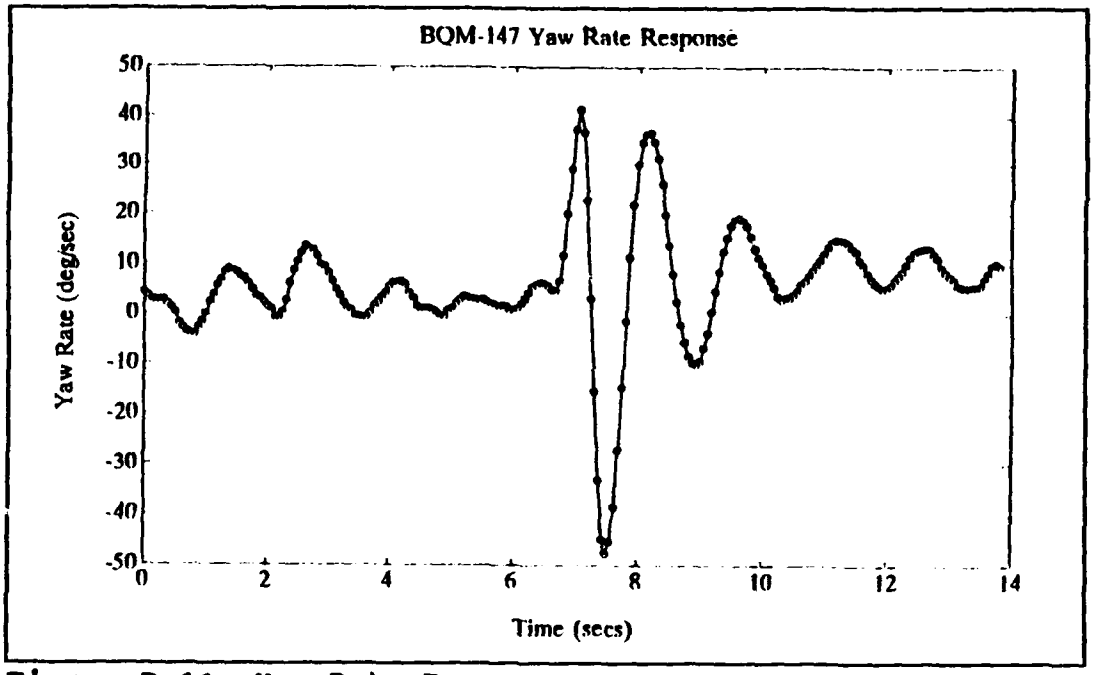

Figure B-11 Yaw-Rate Response

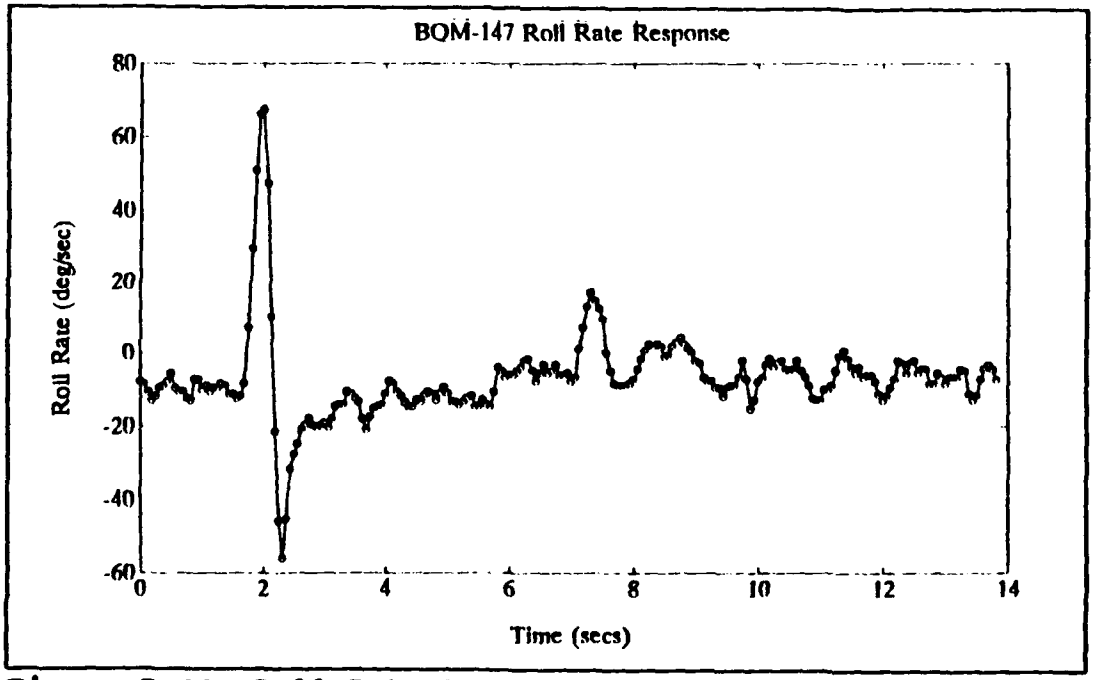

Figure B-12 Roll-Rate Response

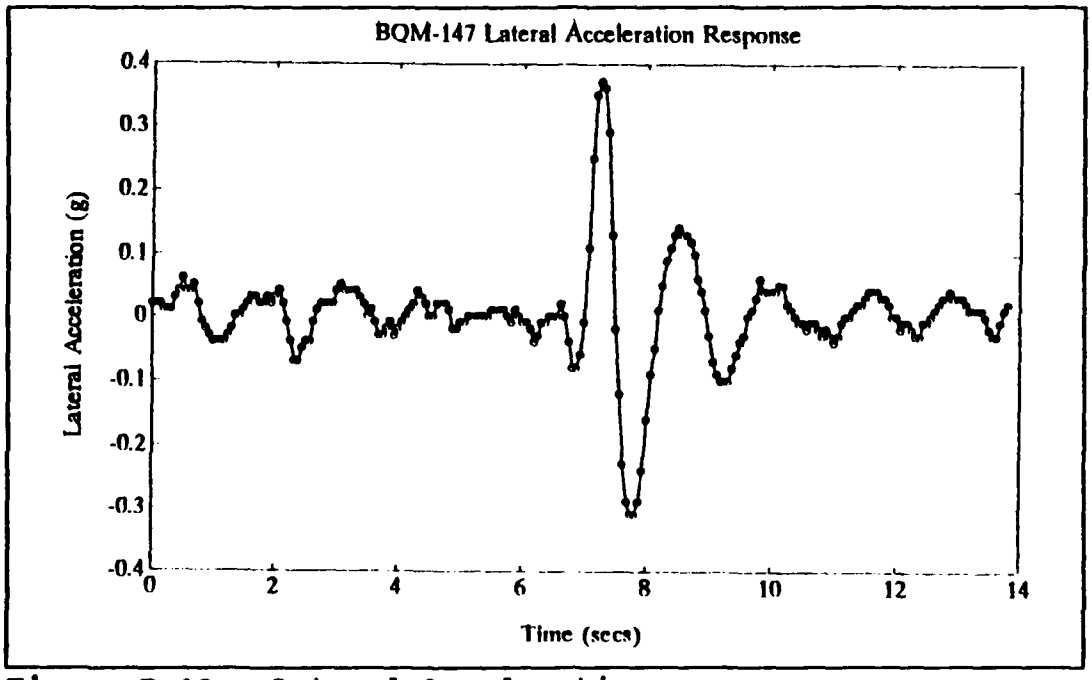

Figure B-13 Lateral Acceleration

INITIAL DISTRIBUTION LIST

		No. Copies
1.	Defense Technical Information Center Cameron Station Alexandria VA 22304-6145	2
2.	Library, Code 052 Naval Postgraduate School Monterey CA 93943-5002	2
3.	Chairman, Code AA Department of Aeronautics and Astronautics Naval Postgraduate School Monterey CA 93943-5000	1
4.	Professor Richard M. Howard, Code AA/Ho Department of Aeronautics and Astronautics Naval Postgraduate School Monterey CA 93943-5000	3
5.	Professor Isaac Kaminer, Code AA/Ka Department of Aeronautics and Astronautics Naval Postgraduate School Monterey CA 93943-5000	1
6.	CDR Patrick J. Quinn 1251 Colby Dr. St. Peters MO 63376	1
7.	CDR Timothy J. Barnes UAV Joint Project Code PEO (CU)-UD Washington D.C. 20361-1014	1
8.	Mr. Paul Heinhold Marine Corps UAV Project Office Intelligence Systems (C2IU) Marine Corps Research Development and Acquisition Command Quantico VA 22134-5080	1
9.	Mr. David J. Fratello MS 355 NASA Langley Research Center Hampton VA 23665	1

10. Mr Albion H. Bowers 1
MS D-2045
Dryden Flight Research Facility
P.O. Box 273
Edwards CA 93523